

Medical University of South Carolina

MEDICA

MUSC Theses and Dissertations

2017

Identification and Characterization of Dioctyl Sodium Sulfosuccinate (DOSS) as an Obesogen and Metabolic Disruptor

Alexis M. Temkin

Medical University of South Carolina

Follow this and additional works at: <https://medica-musc.researchcommons.org/theses>

Recommended Citation

Temkin, Alexis M., "Identification and Characterization of Dioctyl Sodium Sulfosuccinate (DOSS) as an Obesogen and Metabolic Disruptor" (2017). *MUSC Theses and Dissertations*. 344.

<https://medica-musc.researchcommons.org/theses/344>

This Dissertation is brought to you for free and open access by MEDICA. It has been accepted for inclusion in MUSC Theses and Dissertations by an authorized administrator of MEDICA. For more information, please contact medica@musc.edu.

Identification and Characterization
of Dioctyl Sodium Sulfosuccinate (DOSS)
as an Obesogen and Metabolic Disruptor

by

Alexis M. Temkin

A dissertation submitted to the faculty of the Medical University of South Carolina in partial fulfillment of the requirements for the degree of Doctor of Philosophy in the College of Graduate Studies.

Department of Molecular and Cellular Biology and Pathobiology
Marine Biomedicine and Environmental Sciences

2017

Approved by:

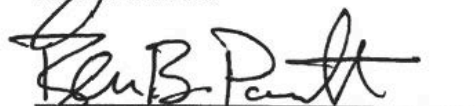
Chairman, Advisory Committee



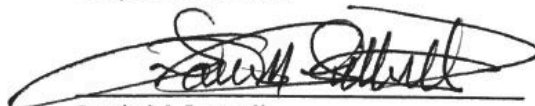
Demetri D. Spyropoulos



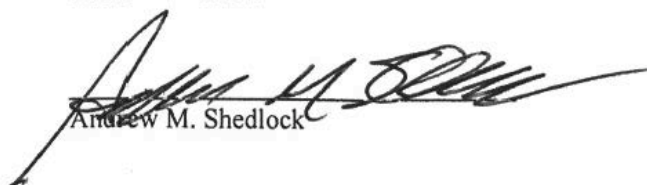
John A. Bowden



Benjamin P. Parrott



Louis M. Luttrell



Andrew M. Shedlock

©2017
Alexis M. Temkin
ALL RIGHTS RESERVED

ACKNOWLEDGMENTS

There are many people, mentors, colleagues, and friends I'd like to thank for their support over the last five years. First and foremost, my major advisor Dr. Demetri D. Spyropoulos for his guidance, support, scientific and worldly wisdom, and comic relief. A special thanks to my committee: Dr. Ben Parrott, Dr. Andrew Shedlock, Dr. John Bowden, and Dr. Louis Luttrell for their insight and enthusiasm. A special thanks to Dr. John Baatz for his role as unofficial, yet necessary, committee member and co-mentor. Dr. Robert Bowers, my fellow lab member for his assistance with experiments and knowledge of the field. My fellow MBES students for their friendships and inspiration. The MUSC Genomics Core for assistance with sequencing experiments. The MUSC SURP students for allowing me to practice my mentoring skills and contributing valuable data to this work. And lastly, Dr. Louis Guillette Jr. whose scientific legacy lives on in all his students. His mentorship is unrivaled and it was an honor to have known and worked with such an extraordinary individual.

TABLE OF CONTENTS

ACKNOWLEDGEMENTS	iii
LIST OF TABLES	viii
LIST OF FIGURES	ix
LIST OF ABBREVIATIONS	xi
ABSTRACT	xv
CHAPTER 1: GENERAL INTRODUCTION.....	1
<i>1.1 Obesity, Diabetes and Metabolic Syndrome</i>	1
<i>1.1.1 It's about communication: Action of Adipokines</i>	3
<i>1.1.2 Obesity and Inflammation</i>	7
<i>1.2 The Developmental Origins of Adult Health and Disease, Endocrine Disrupting Chemicals and Obesogens</i>	10
<i>1.3 The Deepwater Horizon Oil Spill, Surfactants and Dioctyl Sodium Sulfosuccinate</i>	17
<i>1.4 Hypothesis and Specific Aims</i>	22
CHAPTER 2: SCREENING MC252 OIL AND COREXIT 9500A DISPERSANT FOR EDCS USING RECEPTOR TRANSACTIVATION ASSAYS	31
2.1 Introduction	31
2.2 Materials and Methods	33
<i>2.2.1 Preparation of Corexit water accommodated fraction of MC252 crude oil</i>	33
<i>2.2.2 Receptor transactivation and ligand induced activation assays</i>	34
<i>2.2.3 Solid-phase extraction</i>	36
<i>2.2.4 Chemical analysis of CWF sub-fractions using LC-MS/MS</i>	36

2.2.5 <i>Molecular modeling of Corexit components binding to the PPARγ ligand binding domain</i>	38
2.2.6 <i>Statistical analysis</i>	39
2.3 Results	
2.3.1 <i>MC252 oil demonstrates estrogenic activity</i>	39
2.3.2 <i>Corexit may contain progesterone receptor beta antagonist(s)</i>	40
2.3.3 <i>CWAF and Corexit exhibit RXRα activity</i>	41
2.3.4 <i>CWAF and Corexit exhibit PPARγ activity</i>	42
2.3.5 <i>CWAF fractionation and analysis</i>	43
2.3.6 <i>Modeling of Corexit components: PPARγ binding prediction</i>	45
2.4 Discussion	55
CHAPTER 3: VALIDATION OF DOSS, A COMPONENT OF THE DISPERSANT COREXIT 9500A, AS A PROBABLE OBESOGEN <i>IN VITRO</i>	59
3.1 Introduction	59
3.2. Materials and Methods	61
3.2.1 <i>Cell viability assays</i>	61
3.2.2 <i>Receptor transactivation and ligand induced activation assays</i>	61
3.2.3 <i>TR-FRET RXRα and PPARγ binding assays</i>	62
3.2.4 <i>3T3 L1 adipocyte differentiation assays</i>	63
3.2.5 <i>Mouse and human bone marrow derived mesenchymal stem cell adipogenesis assay</i>	64
3.2.6 <i>mRNA gene expression by qPCR</i>	64
3.2.7 <i>Statistical analysis</i>	66
3.3 Results	66
3.3.1 <i>DOSS activates PPARγ</i>	66

3.3.2 <i>Span 80 exhibits RXRα activity</i>	69
3.3.3 <i>Oleic acid has stronger activity for RXRα than PPARγ</i>	70
3.3.4 <i>DOSS increases adipogenesis in preadipocytes and BM-MSCs</i>	71
3.3.5 <i>DOSS increase expression of adipogenic genes</i>	73
3.4 Discussion	88
CHAPTER 4: CHARACTERIZATION OF DOSS AS AN OBESOGEN AND METABOLIC DISRUPTOR <i>IN VIVO</i>	93
4.1 Introduction	93
4.2 Materials and Methods	96
4.2.1 <i>Animal husbandry and treatment</i>	96
4.2.2 <i>Oral glucose tolerance test</i>	98
4.2.3 <i>Body composition assessment</i>	98
4.2.4 <i>Animal sacrifice and tissue collection</i>	99
4.2.5 <i>Circulating adipokines and cytokine levels</i>	100
4.2.6 <i>Gene expression</i>	101
4.2.7 <i>DNA methylation analysis via targeted bisulfite sequencing</i>	102
4.2.8 <i>Plasma lipidomic profiling</i>	104
4.2.9 <i>Statistical analysis</i>	106
4.3 Results	107
4.3.1 <i>DOSS treatment induces glucose intolerance in male mice</i>	107
4.3.2 <i>DOSS treatment increases body mass, fat grams, fat percentage and reduces bone area in male mice</i>	108
4.3.3 <i>DOSS treatment alters circulating adipokines levels</i>	111
4.3.4 <i>DOSS treatment is associated with a persistent inflammatory state</i>	114

4.3.5 DOSS treatment altered DNA promoter methylation of IL-6 and Cox2	116
4.3.6 DOSS treated animals have elevated circulating phospholipids associated with high fat diet induced obesity and diabetes	118
4.4 Discussion	134
CHAPTER 5: CONCLUSIONS, LIMITATIONS AND FUTURE DIRECTIONS	145
References	160

LIST OF TABLES

1.1 Literature Review of <i>In Vivo</i> Obesogen Experiments.....	26
3.1 Genes and corresponding primers used for qRT-PCR analysis	63
4.1 Genes and corresponding primers used for qRT-PCR analysis	95
4.2 Bisulfite sequencing primer sequences, chromosomal location, product size, CpG number and references	135
4.3 Average percent methylation of interrogated genes in IWAT tissue of F1 males from control and DOSS treated dams	136

LIST OF FIGURES

1.1 Molecular signaling in the development of obesity mediated metabolic syndrome	25
1.2 Prevalence of obesity and diabetes in the US correlates with chemical production	26
1.3 Geographic coverage of oil and dispersant from the Deepwater Horizon Oil Spill	29
1.4 Summary of specific aims and broad approach for dissertation research	30
2.1 Receptor transactivation assay validation by positive control dose response curves	46
2.2 PPAR γ and RXR α activity in a GAL-UAS system using serum-free conditions	47
2.3 Activation of estrogen receptors alpha and beta by components of MC252 oil, Corexit and lecithin/tween 80 dispersant	48
2.4 Potential antagonist activity of progesterone receptor beta by components of Corexit	49
2.5 RXR α transactivation activity of the Corexit Water Accommodated Fraction of MC252 crude oil (CWAF), Corexit, the Lecithin/Tween 80 water accommodated fraction of MC252 Oil (LT WAF) and Lecithin/Tween80 (LT)	50
2.6 PPAR γ transactivation activity of the Corexit Water Accommodated Fraction of MC252 crude oil (CWAF), Corexit, the Lecithin/Tween80 water accommodated fraction of MC252 Oil (LT WAF) and Lecithin/Tween80 (LT)	51
2.7 PPAR γ transactivation by the 50/50 ethanol:water CWAF volume fraction	52
2.8 Tween 80 and DOSS are present in the 50/50 ethanol:water fraction	53
2.9 Molecular modeling suggests that Span 80, Tween 80 and dioctyl sodium sulfosuccinate (DOSS) components of Corexit have predicted PPAR γ ligand binding activity	54
3.1 Cytotoxicity of DOSS, Span 80 and Tween 80 in HEK 293 T17 Cells and 3T3 L1 murine preadipocytes	76
3.2 Comparison of Span 80, and Tween 80 potency and efficiency for RXR α and PPAR γ using receptor transactivation assays	77
3.3 DOSS activates PPAR γ	78
3.4 Span80, but not other components of Corexit, activate RXR α	80

3.5 Span 80 and Tween 80 binding affinity for RXR α and PPAR γ using TR FRET assays	81
3.6 Potential activation of other PPAR isoforms by DOSS	82
3.7 Oleic acid has stronger transactivation activity for RXR α than PPAR γ	83
3.8 DOSS increases adipogenesis in preadipocytes and bone marrow derived mesenchymal stem cells	84
3.9 DOSS and Span80 increase adipogenesis in 3T3 L1 preadipocytes	85
3.10 DOSS increase expression of adipogenic genes murine cell lines	86
3.11 DOSS increase expression of adipogenic genes in human BM-MSCs	87
4.1 Developmental DOSS treatment promotes glucose intolerance in male F1 mice ...	120
4.2 Developmental DOSS treatment does not promote glucose intolerance in female F1 mice	122
4.3 Body composition at 12 weeks of age in F1 male and female mice from dams treated with DOSS or vehicle control	124
4.4 Effects of DOSS treatment on body mass, adipose tissue weight and percent adipose tissue and male and female F1 mice	125
4.5 Developmental DOSS treatment alters expression and circulating levels of adipokines in male F1 mice	127
4.6 Developmental DOSS treatment promotes a proinflammatory state in male F1 mice	129
4.7 DOSS promotes changes in DNA methylation in promoter regions of inflammatory genes in IWAT	131
4.8 DOSS treatment promotes changes in circulating phospholipids	133
5.1 Summary of results presented in Chapters 2, 3 and 4	158
5.2 EPA ToxCast data for docusate sodium activation of several nuclear receptors using the NovaScreen radioligand binding assay	159

LIST OF ABBREVIATIONS

ADIPOQ	adiponectin
AP	alkylphenolic
APE	alkylphenol polyethoxylates
BM-MSC	bone marrow derived mesenchymal stem cells
BMC	bone mineral content
BMD	bone mineral density
BMI	body mass index
BPA	bisphenol-A
C/EBP	Ccaat-enhancer-binding proteins
CAN	acetonitrile
cDNA	complementary deoxy ribonucleic acid
CE	cholesterol ester
Corexit	Corexit® 9500
COX2	cyclooxygenase 2
DDE	dichlorodiphenyldrichloroethylene
DDT	dichlorodiphenyltrichloroethane
DEHP	diethylhexyl phthalate
DES	diethylstilbestrol
DiNP	diisononyl phthalate
DMSO	dimethyl sulfoxide
DNA	deoxy ribonucleic acid
DOSS	dioctyl sodium sulfosuccinate

DWH	Deepwater Horizon
DXA	dual-energy X-ray absorptiometry
E2	17 β -estradiol
EDC	endocrine disrupting chemical
EPA	Environmental Protection Agency
ER	estrogen receptor
EWAT	epididymal white adipose tissue
EZH2	enhancer of zeste 2 polycomb repressive complex subunit
FABP4	fatty acid binding protein 4
FDA	Food and Drug Administration
HPRT	hypoxanthine guanine phosphoribosyl transferase
ICP	petroleum distillates
IL-1B	interleukin 1B
IL-6	interleukin-6
IPA	isopropanol
iPSCs	induced pluripotent stem cells
IWAT	inguinal white adipose tissue
LPC	lyso phosphatidyl choline
LT	lecithin/Tween 80
MCP-1	monocyte chemoattractant protein 1
MEHP	Mono (2-ethylhexyl) phthalate
MIM	minimal induction media
MiNP	monoisononyl phthalate

NHANES	Nation Health and Nutrition Examination Survey
NIH	National Institutes of Health
NOX4	NADPH oxidase 4
NP	nonylphenol
NTC	non-treated control
OP	octylphenol
OWAT	ovarian white adipose tissue
PAH	polycyclic aromatic hydrocarbons
PAIN	pan assay interference compounds
PC	phosphatidylcholine
PCB	polychlorinated biphenyl
PCR	polymerase chain reaction
PDM	preadipocyte differentiation media
PE	phosphatidylethanolamine
PFA	paraformaldehyde
PFOA	perfluorooctanoic acid
PG	propylene glycol
PGE2	prostaglandin E2
PPAR	peroxisome proliferator activated receptor
PPRE	PPAR response element
PR	progesterone receptor
Pref1/DLk1	preadipocyte factor one/delta like kinase 1
RA	all-trans retinoic acid

RNA	ribonucleic acid
Rosi	rosiglitazone
RXR	retinoid x receptor
SDBS	sodium dodecylbenzenesulfonate
SDS	sodium dodecyl sulfate
SNP	single nucleotide polymorphism
Span 80	Span 80®
SPE	solid phase extraction
T2D	type-two diabetes
TBT	tributyltin
TNF- α	tumor necrosis factor alpha
TR-FRET	time-resolved fluorescence resonance energy transfer
Tween 80	Tween 80®
TZD	thiazolidinediones
UAS	upstream activator sequence
WAF	water accommodated fraction

ABSTRACT

ALEXIS M TEMKIN. Identification and Characterization of Dioctyl Sodium Sulfosuccinate (DOSS) as an Obesogen and Metabolic Disruptor
(Under the direction of DEMETRI D. SPYROPOULOS)

The National obesity epidemic has reached a point where 36.5% of the adults are obese. While diet, exercise and genetics are major factors driving obesity, recent studies also implicate environmental chemical agents known as ‘Obesogens’. Research efforts have begun to identify obesogens, which promote obesity and metabolic syndrome and are especially potent during fetal and childhood development. The research presented herein provides a logical framework for the identification, characterization and validation of obesogens in environmental samples.

This framework was developed based on potential obesogens present in crude oil (MC252 oil) and dispersant (Corexit) from the Deepwater Horizon oil spill given the magnitude of the spill and cleanup efforts and that components of oil have been previously implicated as obesogens. Receptor transactivation assays for nuclear receptors that regulate metabolic pathways previously implicated were used to identify obesogenic activities. Corexit components were identified to have obesogenic activities, including dioctyl sodium sulfosuccinate (DOSS), Span 80 and Tween 80. These candidate obesogens were then validated *in vitro* using adipogenic differentiation assays. DOSS increased adipogenesis in both mouse and human pre-adipocytes and stem cells. DOSS is a ubiquitous chemical used as a food additive and stool softener often prescribed to pregnant women. As such, DOSS was evaluated *in vivo* using mice in a scenario

imitating human pregnancy-associated exposure. Significantly, DOSS exposure to pregnant dams produced increased weight gain and adiposity, glucose intolerance, decreased bone area, altered adipokine production, a proinflammatory state and dyslipidemia in the male F1 population. Together, these studies provide a framework for investigation of obesogens. Furthermore, the data suggest that DOSS can act as an obesogen *in vivo* at physiologically relevant doses and prompt further research into the safe use of DOSS during pregnancy.

CHAPTER 1: GENERAL INTRODUCTION

1.1 Obesity, Diabetes and Metabolic Syndrome

The number of overweight and obese children, adolescents and adults in the United States has been growing at an alarming rate since the 1980s. The most recent data collected indicates that in the United States, 37.7% of adults are obese and 7.7% are extremely obese, based on data from 2013-2014 [1]. Strikingly, this epidemic affects children and adolescents as well with 17% of children ages 2-19 obese and 5.8% extremely obese [2]. Rates of diabetes, particularly non-genetic type-two diabetes (T2D) characterized by extreme insulin resistance, follow similar trends to those observed for obesity. Data indicates that in the United States, diabetes incidence doubled between 1990 and 2008 for data analyzed from 1980-2012 [3]. A recent study identified nearly half of the US population as diabetic or prediabetic [4].

Obesity and being overweight has been established as major risk factors for T2D with 80% of individuals diagnosed with T2D clinically overweight at time of diagnosis [5]. Obesity is also often associated with other metabolic symptoms including abdominal obesity specifically, dyslipidemia, hypertension, glucose intolerance, and proinflammatory state [6]. Together, this combination of metabolic risk factors stemming from obesity has become classified as metabolic syndrome and can increase one's risk for development of T2D and cardiovascular disease. The prevalence of metabolic syndrome in adults in the United States is similar to that of the obesity epidemic, with 34.7% of US adults diagnosed with metabolic syndrome between 2011 and 2012 [7]. Given that over 30% of the adult population suffers from such a chronic disorder has enormous public health and economic impacts. The economic burden of such a public

health disorder is estimated to increase by \$48-66 billion/year in the United States by 2030 with an estimated 65 million more obese adults by this time [8]. For an individual with metabolic syndrome, individual health care costs are generally \$2000 more per year when compared to individuals without metabolic syndrome [9].

Obesity in adults is characterized as having a body mass index (BMI) greater than 30 and overweight as being in the BMI range of 25-29.9. BMI is a measurement of weight to height ratio. While BMI is still used as a clinical measurement for obesity, some data suggests it is not the most accurate or the best predictor of obesity associated symptoms and that certain types of fat are more pathological than others such as visceral fat compared to subcutaneous fat [10]. Data from the National Health and Nutrition Examination Survey of roughly 15,000 adults indicates that waist circumference better explains obesity related health risks, like metabolic syndrome, better than BMI [11].

For several decades, the general public and the medical community has thought of obesity as a simple issue that could be solved and regulated by the number of calories an individual consumes and burns, suggesting that obesity is ultimately a result of behavioral choices [12]. The negative attitude of our society associated with obesity can lead to severe psychological issues in those afflicted. Obese individuals are often considered lazy, uneducated, and suffer discrimination making this a significant and complicated public health issue [13].

However, great strides have been made in understanding the physiological roles of adipose tissue, pathophysiology of obesity associated adipose tissue and the molecular mechanisms by which obesity and metabolic syndrome develop in an effort to effectively treat and prevent obesity and are discussed as follows.

Additionally, new findings are suggesting that obesity risk might be influenced by factors beyond behavioral choices, including genetic and environmental factors discussed in Sections 1.2 and 1.3.

1.1.1 It's about communication: Action of Adipokines

Obesity research has shed light onto the intricate mechanisms of the disease. For instance, the discovery of fat specific hormones, shifted the field and medical perspective for treatment dramatically. As the biological roles of fat as an organ (adipose tissue) were elucidated, so was the complex nature of treating a disease like obesity as well as understanding the root causes of the disorder. Since the classification of adipose tissue as an endocrine organ and discovery of adipokines, signaling molecules secreted from adipose tissue, their functional role in normal physiology as well as how they are altered in disease states has been an active area of investigation [14].

Along the lines of genetics, the first spontaneous mouse model of obesity was discovered in 1949, when an unknown mutation, deemed *ob*, for obese, caused extreme weight gain, hyperglycemia and hyperlipidemia in the mutant mice [15]. Ten years later another obese mouse model was observed and classified as *db/db* due to the onset of insulin resistance and diabetes in this mouse strain [16]. It wasn't until roughly 50 years later in the mid 1990's that the genes responsible for the mutations, *Lep* and *Lepr*, were discovered. *Lep* encodes for the protein Leptin and *Lepr* encodes for the receptor in which leptin binds [17, 18]. Leptin binds to the leptin receptor primarily expressed in the brain and results in satiety signaling. While some researchers may have hypothesized that similar mutations would be observed in the obese human population, one study describes only two individuals with a mutation in the leptin gene leading to early-onset morbid

obesity [19]. Similarly, recent investigation into polymorphisms in the LEP and LEPR genes are inconclusive with half of the studies showing association and half showing no correlation [20]. However, there is consistent observation that circulating levels of leptin are positively correlated with obesity in humans [21]. This observation indicates perhaps a resistance to leptin in obesity and ultimately a more complicated regulatory system driving disease development and progression.

Adiponectin is a signaling molecule exclusively secreted by adipocytes and was discovered as a prevalent plasma protein in an adipose tissue cDNA screening effort to identify novel drug and pathological targets in obesity [22]. The murine homologue was discovered in 1995 as a novel protein secreted by 3T3-L1 mouse adipocytes, a common cell culture model for adipogenesis [23, 24]. Adiponectin can bind to the adiponectin receptor, which upon complex formation activates AMP kinase signaling, an important step in regulating energy metabolism signaling cascades. A reduction in both adiponectin and adiponectin receptor has been observed in both diet induced and genetically induced models of obesity in mice. While mice homozygous for adiponectin deletions do not develop obesity like *ob/ob* mice do, they do develop diet induced obesity and hyperglycemia more rapidly and severely than wild type mice [25]. When supplemented with adiponectin, this phenotype is reversed. Similarly, mice that over express adiponectin display increased insulin sensitivity, resistance to high fat diet-induced hyperinsulinemia, and impaired glucose tolerance [26].

In summary, these observations indicate that adiponectin plays an important protective role in preventing obesity development and associated insulin resistance. Further supporting the plausible protective role of adiponectin in human incidence of

obesity and T2D is the negative correlation often observed between circulating adiponectin levels and incidence of diabetes, insulin resistance and obesity in human disease [27-30]. This relationship is generally reproduced in animal models of T2D and obesity. However, some animal studies report no change in circulating adiponectin levels despite increased adiposity and reduced adiponectin gene expression in white adipose tissue deposits [31] indicating a possible need to interpret circulating adiponectin levels as relative to adiposity in animal models. Similarly, higher circulating levels are observed in lean individuals and patients with anorexia nervosa and extremely low levels of body fat [32]. Furthermore, treatment of diabetic individuals with agonists of PPAR γ , a lipid sensing nuclear receptor that promotes insulin sensitization, such as Rosiglitazone, increase adiponectin levels and improves insulin sensitization suggesting a direct role for adiponectin in glucose intolerance and insulin resistance present in T2D [33]. Importantly, some clinical data suggestions that circulating adiponectin levels can predict T2D disease trajectory, indicating that individuals with the lowest levels of adiponectin are more likely to develop diabetes than those with higher levels [34-36]. In summary, these data indicate that reduced production of adiponectin can promote the development of obesity and subsequent T2D and determining the mechanism contributing to reduced adiponectin expression can identify treatment and prevention targets. One such mechanism may be by epigenetic regulation.

Given that diet and lifestyle are fundamental to weight gain and metabolism, the study of environmental and epigenetic regulation of adipokines signaling are likely to further our understanding of the molecular mechanisms associated with metabolic syndrome. DNA methylation occurring at CpG sequences within a regulatory region of a

gene can influence recruitment of transcription factors thereby influencing gene expression of a given gene. Generally, hypermethylation of a promoter region results in reduced gene expression for a given loci [37]. However, CpG methylation can also serve to recruit certain methylation dependent transcription factors at cis regulatory elements promoting gene expression [38]. DNA methylation can also be directly influenced through diet since folate, a common dietary supplement especially in the diets of pregnant women, is a key source for the carbon group required to methylate DNA. In fact, dietary supplementation with folate results in hypermethylation of DNA and can ameliorate gastrointestinal pathologies associated with DNA hypomethylation [39-41]. Additionally, maternal supplementation with folate can also rescue bisphenol-A (BPA) induced hypomethylation [42]. Specifically relating DNA methylation to obesity, changes in DNA methylation as a result of exercise or weight loss surgery have been observed [43, 44] and adipose tissue DNA methylation profiles differ in identical twins discordant for obesity and BMI [45]. Together these observations not only implicate DNA methylation as a potential mechanism of gene regulation and disease development in metabolic syndrome and metabolic disruption but also simultaneously a target for treatment and prevention of such disease development.

Investigation of the adiponectin promoter region reveals hypermethylation of four CpG sites in high fat diet-induced obesity animal models however, two other CpG sites nearby (within 50 base pairs) seem to be unaltered [46]. This promoter site-specific hypermethylation correlated with reduced expression of the *AdipoQ* gene [46]. In human samples, *ADIPOQ* methylation of one CpG site is associated with BMI while another is associated with waist circumference. These data indicate DNA methylation as a plausible

gene regulatory mechanism by which adiponectin expression and regulation are augmented in obesity [47]. For leptin, a diet-induced obesity animal model revealed a curious positive correlation between average promoter methylation and leptin gene expression in adipose tissue [48]. The same study identified other types of epigenetic modifications such as histone modifications that may play a more dominant regulatory role in leptin expression than that of DNA methylation. In human adipose tissue samples, negative associations between specific CpG sites and leptin expression have been observed but are dependent on leptin SNP genotypes of individuals [49] highlighting the importance of gene by environment interactions in metabolic phenotypes. So, while preliminary investigation has been done to establish a role for DNA methylation in regulation of adipokine expression and function, the evidence does not articulate a common mechanism in terms of CpG site, gene or phenotype. This subject warrants further investigation especially in the context of how changes in DNA methylation due to environmental contributors can lead to aberrant signaling and metabolic syndrome development.

1.1.2 Obesity and Inflammation

The role of inflammation in chronic diseases like obesity and diabetes is an active area of investigation. In both mouse and human studies, it has been observed that disease states of these disorders coincide with markers of chronic inflammation. Understanding if inflammation in fact can cause obesity or occurs after the fact is still relatively unanswered although obesity is associated with an infiltration of macrophages into white adipose tissue, which in turn secrete proinflammatory cytokines [50]. Several inflammatory cytokines, such as IL-6, TNF- α IL-1B and MCP-1, have been documented

to be upregulated in obesity, classifying the disease as associated with systemic inflammation or a proinflammatory state [51]. It is hypothesized that the action of these cytokines contribute to insulin resistance and other symptoms observed in metabolic syndrome. The majority of research has focused on IL-6 and TNF- α since they are the most prevalent and pathological associated.

IL-6 can be secreted by adipose-associated macrophages and by adipocytes themselves, although adipocytes contribute only a small percentage of overall tissue IL-6 levels [52]. Interestingly, different adipose tissue deposits can secrete different levels of IL-6 [52]. Increases in IL-6 levels have been shown to predict the development of T2D, suggesting a pathogenic role for the cytokine, although a combination of inflammatory cytokines is likely a better predictor [53, 54]. Conversely, IL-6 knockout mice develop obesity and have impaired glucose metabolism which would suggest a protective role for the cytokine [55]. It will be important to determine the factors influencing whether IL-6 has a pro- or anti-inflammatory action in obesity and T2D development although the majority of studies point to its role as a pathological pro-inflammatory cytokine. For example, a positive correlation between serum IL-6 levels and presence of obesity and diabetes is consistently observed in human cohort studies [56, 57]. Additionally, weight loss can reduce circulating IL-6 levels and improve insulin sensitivity [58]. When used in *in vitro* studies, IL-6 treatment promotes insulin resistance in cultured adipocyte cell lines, with reduced adiponectin and insulin receptor substrate-1 as possible mechanisms of action [59, 60]. Regulation of IL-6 in adipose tissue by DNA methylation has not been evaluated in rodent or human studies and could be an unidentified but important mechanism by which IL-6 pathogenicity in adipose tissue occurs during obesity.

Like IL-6, TNF- α is similarly upregulated in proinflammatory-dependent obesity, often concomitantly with IL-6 [61]. Adipose derived TNF- α is produced exclusively by adipose associated macrophages and can play a direct role in mediating obesity-linked insulin resistance [50]. Seminal work from Spiegelman, et al., showed that neutralization of circulating TNF- α in obese rats resulted in improved insulin response as measured by uptake of glucose [62]. TNF- α has also been the target of therapeutics to treat obesity and insulin resistance with some successful results, and similarly, circulating TNF- α can be reduced after weight loss [63, 64]. Taken together, our current view is that cytokine signaling is an important contributor to metabolic syndrome but that more research into the mechanisms (epigenetic) controlling cytokine production in adipose tissue is needed.

In summary, as depicted in Figure 1, adipocyte dysfunction in obesity is marked by hypertrophy and/or hyperplasia of adipose tissue, infiltration of macrophages that increase adipose tissue associated proinflammatory cytokines (IL-6 and TNF- α), which in turn promotes insulin resistance (hyperinsulinemia), reduced adiponectin and increased leptin secretion, impaired glucose tolerance, and dyslipidemia [65]. Together these measureable observations signify metabolic syndrome.

While the symptoms classifying metabolic syndrome and the associated health risks are well established, the causes of obesity and metabolic syndrome are still under investigation. A recent notable observation indicates a direct correlation between the rising rate of chemical production in the US and the increase in rates of obesity in the US (Figure 2A) [66]. Beginning in the 1940s there have been dramatic increases in chemical production, with approximate 20 billion kg/year produced by the 1960s and climbing to about 250 billion kg/year by 2010. Obesity incidence began its dramatic increase in the

1980s, beginning with approximately 15% percent of the adult population being obese in 1980, and climbing to over 35% by 2010. As described by Sargis et al., a steady increase in diabetes rates turned to dramatic increases from the late 1990s onward. (Figure 2B) [67]. It is not clearly defined why the dramatic increases in obesity began in the 1980s and in diabetes in the late 1990s, but it may be related to the total chemical burden mixture, synthesis of specific types of chemicals or because obesity often precedes the development of diabetes [68, 69]. Domesticated animals and animals living within close proximity to industrialized cities and humans have also experienced unprecedented increases in weight gain and obesity [70]. Identification of this correlation helped in the development of the obesogen hypothesis, which suggests a causal link between exogenous chemical exposure and obesity development. This general hypothesis is explored in section 1.2 and foundational to the work performed and discussed in the following chapters

1.2 The Developmental Origins of Adult Health and Disease, Endocrine Disrupting Chemicals and Obesogens

The developmental origins of adult health and disease (DOHAD) hypothesis was first proposed by Barker in the 1980s [71]. Barker linked the incidence of cardiovascular disease in adults who experienced poor fetal nutrition in the Netherlands as a result of Nazi occupation during WWII [72]. Research later documented incidence of obesity and diabetes in offspring of mothers who experienced malnutrition during pregnancy as a direct result of the Irish potato famine [73]. Together, this research provides evidence to support the hypothesis that the maternal environment during fetal development might result in fetal epigenetic reprogramming that influences disease susceptibility and development later in life. Development being exquisitely sensitive is likely related to the

prevalence of stem cells whose patterning is not hard-wired but highly amenable to epigenetic reprogramming [74].

Similar observations connecting conditions experienced during early life to later onset phenotypes were being made in wildlife and environmental studies. Rachel Carson's publication of Silent Spring in 1962 enlightened the public to the harsh –level effects caused by the widespread use of the pesticide dichlorodiphenyltrichloroethane (DDT) on the ecosystem. Similarly, the foundational work of the Guillette lab on the alligator population of the heavily polluted Lake Apopka in Florida clearly demonstrated reproductive abnormalities in the field could be reproduced under chemical exposure in the lab [75-77]. The terms endocrine disruptor, environmental endocrine disruptor and endocrine disrupting chemicals (EDCs) became commonly used and an active area of study in the 1970s. Environmental endocrine disruptors have long been studied for their interactions and effects primarily within the reproductive system. A pharmaceutical example of endocrine disruption on reproduction is diethylstilbestrol (DES), a potent pharmaceutical estrogen prescribed to pregnant women to help prevent preterm birth. It was only later learned, that daughters exposed to DES in the womb experienced severe reproductive disorders including a rare vaginal cancer [78]. Virtually all of the adverse reproductive phenotypes described in the DES-exposed mouse model have now been identified in daughters of DES exposed women [79-81]. This work was foundational evidence supporting the presence of endocrine disruption and validated the use of mouse models as strong models for study of potential EDCs with translatable human results.

Once a clear link was established between contaminant exposure and disease outcomes, investigators began to tease apart the multiple mechanisms whereby endocrine

disrupting chemicals act. The most commonly studied mechanism of endocrine system regulation is via hormone/endogenous ligand interaction with target nuclear hormone receptors (either in the binding pocket or allosterically). Upon ligand binding, the receptor is translocated to the nucleus where it regulates targeted gene expression via specific response element binding and recruitment of transcription machinery and co-regulatory proteins [82]. Through a variety of interactions with the receptor, exogenous EDCs can act as agonists, antagonists or simply block endogenous ligands from binding. (i.e., acting as competitive inhibitors) [83]. EDCs could also sequester the ligand preventing action on its receptor, block receptor nuclear translocation, and alter co-factor (activators and repressors) recruitment to target response elements resulting in gene expression of select genes [84-86]. Additionally, synthesis of endogenous steroid hormones involves the activity of several enzymes including but not limited to aromatase for conversion of testosterone to estrogen and estrogen sulfotransferases, both of which can be inhibited by EDCs [87]. Lastly EDCs can alter epigenetic patterning of genes committing cells towards specific disease lineages [88].

Historically, reproductive effects have been the primary focus of research on EDCs, and more recently, metabolic disorders have emerged as likely targets of chemical exposures in combination with diet, exercise and lifestyle [88]. More research has been devoted to identifying novel metabolic disrupting chemicals, as well as identifying additional effects of legacy chemicals, as they relate to metabolic systems. For example, canonically estrogenic compounds including DES, BPA and polychlorinated biphenyls (PCBs), known for their adverse reproductive effects, also exhibit weight gain and impaired glucose tolerance and thus result in metabolic disorder phenotypes [89-91].

These novel compounds have been termed “obesogens” and more recently classified as a subset of EDCs known as metabolic disruptors [92]. The most well studied obesogen to date is tributyltin (TBT). Exposure of pregnant mice to TBT, whether throughout or at a single time point in pregnancy, produce obesogenic effects in offspring [93, 94]. Alternatively, daily TBT exposure over several weeks promotes weight gain and increased adiposity in adult mice [95]. The proposed mechanism by which TBT elicits its obesogenic effects is through the PPAR γ /RXR α signaling pathway, whereby it acts as a ligand that activates both PPAR γ and RXR α in receptor transactivation assays and promotes adipogenesis *in vitro* through either a PPAR γ -dependent mechanism [96] or through a PPAR γ -independent mechanism (e.g. RXR α) [97].

PPAR γ is a member of the nuclear receptor super family functioning as a ligand activated transcription factor. In order to elicit a transcriptional response, PPAR γ first forms a heterodimeric complex with RXR α , a common partner for orphan nuclear receptors, then binds to a PPAR response element (PPRE) [98-100]. PPRE sequences are found in the promoter of several genes that are integral in lipid metabolism and homeostasis [101, 102] and PPAR γ , along with other transcription factors including the Ccaat-enhancer-binding protein (C/EBP) family, is known as the master regulator of adipogenesis [103]. Endogenous ligands for PPAR γ include fatty acids, such as arachidonic acid, and their fatty acid derivatives, specifically eicosanoids [104]. There are two alternatively spliced isoforms of PPAR γ , PPAR γ 1 and PPAR γ 2. While PPAR γ 2 is primarily expressed in mesenchymal stem cells and preadipocytes during adipogenesis, PPAR γ 1 is more highly expressed in adipose tissue and also involved in lipid homeostasis [105-107].

In addition to adipogenesis, activation of PPAR γ results in several metabolic outcomes including insulin sensitization, lipid metabolism, hepatic lipid storage, and glucose-stimulated insulin secretion [108]. Due to the role of PPAR γ in insulin sensitization, it has been the target of a class of drugs, termed the thiazolidinediones (TZD), that are aimed at ameliorating the symptoms and pathologies of T2D and metabolic syndrome [109]. The multiple pathways downstream of PPAR γ are particularly vulnerable to disruption due to activation or inhibition of the receptor by exogenous ligands [110].

The approach used to identify TBT as a PPAR γ agonist and its further classification as an obesogen primarily focused on receptor activity and has been used to identify other potential obesogens [111]. A list of publications that provide evidence for metabolic disruption in mouse models by exogenous chemicals is summarized in Table 1. Such compounds include air pollutants like PAHs, the antifouling agent TBT, the stain and water repellent perfluorooctanoic acid (PFOA), the plasticizer diethylhexyl phthalate (DEHP) and its metabolite mono (2-ethylhexyl) phthalate (MEHP), the pesticides triflumazole and tolyfluanid, and the estrogenic compounds DES and BPA. Despite their diversity in utility, structure and function, many obesogens appear to act through a common mechanism, that is, binding and/or activating the PPAR γ receptor, although this observation could be due to an imbalance in research efforts focusing primarily on PPAR γ mediated obesogen mechanisms of actions. In fact, EPA obesogen screening efforts (ToxCast) have primarily focused on chemicals that activate PPAR γ while a less characterized and emerging mechanisms of action for obesogens is through interaction with the glucocorticoid receptor [112, 113]. An appreciation for which

obesogenic/metabolism-disrupting chemical compounds came into production at different times may help shed light on the dramatic increases in obesity and diabetes shown in Figure 2.

Also shown in Table 1, is the variability in timing of dose on outcomes. Broadly, studies fall into two categories, gestational/perinatal exposure and adult exposure. Even within those studies treating during times of development, there is extreme variability for dose timing and mode of delivery. Several studies provide a single dose during gestation, while others provide daily injections delivering a desired dose from gestation through weaning. Understanding the environmental relevance of dose, time, and mode of delivery when considering experimental design is paramount in order to provide research with results that better inform exposure and health effects observed in human populations. While there may be diversity among type of EDC and timing of dose, the obesogenic end points of analysis generally remain consistent. Based on this literature (Table 1), end points that should be included in a study evaluating obesogens and metabolic disruptors include, glucose tolerance tests, body weight, adiposity as a function of adipose tissue weight specifically, general body composition, adipokine, cytokine and hormone analysis in serum or plasma, and gene expression of obesity associated genes in adipose tissue. Importantly, these are the same parameters that help define metabolic syndrome in human patients.

One significant weakness amongst the animal data presented in Table 1 is the inadequate presentation of sex-specific differences in outcomes resulting from EDC exposure. Often studies analyze one sex with unclear reasoning for the omission of the other sex. In these cases it is unclear if the other sex was tested or if this omission

represents inconclusive or negative results and likely an overgeneralization because multiple different phenotypes could be assayed for and identified. Previous publications that utilize one sex, such as high-fat diet induced obesity studies that use males [114], may be driving choices to use one sex over the other. For those studies reporting results in both sexes, there is often clear sexual dimorphism in regard to exposure effects, as is the case with the metabolic disruptor tolyfluanid [115]. If results are not clearly and fully reported in the context of different sexes, it is possible for the results to be interpreted incorrectly. Additionally, female mice have traditionally been underrepresented in studies and a call to research was made the NIH to begin examination of both sexes for their outcomes in order to gain a more complete understanding of biological variables that contribute to disease [116]. This may be particularly relevant for the role of endocrine disruptors in the promotion of obesity, diabetes and metabolic syndrome.

While there is strong evidence for metabolic disruption induced by exogenous chemicals in animal models, epidemiological studies in humans are not conclusive. Many of the data for the effects of obesogens in humans is based on cross sectional studies, particularly for studies on phthalate plasticizers. Using urinary phthalates levels from the National Health and Nutrition Examination Survey (NHANES) data, multiple groups have identified correlations between certain phthalate metabolite levels and markers of obesity like BMI and waist circumference in adult men and women [117, 118]. Other studies examine single time point analyses during pregnancy and single time point analyses in offspring. For example, child adiposity at 8 years of age was the single time point used and found to be associated with higher maternal serum levels of PFOA during pregnancy [119]. Interestingly, while cross sectional studies for BPA levels have been

observed to be associated with markers of obesity [120], maternal BPA levels negatively correlate with BMI in children [121, 122]. Well-designed longitudinal studies are necessary in order to determine how results from animal models studying metabolic disruptors can be translated into human health. The “Obesogenic Endocrine disrupting chemicals: Linking prenatal exposure to the development of obesity later in life” (OBELIX) project was funded with this intention in mind and will provide data to fill a knowledge gap in this field [123]. The objective of this project is to use four mother-child cohorts to evaluate the link between contaminant exposure to pregnancy and obesity endpoints in children. Data from the OBELIX project has already identified a link between prenatal dichlorodiphenyldichloroethylene (DDE) exposure and increases in infant growth [124].

1.3 The Deepwater Horizon Oil Spill, Surfactants and Dioctyl Sodium Sulfosuccinate

The Deepwater Horizon Oil Spill breach occurred in April 20, 2010. It was a massive industrial disaster in which 200 million gallons of oil was released into the Gulf of Mexico due to an oil rig explosion, the largest oil spill in US history [125]. In order to remediate the effects of the spill, 1.8 million gallons of Corexit® dispersant was applied to the spill both at the surface and in an unprecedented event via injection underwater near the well head. Dispersants are used as detergents to remove oil from surface slicks, break it into droplets and disperse it throughout the water column to prevent oiling of fragile shoreline habitats and ecosystems. This is done through the combined use of surfactants and solvents that contain both hydrophobic and hydrophilic moieties. The majority of dispersants used was Corexit 9500,® (from here on referred to as Corexit)

which contains approximately 10-30% ,dioctyl sodium sulfosuccinate (DOSS), an active surfactant (MSDS for Corexit® EC9500A, Nalco Environmental Solutions).

The massive nature of the spill and contamination of the surrounding environment has persisted well past the capping of the well head on July 25, 2010. The staggering geographic coverage of the oil spill and aerial dispersant coverage depicted in Figure 3, emphasize the broad impacts of such a natural disaster on multiple marine habitats (pelagic, benthic, coastal), organismal life stages, and several species, including humans, highlighting the need for research across all levels involving multiple disciplines.

Toxicological effects of oil and dispersant have been the primary area of research to understand the immediate impacts of the DWH oil spill with some focus on sub lethal effects. Many studies indicate that dispersed oil is more toxic than either crude oil or dispersant on its own, with one argument being that dispersant makes toxic compounds (e.g. polycyclic aromatic hydrocarbons; PAHS), in crude oil more bioavailable to marine organisms [126, 127]. Other studies indicate that exposure to oil and dispersant during the vulnerable life stages of development and embryogenesis, can cause teratogenic effects in zebrafish animal models [128] and impact cardiovascular development of several commercially and ecologically important Gulf of Mexico large, pelagic, predatory fish species [129]. Marine mammals were also impacted from the spill; one study observed higher prevalence of disease and worse health prognosis in dolphins from a population that resides in a heavily oiled area when compared to a population from an unoiled site [130]. With regard to human health, acute exposure to Corexit caused respiratory distress in oil spill remediation workers as Corexit can be harmful to human airway epithelial cells via surfactant perturbation [131-133]. Moreover, exposed workers

experienced significantly altered blood profiles and liver function and enzyme levels [131, 132]. Together these data indicate overall adverse health effects across a multitude of species impacted by the oil spill and use of Corexit, potentially implicating both immediate and long-term effects on Gulf of Mexico human and marine species populations.

Despite large amounts of research efforts assessing the effect of MC252 oil and Corexit on several species, few studies have focused on potential endocrine disrupting effects of such a large environmental exposure, including the identification of EDCs present in the complex mixtures of oil, dispersant and dispersed oil specific to the DWH spill. However, some evidence for endocrine disrupting effects in other types of oils and dispersants/surfactants exists for both terrestrial mammals and marine organisms, as follows. One week of dietary exposure to Nigerian bonny light crude oil reduced testicular steroidogenesis in male rats as measured by enzyme function and circulating hormone levels [134]. Work by Skinner et al., reported jet fuel exposure via intraperitoneal injection of pregnant dams during development resulted in transgenerational inheritance of obesity (F3 only), polycystic ovarian diseases and changes in sperm epigenetic marks observed in subsequent generations [135]. In both of the above examples, the exposure routes are unlikely real world scenarios making the implications and translatability of observed results difficult to interpret.

Environmentally relevant exposure to ambient PAH's, compounds known for their prevalence in oil and associated toxicity and carcinogenicity, resulted in increased adiposity in mice and associated changes in adipose tissue gene expression and DNA methylation in offspring and grand offspring of exposed dams [136]. Similarly, Kim et al.

(2005) reported several PAHs to activate PPAR signaling providing a potential mechanism by which PAHs can influence lipid metabolism and homeostasis [137]. These two studies together provide a plausible mechanism by which crude oil may be a metabolic disruptor but replication and consideration for different types of crude oil and exposure routes is necessary.

Water accommodated fractions prepared from crude oil bunkers in South Africa display multiple endocrine disrupting properties including thyroid, estrogen, androgen, and PPAR activities when screened *in vitro* with some translatable effects to *in vivo* studies in amphibian and freshwater fish animal models [138]. With regard to mammalian responses to crude oil, investigators observed potent estrogenic effects of several types of oil *in vitro* measured by receptor transactivation assays and increased proliferation of a human breast carcinoma cell line [139].

With regard to dispersant, one group did perform receptor transactivation screening assays in eight dispersants, including Corexit [140]. Like most EDC screening efforts, priority was put on screening for estrogens and androgens using receptor transactivation assays. Investigators observed no androgenic activity for any of the dispersant analyzed while weak estrogenic activity was detected for two dispersants (not Corexit). This group also performed a multiplexed reporter assay screen and identified PPAR activity for many dispersants, particularly Corexit. Validation of this activity required more detailed experimentation, which was pursued in research efforts described in subsequent chapters.

Other surfactants that are widely used in cleaning products, pesticides and cosmetics and have been evaluated for the endocrine disrupting properties are

alkylphenolic (AP) compounds and alkylphenol polyethoxylates (APEs). While APEs have been used in other oil dispersants, they were not part of the Corexit® composition. In the environment AP and APEs can break down into multiple nonylphenol (NP) and octylphenol (OP) compounds, which are more persistent, bioactive and toxic molecules and can be detected in surface waters and sewage sludge [141, 142]. In *in vitro* receptor transactivation assays, breast cancer cell line growth assays and vitellogenin assays, multiple investigators have reported weak estrogenic activity for NP- and OP-like biodegradation products [140, 143, 144]. *In vivo* studies also indicate that these compounds and mixtures of these surfactants with other pesticides behave as estrogenic endocrine disruptors, functioning to increase vitellogenin expression in fish [142, 145] although secondary sex characteristics seem to be unaffected [146]. However, these studies describe effects observed in laboratory experiments using concentrations higher than those observed in the field and documenting population-based effects is difficult. Because NPs can also be found in several commercial food products, including infant formula [147], determining physiologically relevant exposure doses for humans is feasible and could inform the experimental design of animals studies to determine if these concentrations of NPs have endocrine disrupting effects in mammalian species.

Similar to NPs, several components of Corexit have broad commercial use as many serve multiple purposes including acting as food additives, pharmaceutical stool softeners, and house hold cleaning products. While DOSS is a prevalent component of Corexit (10-30%) it is also a food additive particularly in dried beverages (75 ppm) [148] and prescribed as a stool softener (Colace/docusate sodium) at recommended doses of 200-300 mg/day with a maximum dose of 500 mg/day. Toxicity data for DOSS does not

indicate it as carcinogenic, teratogenic or to have an effect on reproductive function in rodents exposed to 1% DOSS in their food [149, 150]. Similarly, use of DOSS as a stool softener during pregnancy and breast feeding were not previously found to produce any apparent adverse health effects in the children [151-154]. However, DOSS can alter absorption of other compounds (Danthron; a stimulant laxative) and a caution is advised when taking docusate in combination with certain medications [155]. To the best of my knowledge, DOSS has not been evaluated as a metabolic disruptor at environmentally relevant concentrations.

In summary, evaluation of Corexit and its components for their endocrine disrupting potential at physiologically relevant doses and primary routes of exposure are particularly necessary given that human exposure to these compounds is likely widespread and can occur through multiple routes. For example, exposure to Corexit and oil components could occur through consumption of contaminated seafood. And while direct human exposure to Corexit via oil spill remediation is likely acute and would have immediate effects such as respiratory distress and alterations to hepatic function, exposure to the Corexit component DOSS via Colace use during pregnancy or long-term dietary intake could result in sub lethal endocrine/metabolic disrupting effects.

1.4 Hypothesis and Specific Aims

Due to the massive nature of the DWH oil spill, and given the lack of research on EDCs specific to MC252 oil and Corexit dispersant, I sought to identify and characterize potential EDCs present in these mixtures. ***The overarching hypothesis of this Dissertation is that DOSS, a major functional component of Corexit, is a metabolic disruptor.*** Particular emphasis was put on identifying potential novel obesogens given the

rise in obesity and diabetes epidemics. Furthermore, *in vitro* and *in vivo* validation and characterization of obesogens was performed and designed in a context relevant for human health. The specific aims testing the above hypothesis are summarized as follows and in Figure 4:

Specific Aim 1: Identify potential obesogens present in MC252 oil and/or Corexit® 9500 dispersant via effects based screening (Chapter 2).

Hypothesis: Components of oil, primarily PAHs would be potential obesogens. These experiments included screening several types of oil and dispersant mixtures for PPAR γ , RXR α and estrogen receptor activation using receptor transactivation assays to determine if the oil itself, components of oil and/or DOSS, exhibited obesogenic activity.

Specific Aim 2: Validate candidate obesogen/s *in vitro* (Chapter 3).

Hypothesis: Potential obesogens identified in Aim 1 (ie. DOSS) will act as an obesogen *in vitro* via PPAR γ agonist activity promoting adipogenesis and gene expression of PPAR γ regulated proadipogenic genes. This hypothesis was tested using adipogenic differentiation assays of three adipocyte progenitor cells in the presence of DOSS or a vehicle control.

Specific Aim 3: Characterize validated obesogen *in vivo* in an environmentally relevant manner (Chapter 4).

Hypothesis: DOSS can act as a metabolic disruptor *in vivo* promoting a unique phenotype associated with developmental DOSS exposure. To

test this hypothesis the F1 population of dams treated with DOSS from mid gestation through weaning was analyzed for markers of metabolic syndrome including glucose tolerance tests, circulating adipokines and cytokines, dyslipidemia, adipose tissue gene expression and DNA methylation.

The work presented herein strives to build evidence for the overall metabolic disruptor hypothesis, that is exposure to exogenous chemicals during development can predispose an individual to develop metabolic syndrome in their adult life. Given the potential for human exposure to MC252 oil and Corexit via consumption of contaminated seafood, ambient exposure due to proximity to the spill or exposure to a specific Corexit component (DOSS) via stool softener/Colace use during pregnancy (critical windows of development), there is a need to fully evaluate the potentially adverse effects associated with exposure to these compounds, including their potential role as endocrine/metabolic disruptors.

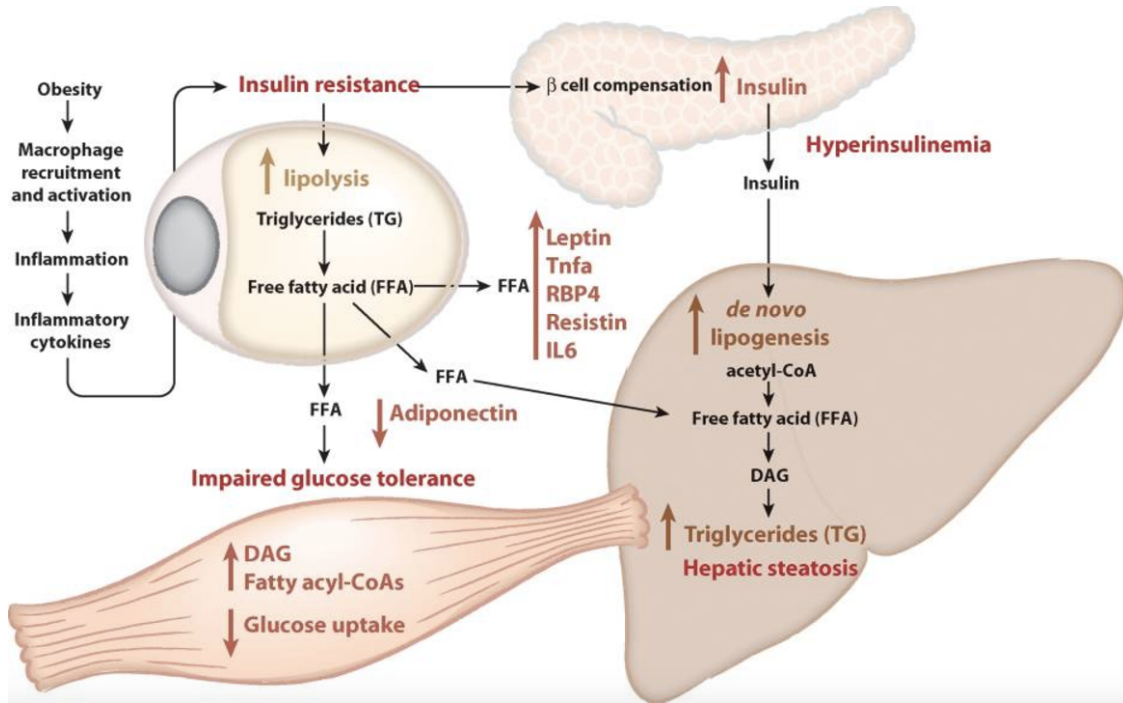


Figure 1. Molecular signaling in the development of obesity mediated metabolic syndrome.

Metabolic syndrome is characterized as increased adiposity particularly in the abdomen, impaired glucose tolerance and insulin resistance, dyslipidemia and a proinflammatory state. Together these symptoms increase an individual's risk for development of T2D and cardiovascular disease. Figure adapted from [65].

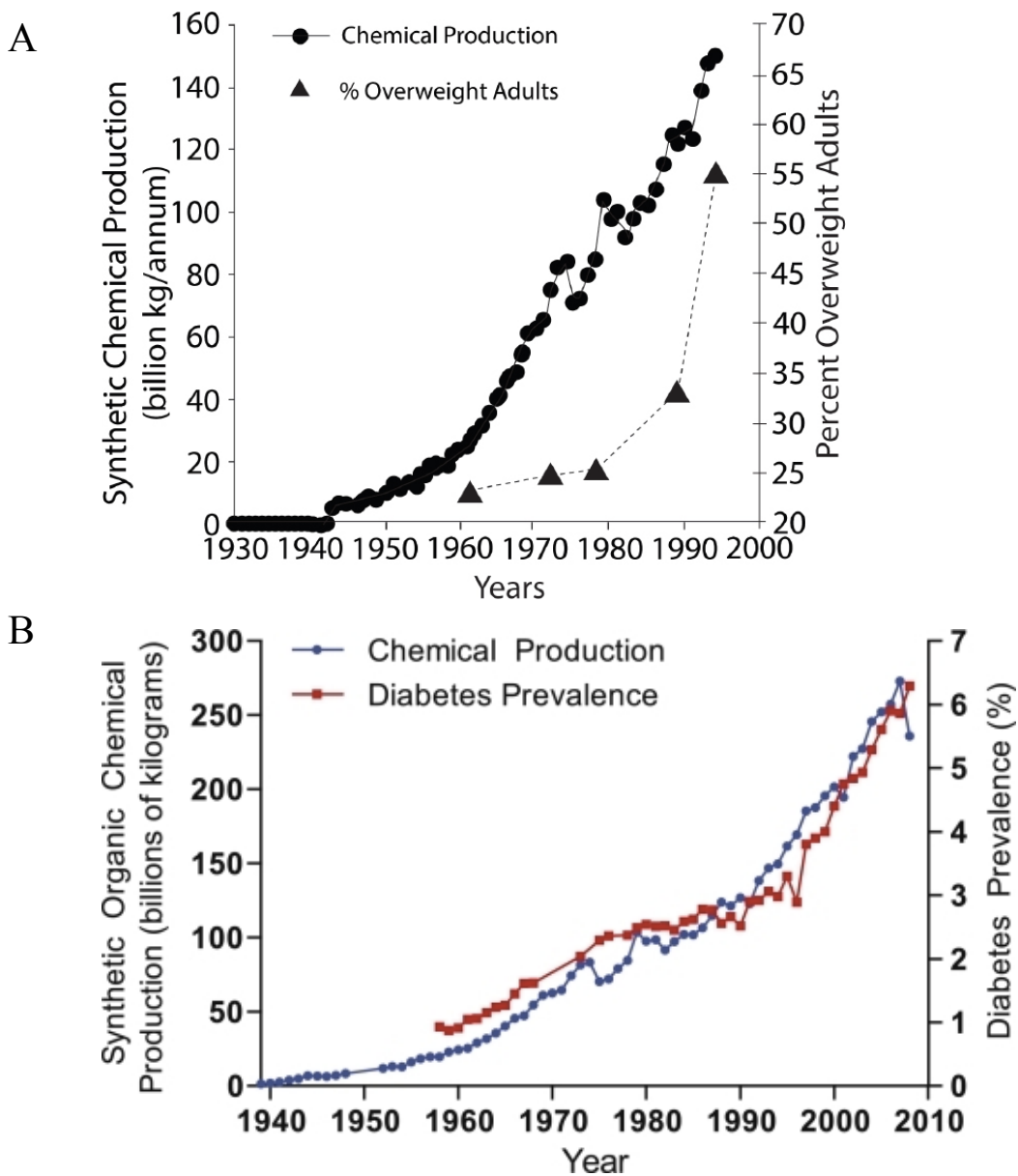


Figure 2. Prevalence of obesity and diabetes in the US correlates with chemical production.

Annual chemical production data was collected from US Tariff Commission reports and Chemical and Engineering News and data for obesity (A) and diabetes (B) incidence were provided by the CDC. Figures were adapted from [66] and [67] for A and B respectively.

Table 1. Literature Review of *In Vivo* Obesogen Experiments

Chemical and Reference	Mouse Strain	[Dose]	Dose Time	Mechanism	End Points	Results
PAH mixture [136]	BALB/cByj – 9wk	7.38-40 ng/m ³ Prenatal	Every day from GD 1/3 – 19-21	?	- Body weight –PND21 – PND 60 - Body lean and fat mass – MRS - histological and morphometric analysis of adipose tissue (number and size) - qPCR of inguinal WAT and BAT – PND 60, PPAR γ , Cox2, CEBP α , FAS, adiponectin - DNA methylation - F2 cohort – same endpoints as F1	- inc. PAH \rightarrow inc. F1 weights - inc. PAH \rightarrow inc. WAT - inc. PAH \rightarrow inc. adipocyte size - inc. PAH \rightarrow dec. PPAR γ promoter methylation in fat
TBTa [94]	C57BL/6J	0.1 mg/kg with 0.5% CMC vehicle Prenatal	Gavage at E16.5	PPAR γ /RXR α	- stem cell differentiation of mADSCs - methylation of Fabp4 promoter	-no indication of sex differences -TBT \rightarrow promotes adipogenic differentiation mADSCs - TBT \rightarrow reduces osteogenic capacity of mADSCs TBT \rightarrow reduces Fabp4 promoter methylation
TBTb [93]	C57BL/6J	5.42, 54.2, 542 nM in 0.5% CMC	7 days before pregnancy and throughout pregnancy	PPAR γ /RXR α	- Adipose Tissue Histology - Adiposity - Liver Histology and gene expression - BM-MSc differentiation and gene expression	-male and female have same response -TBT \rightarrow inc. adipocyte size and number -TBT \rightarrow inc. expression of proadipogenic genes in BM-MSCs -TBT \rightarrow inc. liver lipid accumulation
PFOA [156]	CD1	0.01, 0.1, 0.3, 1, 3 or 5 mg/kg BW	oral gavage once daily from GD 1-17	PPAR	- glucose tolerance test –young (15-16 wk) and old (70-74 wk) - body mass composition (42 wks) - serum adipokine – leptin and insulin (21-33 wk)	-only female analyzed -low PFOA \rightarrow inc. body weight -low PFOA \rightarrow inc. leptin and insulin -low PFOA \rightarrow no change in adiposity
DEHP [157]	129S6 – obesity resistant	0.05 mg/kg Adult	Daily in chow from 10wk-20 wk	PPAR Oxidative stress	- insulin tolerance test – 6wks - glucose tolerance test – 8 wks female - body composition – 10 wks - adipokine and hormone ELISA - metabolics	- DEHP \rightarrow increased body weight - DEHP \rightarrow alters insulin tolerance - DEHP \rightarrow reduced adiponectin and PPAR γ protein levels - DEHP \rightarrow inc. PCs 38:X

					- qPCR – adiponectin, PI3K, Igfr1r, Vamp4	
MEHP [158]	C57BL/6J	0.5, 0.25, 0.05 mg/kg/day	Oral gavage E12 to PND 7	PPAR γ	-8 wks - body weight - adipose and liver tissue weight - blood glucose level - serum cholesterol and TAGs	-only males effected high MEHP \rightarrow inc. body weight, adiposity - high MEHP \rightarrow inc. cholesterol, TAGs, glucose - MEHP \rightarrow PPAR γ adipose gene expression
Triflumazole [159]	CD1	0.1, 1.0, 10 uM in 0.5% CMC	During breeding and throughout pregnancy	PPAR γ	- Adipose Tissue Weight - Adipose MSC qPCR – PPAR γ , ZFP423, Pref-1, FABP4	-only males analyzed - 0.1 TFZ \rightarrow inc. adiposity - TFZ \rightarrow inc. PPAR γ , ZFP423, FABP4 aMSC gene expression
Tolyfluonid [115]	C57BL/6	100ppm in diet Adult	12 wk adult	GR	- ITT – 5 wk and 10 wk - Body composition - Adipokine and metabolites - Adipose qPCR	- effects males only - TF \rightarrow inc. weight gain and adiposity - TF \rightarrow glucose intolerance and insulin resistance - TF \rightarrow impairs adiponectin and leptin signaling
DES – summarized in [160]	CD1	0.001 mg/kg/day	GD 9-16 via subcutaneous injections	ER	- body weight gain - adipose tissue weight	-DES \rightarrow inc. body weight over time (6-14 wks) -DES \rightarrow inc. adipose weight and body fat percentage
BPA [161]	CD1	5, 50, 500, 5000, 50000 ug/kg.day	GD 9-18 daily via micropipetter	ER	- GTT and ITT – 18 wks - adipose tissue number and volume - serum hormones	-only males analyzed - non-monotonic dose response -BPA \rightarrow body weight at certain time points -BPA \rightarrow fat pad weight -BPA \rightarrow impaired glucose tolerance -BPA \rightarrow inc. insulin, leptin and dec. adiponectin

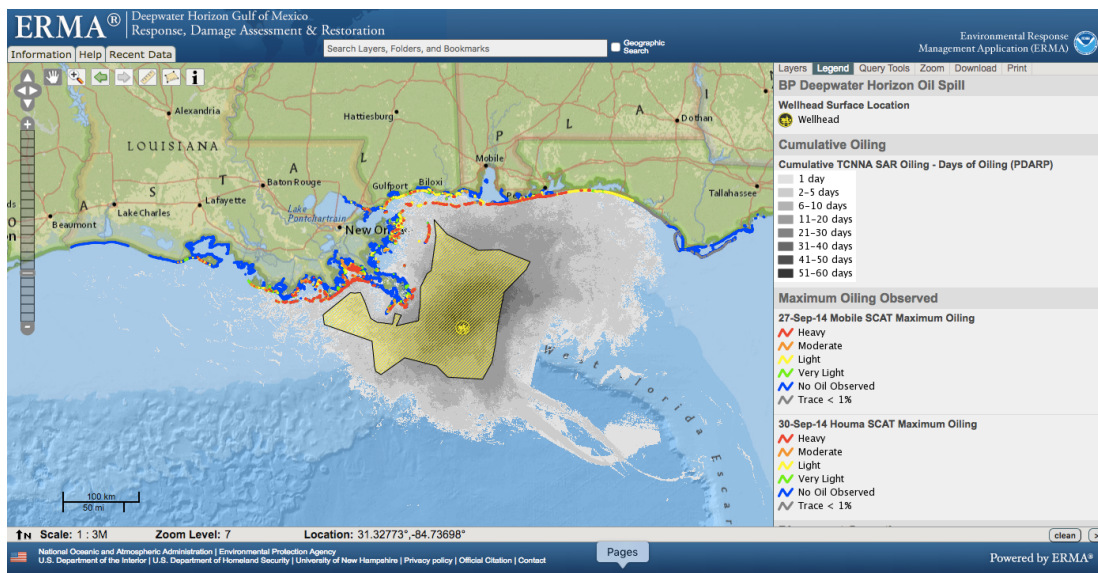


Figure 3. Geographic coverage of oil and dispersant from the Deepwater Horizon Oil Spill.

Data and figure were obtained from the NOAA Emergency Response Management Application. Total oil coverage is represented in grey with overlaid aerial dispersant release in yellow. Oiled shorelines range from no oil observed (blue) to heavily oiled (red). <https://erma.noaa.gov/gulfofmexico/erma.html>

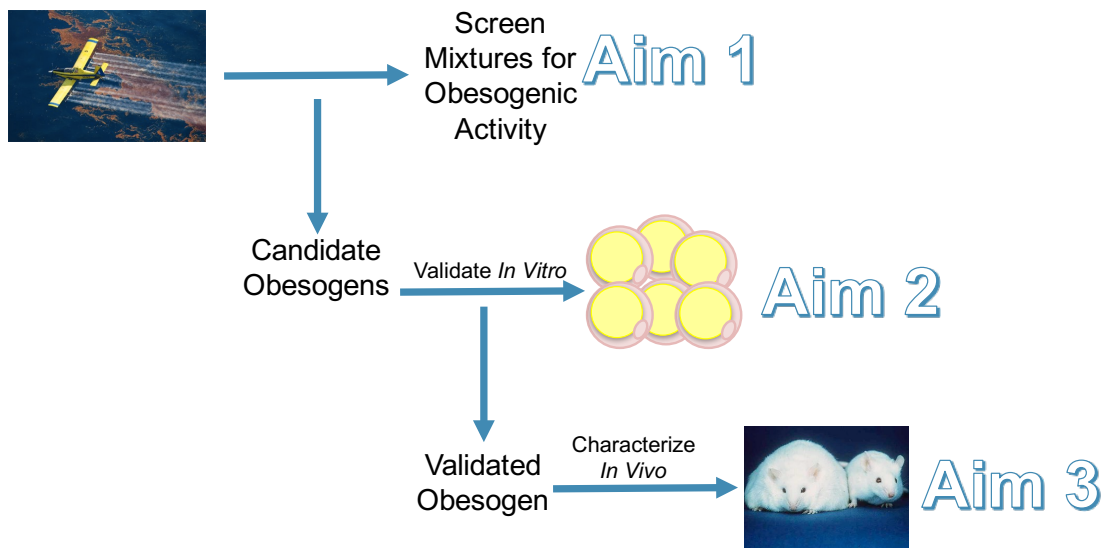


Figure 4. Summary of specific aims and broad approach for dissertation research.

CHAPTER 2: SCREENING MC252 OIL AND COREXIT 9500A DISPERSANT FOR EDCS USING RECEPTOR TRANSACTIVATION ASSAYS

2.1 Introduction

The *Deepwater Horizon* (DWH) oil spill, which began April 20, 2010, resulted in the release of approximately 205 million gallons of MC252 (Mississippi Canyon block 252) crude oil into the Gulf of Mexico, exceeding the Exxon *Valdez* spill by an order of magnitude [125]. Approximately 2.1 million gallons of dispersant was used to dissolve the oil into the water column, presumably aiding in oil biodegradation and preventing the oil from reaching fragile near shore habitats [162]. The dispersant applied by aerial spray and at the wellhead oil source was primarily Corexit 9500 (EC9500, EC9500A and EC9500B) and secondarily Corexit 9527 (Nalco Environmental Solutions, Sugar Land, TX). Since the spill, many studies have focused on the toxicity of crude oil, dispersed oil or dispersant alone in a variety of species and animal models, many of which concluded that dispersed oil to be the most toxic mixture [126, 163, 164]. Contributing to this toxicity, dispersant has been shown to increase the bioavailability of oil components, such as polycyclic aromatic hydrocarbons (PAHs) to fishes [127].

Given the unprecedented use of dispersant during the DWH oil spill and large scale of the spill itself, it was crucial to go beyond acute toxicity testing to carefully evaluate sublethal and potential long-term health effects of oil and dispersant to improve oil remediation safety. Both oil and dispersant, or their components have been implicated as potential endocrine/metabolic disruptors but only a few studies have been performed addressing this question [134, 140, 145, 165]. Similarly, to our knowledge, no studies have looked at the combination of MC252 oil and Corexit 9500 specifically for endocrine disruption.

Endocrine disrupting chemicals (EDCs) have multiple types of mechanism of action. They can prevent or alter synthesis of hormones through interaction with enzymes

in tightly regulated pathways, affect clearance of hormones from the body, and alter epigenetic marks and signaling, such as DNA methylation [166-169]. Arguably, the most well studied mechanism of action is through direct binding and interaction of EDCs with nuclear receptors, the class of receptors that endogenous hormones bind to as ligands. Nuclear receptors are ligand activated receptors that translocate to the nucleus and regulate gene expression once activated, resulting in downstream signaling cascades [170]. EDCs can mimic endogenous ligands leading to unintended activation of receptors or they can block endogenous hormones from binding to receptors causing antagonistic effects [171]. For example, legacy EDCs like DES [172] and PCBs [173, 174] and more recently BPA [175], elicit their adverse reproductive effects via direct interaction with and binding to the estrogen receptor. Additionally, these types of exposures can be more harmful when they occur during vulnerable life stages including developmental and larval stages, which are more sensitive to very low doses (many EDCs have non-monotonic dose response curves) [176].

The objective of this study was to screen MC252 oil, Corexit® 9500A (from here on referred to as Corexit), and water accommodated fractions of dispersed oil for different endocrine disrupting activities using receptor transactivation assays for human estrogen receptor alpha ($ER\alpha$) and beta ($ER\beta$), human progesterone receptor beta ($PR\beta$), human retinoid x receptor alpha ($RXR\alpha$), and mouse peroxisome proliferated receptor gamma ($PPAR\gamma$). It was hypothesized that components of MC252 oil in particular, would contain obesogenic EDCs given previous studies that identified PAHs as $PPAR\gamma/ER\alpha$ agonists and others that found correlations between human and animal prenatal PAH exposure and offspring obesity [136, 137, 177, 178]. Identifying these obesogenic EDCs

and understanding their potential sublethal effects should help predict outcomes of exposures and provide more context for their appropriate use and regulation. Particular emphasis was put on identifying novel obesogenic compounds given the rise of the obesity epidemic and considering that some Corexit components are commonly used as food additives, and in personal care products (multiple exposure sources and routes relevant for human health).

2.2 Materials and Methods

2.2.1 Preparation of Corexit® water accommodated fraction of MC252 crude oil

To distinguish between activity originating from dispersant versus MC252 oil, a suite of water accommodated fractions was prepared using alternative oils, solvents and dispersants. All water accommodated fraction (WAF) mixtures were prepared the same way by vigorously stirring the components at specified ratios overnight followed by 12 hrs of gravity-based separation and aqueous phase collection. All solutions were stored at 4°C in glass vials. Lecithin/Tween 80® (LT) dispersant was prepared as described in Athas et al. (2014) [179]. Briefly, Lecithin, L- α -phosphatidylcholine, (Avanti Polar Lipids) was mixed with Tween 80® (Sigma Aldrich and here on referred to without ®) at a weight ratio of 60/40, respectively and dissolved in ethanol with the total surfactant concentration at 60 wt %. CWAF (Corexit Water Accommodated Fraction) is Corexit 9500 (Nalco Environmental Solutions, LLC), MC252 oil (Louisiana sweet crude oil collected from the Macondo wellhead 08/15/2010 by AECOM) and DMEM/F12 cell culture media mixed 1:20:200 (v/v/v; ratios by volume). LT WAF is LT dispersant, MC252 oil and DMEM/F12 culture media mixed at 1:20:200 (v/v/v). WAF is MC252 oil and DMEM/F12 mixed 1:10. C_MWAF (Corexit Mazola corn oil Water Accommodated

Fraction) is Corexit, Mazola® corn oil and DMEM/F12 mixed 1:20:200 (v/v/v). Corexit only or LT only mixtures are Corexit or Lecithin/Tween 80 dispersant and cell culture media at a ratio of 1:200. DWAF (dimethyl sulfoxide water accommodated fraction) is DMSO, MC252 oil and cell culture media mixed 2:20:200 (v/v/v).

2.2.2 Receptor transactivation and ligand induced activation assays

Estrogen-receptor alpha and beta (ER α and ER β) and progesterone-receptor beta (PR β) plasmids were kindly provided by Dr. Satomi Kohno and Dr. Louis Guillette Jr at the Medical University of South Carolina. PPAR γ and RXR α plasmids were kindly provided by Dr. Bruce Blumberg of UC Irvine. Estrogen receptor and progesterone receptor assays were performed in collaboration with Merry Anderson and Caitlin Sojka respectively, both students in the MUSC Summer Undergraduate Research Program (SURP). For estrogen and progesterone receptor assays, full-length human receptors and their corresponding response element-luciferase reporters were used. For PPAR γ and RXR α assays, a GAL4 (yeast transcription activator protein) DNA binding domain with the receptor ligand binding domain fusion protein and upstream activation sequence (UAS)-luciferase reporter system derived from yeast was used and referred to as ligand induced activation assays.

For all receptor activity based assays, HEK293T/17 cells (ATCC CRL-11268) were maintained in DMEM/F12 (Gibco by Life Technologies; Grand Island, NY) containing 10% fetal bovine serum (ThermoScientific; Waltham, MA), 2 mM glutamax, 100 mM nonessential amino acids and antibiotic/antimycotic. Cells were transfected with Lipofectamine® 2000 according to the manufacturer's protocol (Invitrogen by Life Technologies; Grand Island, NY) and plated in 96-well dishes at a density of 20,000 cells

per well. Each well of cells was transfected with full length receptor (human ER α , ER β , PGR β) or LBD-GAL4 fusion protein vectors (mouse PPAR γ ligand-binding domain [a.a. 163-475] or human RXR α LBD [Glu203-Thr462] with GAL4 DNA-binding domain [amino acids 1-147] [180]), receptor response element luciferase reporter plasmids (4xERE-luc [181], MMTV-luc [182]) or UASx4 TK-luc (contains four copies of the GAL4 Upstream Activating Sequence and the herpes virus thymidine kinase promoter [-105/+51] driving firefly luciferase) and pRL vector (encoding *Renilla* luciferase to control for transfection efficiency) at a ratio of 1:5:0.1 respectively. During transfection, media containing charcoal stripped FBS (ThermoScientific) was used to prevent activation of receptors from serum components. The next morning, media was replaced with fresh charcoal stripped media to remove excess Lipofectamine[®] reagent that could potentially react with test ligands. In the afternoon, triplicate wells of cells were treated as described in serum free or 0.10% FBS conditions, as this was shown to increase assay sensitivity using the RXR α and PPAR γ assays (Figure 2). Cell lysates were harvested after 18 hours (based on assay time optimization shown in Figure 2) of treatment and the Dual-Luciferase[®] Reporter Assay System (Promega; Madison, WI) and a BioTek luminometer were used to measure firefly and *Renilla* luminescence according to the recommendations of the manufacturers. Data are represented as normalized firefly:renilla ratios expressed as fold change over the non-treated control (NTC). For EC50 curves, data are expressed as percent activation normalized to 100% activation for a given receptor by its positive control or endogenous ligand. For positive control hormone ligands, DMSO was used as the vehicle/NTC. For oil/dispersant mixtures, cell culture media was used as the vehicle/NTC.

2.2.3 Solid-Phase Extraction

Solid phase extraction (SPE) protocols and fraction testing in transactivation assays was performed in collaboration with Margaret Magaletta, a student in the MUSC SURP. Fractionation of CWAF was performed to determine that compounds from Corexit and not oil were responsible for the observed PPAR γ activity. Bond Elut® 3 mL silica SPE columns (Agilent Technologies; Santa Clara, CA) and vacuum manifold chambers were employed to fractionate CWAF. Before fractionation, the silica chromatography columns were prewashed with 2 mL of water. Four fractions bearing differential polarities and hydrophobicities were collected using 2 mL of: 50:50 water:ethanol v/v, methanol, dichloromethane, followed by hexanes. For every 75 μ L of CWAF loaded into the column, an additional 100 μ L of water was used to pull the sample through the column, and 2 mL of solvent was used to collect each fraction. Before further testing of fractions the solvents were removed from the fractions by centrifugal vacuum evaporation using a Savant ISS110 SpeedVac Concentrator (Thermo Scientific; Waltham, MA) and resuspended in 10 μ L DMSO per 500 μ L of fraction evaporated.

2.2.4 Chemical analysis of CWAF Sub-fractions using LC-MS/MS

Composition of the CWAF ethanol:water extractable SPE fraction was determined using liquid chromatography (LC) for compound separation followed by detection and identification of compounds using tandem mass spectrometry (MS/MS). For separation of compounds in each SPE fraction, samples were injected onto a heated (50°C) Kinetex C-18 LC column (100 mm x 2.1 mm, 1.7 μ m; Phenomenex, Torrance,

CA) on an Agilent 1100 LC with autosampler. The mobile phases used for separation by LC were (A) milli-Q water with 1.0 M ammonium acetate (pH 6.5, Fisher Scientific) and 0.1% formic acid:water (volume fraction, 98%, ACS grade, EMD Millipore) and (B) 1:1 (v/v) isopropanol:acetonitrile (IPA:ACN; ACS plus, Fisher Scientific; Optima LC/MS grade, Fisher Scientific, respectively) with 1.0 M ammonium acetate (pH 6.5) and 0.1% formic acid:IPA/ACN (volume fraction). After sample injection (5 μ L), the components of CWAF were separated using a flow rate of 200 μ L/min that started at 40 % solvent A (for 5 min) and changed to 20 % A (0 min to 5 min), to 0 % A (5 min to 19 min), back to 40 % A (19 min to 20 min), and equilibrated at 40 % A for 5 min. Chromatographically separated components were detected using an AB Sciex API 4000 triple quadrupole mass spectrometer (equipped with a TurboV electrospray ionization source) operating with Analyst software (v. 1.5.2). Full scan mass spectrometric experiments (scanning m/z 200 to 1200) were performed in both positive and negative polarity mode to identify potential target masses in the ethanol/water fraction. The scan parameters (positive/negative) were: a) scan rate (2 s), b) entrance potential (10/-10 V), c) declustering potential (75/-75 V), d) curtain gas (20 psi), gas 1 (nebulizer gas; 20 psi), gas 2 (heater gas; 20 psi), ion spray voltage (5000/-4500 V), source temperature (500 $^{\circ}$ C) and the on. To further characterize the target masses, product ion scans (MS/MS) were collected (collisionally activated dissociation (4), collision energy (30 eV), cell exit potential (15 V). Upon identification of commonalities in the fragmentation of the target masses, precursor ion scans (PIS) of m/z 307.3, 309.3 and 311.3 (corresponding to fragments of ethyl linoleate, ethyl oleate and ethyl stearate, respectively) were employed to highlight analyte classes that exhibited specific in-source fatty acid fragments commonly associated with Polysorbate (Tween[®])

materials [183]. Noting the recently reported ingredients of Corexit (EPA), tentative identification of two dominant components of the CWAF ethanol/water extract, Polysorbate 80 (Tween 80®) and dioctyl sodium sulfosuccinate (DOSS), was made by comparing the acquired mass spectrometric data to previously published reports [183-187].

2.2.5 Molecular modeling of Corexit components binding to the PPAR γ ligand binding domain

Molecular modeling was assessed using MOE Software (Molecular Operating Environment; Chemical Computing Group; Inc. Montreal, Canada). Two crystal structures from the Protein Data Bank [188] comprising the human PPAR γ ligand binding domain bound to different ligands (4EMA; human PPAR γ in complex with rosiglitazone [189] and 2HFP; crystal structure of PPAR γ with N-sulfonyl-2-indole carboxamide ligands [190]) were compared,. Using MOE's superposition function, no significant differences were observed in the active site of PPAR γ (RMSD < 2Å). Because 4EMA contained our positive control Rosiglitazone (Rosi) it was chosen as the model. Ten compounds (Span 80 full and cleaved, DOSS full and cleaved, Tween 80 full and cleaved, rosiglitazone, propylene glycol, 2-butoxyethanol, and 17 β -estradiol), including some metabolites, were docked to PPAR γ . Molecular parameters were set for maximum energy minimization and Amber12 liquid state. Five compounds that comprise Corexit, a negative control (17 β -estradiol) and a positive control (Rosi) were assessed and virtually synthesized based on liquid state parameters at pH 7.4. The run was set to 30 different poses, with an area for 30 refinements if necessary. After parameters were set, a continuous run of all compounds were docked, and descriptors of binding data were given in ascending order related to E score. The E score gives binding efficiency in terms

of energy state, with lower E scores indicating higher affinity. Compounds that had the capability to be cleaved by esterases were assessed with and without the fatty acid chains.

2.2.6 Statistical analysis

All data analyses were performed using GraphPad Prism software (GraphPad v7 Software Inc.; La Jolla, CA). Prior to statistical analysis, data represented as fold change or percentages were log transformed to meet Gaussian distribution and equal variance conditions for ANOVA analysis. Normality and equal variance was assessed via graphical display and confirmed using the Kolmogorov-Smirnov test and Brown-Forsythe test, respectively. Significantly different values were identified as having P-values < 0.05 using one-way ANOVA with Dunnett's Multiple Comparison post hoc test. Two-way ANOVA was used for multiple comparison analysis with Sidak's or Tukey's test and significant p-value < 0.05. GraphPad Prism software was used to calculate EC50 data using sigmoidal, 4PL curves.

2.3 Results

2.3.1 MC252 oil demonstrates estrogenic activity

Estrogen receptor transactivation assays were optimized and validated using 17- β -estradiol (E2) as a positive control (Figure 1 A and B). EC50s of E2 for ER α and ER β were calculated to be 170pM and 7.6pM, respectively (Figure 1 A and B). The assays were determined to be specific given that the non-estrogenic compound rosiglitazone did not activate the receptor (data not shown).

MC252 oil-Corexit water accommodated fractions (CWAF), Corexit only, LT WAF and LT only mixtures were tested for estrogenic activity using human ER α and ER β receptor transactivation assays (Figure 3). CWAF significantly activated both

receptors at all concentrations tested (6.25, 12.5 and 25 ppm), however ER β showed significantly higher fold induction than ER α at all concentrations (Figure 3A). In fact, ER β activation by 25ppm CWAF reached 100% activity (normalized to 100nM E2) whereas ER α activation by CWAF only reached 13% maximal induction (Figure 3A). To determine if estrogenic activity detected in CWAF was from oil or Corexit, Corexit alone was tested as well as WAF from LT dispersed MC252 oil. Corexit only treatments weakly activated both ER α and ER β approximately 2 fold, suggesting activity observed in CWAF was primarily MC252 oil derived. Additionally, WAFs prepared with Corexit and Mazola corn oil showed no significant estrogenic activity (Figure 3A). LT WAF fractions also significantly activated both ER α and ER β in a dose dependent manner with significant activation at all treatments (Figure 3B). While comparable activation was observed for ER β between CWAF and LT WAF, LT WAF increased ER α activation relative to WAF, suggesting that LT may be contributing estrogenic activity. In fact, when LT alone was interrogated for estrogenic activity, activity was observed for ER α but not ER β . Together these data indicate that MC252 oil has estrogenic activity, with oil components having higher transactivation potential for ER β than ER α and LT components lecithin and/or Tween 80 having higher transactivation potential for ER α .

2.3.2 Corexit may contain progesterone receptor beta antagonist(s)

Progesterone receptor beta transactivation assays were optimized using the endogenous ligand progesterone (P4) (Figure 1C). The EC50 for P4 was determined to be 0.75nM. Additionally, non-progestin compounds like E2 were used in validation as negative controls (data not shown). Antagonist assays were optimized using the known progesterone antagonist RU486 (Figure 4D).

We observed significant decreases in progesterone activation by CWAF and Corexit relative to the non-treated control (Figure 4A). In LT WAF treatments we observed no differences from the NTC and a slight increase in transactivation activity of LT (Figure 4B). These data indicate that Corexit may contain a progesterone antagonist. We tested the most abundant component of Corexit, dioctyl sodium sulfosuccinate (DOSS), and found antagonist activity at 1, 2 and 4 ppm DOSS (Figure 4E). Whether this activity is due to direct antagonism of ligand binding or another mechanism requires further investigation. However, the fact that DOSS at a relatively high concentration of 4 ppm (9 μ M) reduced the activity of 5nM P4 by ~90% (similar to 10nM of the well-characterized and specific antagonist RU486), suggests DOSS has low affinity binding (9 μ M vs 10nM) or causes interference through receptor interaction at a different site.

2.3.3 CWAF and Corexit exhibit RXR α activity.

To set up and validate this system (GAL4/UAS ligand induced activity assay), RXR α reporter transfected HEK293 cells were first treated with negative control ligands estrogen (17- β -estradiol; E2) or the PPAR γ agonist rosiglitazone (Rosi), which did not activate luciferase reporter expression, whereas treatment with the positive control RXR α agonists all-trans-retinoic acid (RA) or tributyltin (TBT) resulted in robust, dose-dependent increases in luciferase levels (Figure 5A).

RXR α reporter transfected HEK293 cells were then treated with CWAF and Corexit, which exhibited dose- dependent RXR α activation (Figure 5B). The demonstration that the RXR α activity of Corexit alone is comparable to or even slightly elevated relative to CWAF suggested that one or more components of Corexit, not crude oil, was primarily responsible for the RXR α activity observed in the CWAF. Similarly,

C_MWAF (that uses Mazola corn oil in place of crude oil) exhibited RXR α activation comparable to that of CWAF or Corexit-only treatments. Additionally, when LT WAF was tested for RXR α activity, significantly reduced activation was observed compared to CWAF (Figure 5C). However, LT WAF did activate RXR α significantly above the NTC at 25 ppm suggesting components of oil do, albeit weakly, activate RXR α . Perhaps LT dispersant makes these compounds more bioavailable to cells than Corexit (Figure 5C). LT dispersant alone showed no significant differences compared to NTC. Collectively, these data suggest that Corexit contains one or more compounds that activate RXR α .

2.3.4 CWAF and Corexit exhibit PPAR γ activity

PPAR γ GAL4/UAS ligand induced activity assays were first validated and optimized with E2 or RA treatment as negative controls, which as anticipated did not increase luciferase activity, and Rosi treatment as a positive control, which did induce marked luciferase activity (Figure 6A). The EC₅₀ for Rosi was calculated to be 5nM (Figure 1E).

To distinguish between PPAR γ activity originating from dispersant versus MC252 crude oil several mixtures of MC252 crude oil, with and without Corexit, were prepared and analyzed for PPAR γ activation including: CWAF, WAF, C_MWAF and Corexit only. Dose-dependent PPAR γ activation was detected in CWAF, C_MWAF, and Corexit dilutions but not in WAF (Figure 6B). The CWAF and C_MWAF fractions comprise an emulsified aqueous-oil fraction of the original mixtures of oil and dispersant and a portion of the amphipathic compounds present in the original mixtures are expected to partition to the organic phase. As the dose-dependent PPAR γ activation by Corexit alone substantially outstripped those of CWAF and C_MWAF, these results suggest that

components of Corexit were responsible for the activity detected. To further rule out oil as a primary contributor to the PPAR γ activity in the fractions, two alternate solvents were used to prepare water-accommodated fractions, which lack Corexit, DMSO and LT dispersant. Although twice the amount of DMSO was used to prepare DWAF than Corexit used in preparing CWAF and C_MWAF, no PPAR γ activity was observed in any DWAF dilutions tested (data not shown) further implicating a Corexit ingredient and not a component of oil. Similarly, we observed significantly reduced PPAR γ activation of LT WAF compared to CWAF and no differences between LT only and NTC (Figure 6C). Albeit, we did observe weak but significant activation of PPAR γ by 12.5 ppm and 25 ppm LT WAF (Figure 6C).

2.3.5 CWAF fractionation and analysis

To further investigate CWAF activation of PPAR γ , SPE was employed to fractionate CWAF based on polarity and hydrophobicity; CWAF was fractionated into 50:50 water:ethanol, methanol, DCM and hexane soluble fractions. Substantial PPAR γ activation was detected in the 50:50 water:ethanol fraction, whereas no activity was detected in the other fractions (Figure 7).

Initial mass spectrometric experiments using LC-MS and LC-MS/MS were performed to identify major components in the CWAF ethanol/water sub-fraction. The approach first focused on analyzing the sub-fraction in positive full scan mode, which resulted in the selection of over 200 unique target masses. A representative total ion chromatogram is shown in Figure 8A. Manual inspection of the chromatogram revealed several unique mass profiles with mass differences (between adjacent ions) of 22 and 44 amu, reported to be $[M+NH_4]^+$ and $[M+2NH_4]^{2+}$ ions of polysorbate species [187].

Product ion scans (PISs) showed that the m/z 309.3 ion was the most frequent top fragment for the target masses (present in almost 50% of the product ion spectra). Previous reports attributed the m/z 309 fragment ion to an in-source loss of specific fatty acid esters (ethyl oleate, for m/z 309.3) characteristic of polysorbate species [183], or more recently to a strong presence of oleate-related species in Tween 80® [187]. PIS scan of m/z 309.3 demonstrated several mass spectral profiles relating to sorbitan monooleates (specifically 16 – 27 polyoxyethylene units, as shown in inset B; Figure 8), isosorbide monooleates, and sorbitan dioleates, indicating the presence of Tween 80. The PIS approach was also able to identify other fatty acid esters, including trace ethyl stearate (PIS m/z 311.3) and ethyl linoleate (PIS m/z 307.3) species. Thus, this highly abundant component is likely Tween 80.

Analyzing the sub-fraction in negative full scan mode produced the other highly abundant component of the CWF ethanol/water sub-fraction, namely DOSS. Initial investigation revealed an intense ion at m/z 421. A total ion chromatogram performed in negative FS mode is shown in Figure 8C with the peak at 2.45 min largely representing the $[M-H]^-$ ion of DOSS. To confirm the presence of DOSS, a PIS of m/z 421.1 was performed and the resultant fragmentation profile is shown in inset D of Figure 8. Based on previous reports, which indicate the presence of fragment ions m/z 81 and m/z 227 [185, 186], it was confirmed that DOSS was abundantly present in the ethanol/water sub-fraction

Collectively, these transactivation assays and mass spectrometry analyses of the active fraction of CWF argued that relatively hydrophilic components of Corexit and not MC252 oil were responsible for the observed PPAR γ activity.

2.3.6 Modeling of Corexit components: PPAR γ binding prediction

Since Corexit is a complex mixture of solvents and surfactants, molecular modeling was employed, in conjunction with the LC MS/MS results described in Section 2.3.5, to aid in predicting which components could function as ligands for PPAR γ . Span 80, Tween 80 and DOSS were predicted to bind to the PPAR γ ligand-binding domain as shown by their low E scores whereas propylene glycol and 2-butoxyethanol were not (Figure 9A). Span 80 and Tween 80 have an ester bond that could be cleaved by cellular esterases and, once cleaved, neither cleavage product is predicted to bind tightly (Figure 9A). For DOSS docking, the basic lysine 367 residue has a strong hydrogen bond with the sulfonyl oxygen (Figure 9B). The α -carbon adjacent to the sulfonyl group of DOSS shows potential for strong donation to a hydrogen of Methionine 364, which is slightly exposed. PPAR γ has multiple basic residues that allow a great pairing with the acidic sulfhydryl group of DOSS, thus increasing the efficacy of H-bonding between the ligand and receptor. Tween-80 along with other compounds that exhibit low E scores, either have too large a fatty acid group to effectively fit and bind into the binding site of PPAR γ or have a charge that is too basic, and reject acid-base chemistry; therefore, they have higher binding scores (Figure 8B).

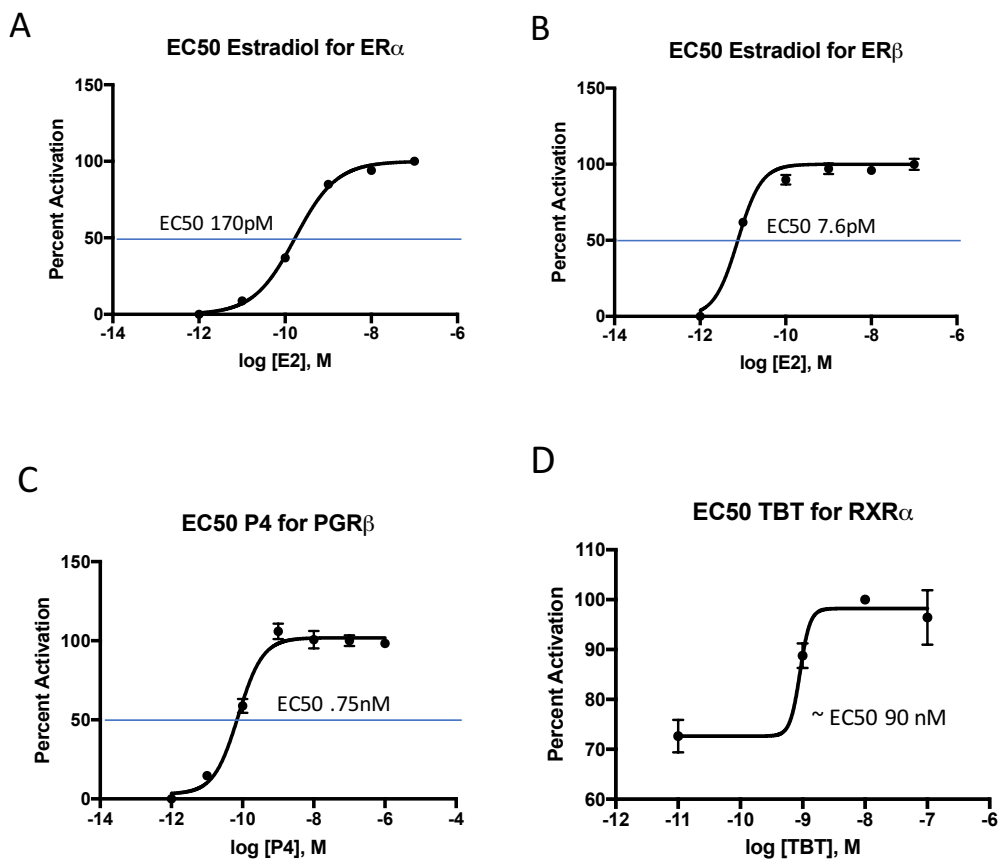


Figure 1. Receptor transactivation assay validation by positive control dose response curves.

HEK293/T17 cells were transfected with receptor and reporter ligands as indicated in methods and treated with positive control ligands for 18 hours in serum free media. EC50 values were calculated for positive control ligands for each receptor transactivation assay used including A) ER α by 17-b-estradiol, B) ER β by 17-b-estradiol, C) PR β by progesterone (P4), D) RXR α by tributyltin (TBT), and E) PPAR γ by Rosi).

EC50 values were calculated using GraphPad Prism using Sigmoidal, 4PL non-linear regression curves.

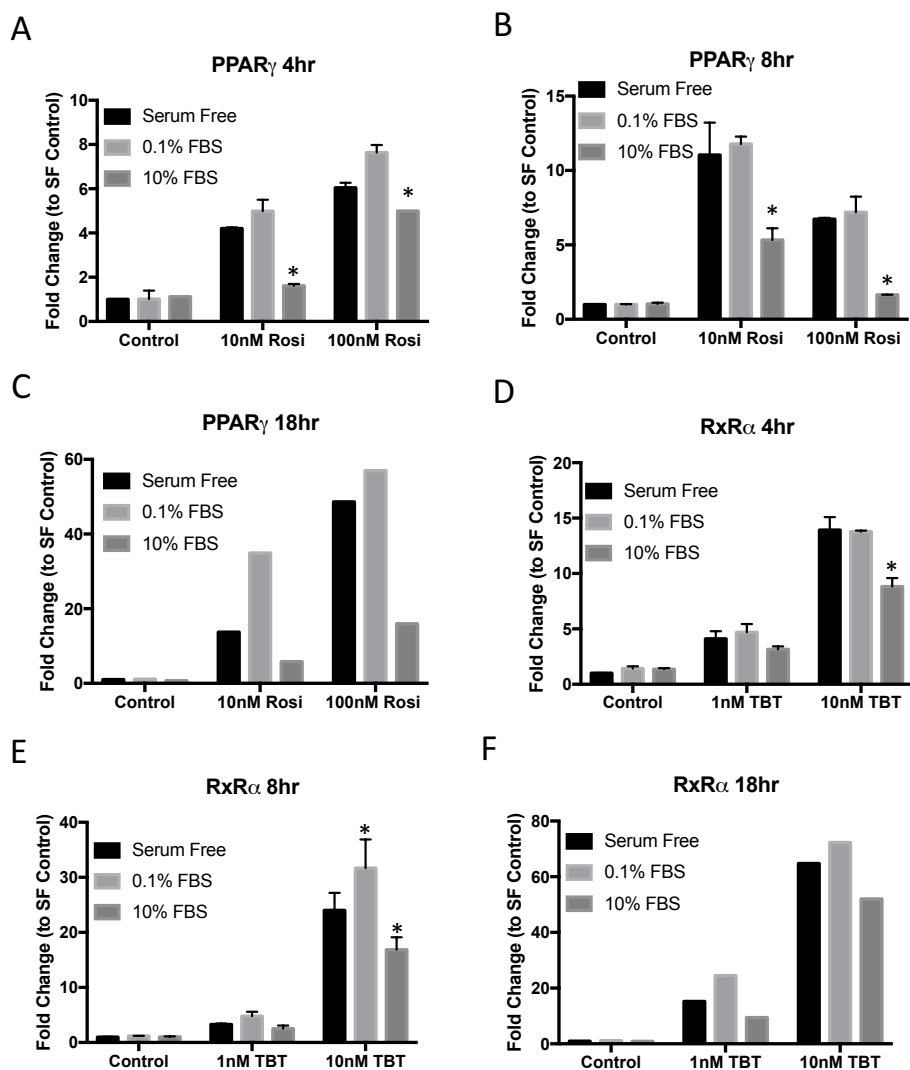


Figure 2. PPAR γ and RXR α activity in a GAL4-UAS system using serum-free conditions.

HEK293T/17 cells were transfected and exposed to the PPAR γ agonist Rosi or RXR α agonist TBT under serum-containing (10% FBS and 0.1% FBS) and serum-free (SF) conditions in triplicate and luciferase activities were measured following exposure for: A) and D) 4 h, B) and E) 8 hr and C) and F) 18 h. Data are normalized to the serum free control in each time point. As shown, assay sensitivity is greatly enhanced under SF or 0.1% FBS conditions. Data are expressed as Mean \pm SD; n = 1-3 per group (* p < 0.05 versus serum free for each treatment group).

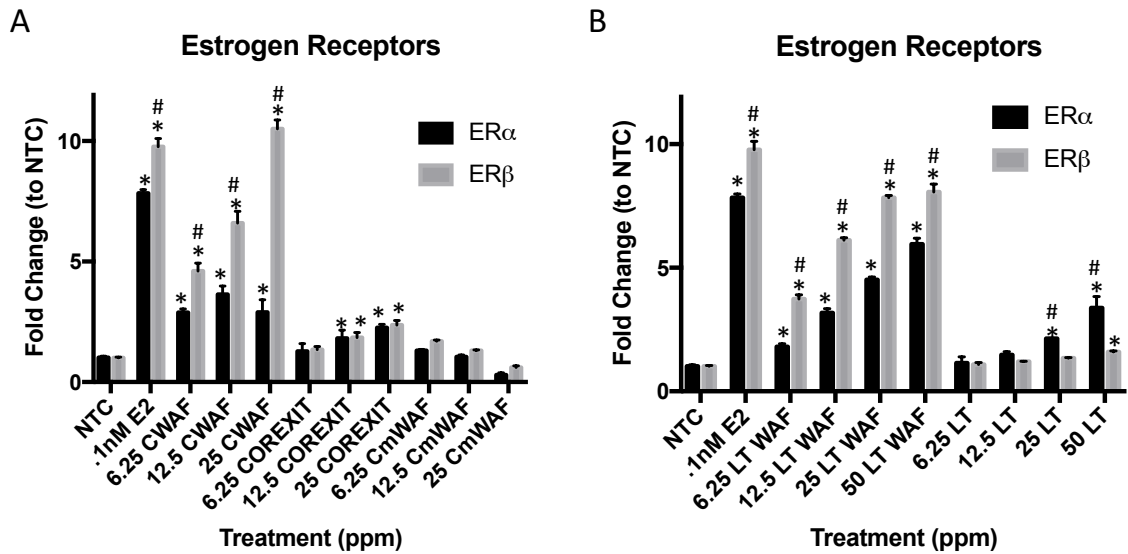


Figure 3. Activation of estrogen receptors alpha and beta by components of MC252 oil, Corexit and lecithin/tween 80 dispersant.

HEK293T/17 cells were transfected with full length human estrogen receptor alpha or beta, estrogen response element luciferase reporter and *Renilla* luciferase transfection control. Cells were exposed A) C-WAF, Corexit and CmWAF and B) LT WAF and LT. Data are expressed as fold change normalized to the non treated/vehicle control. Data were analyzed using two-way ANOVA analysis * $p < 0.05$ compared to NTC, # $p < 0.05$ between receptors for a given treatment.

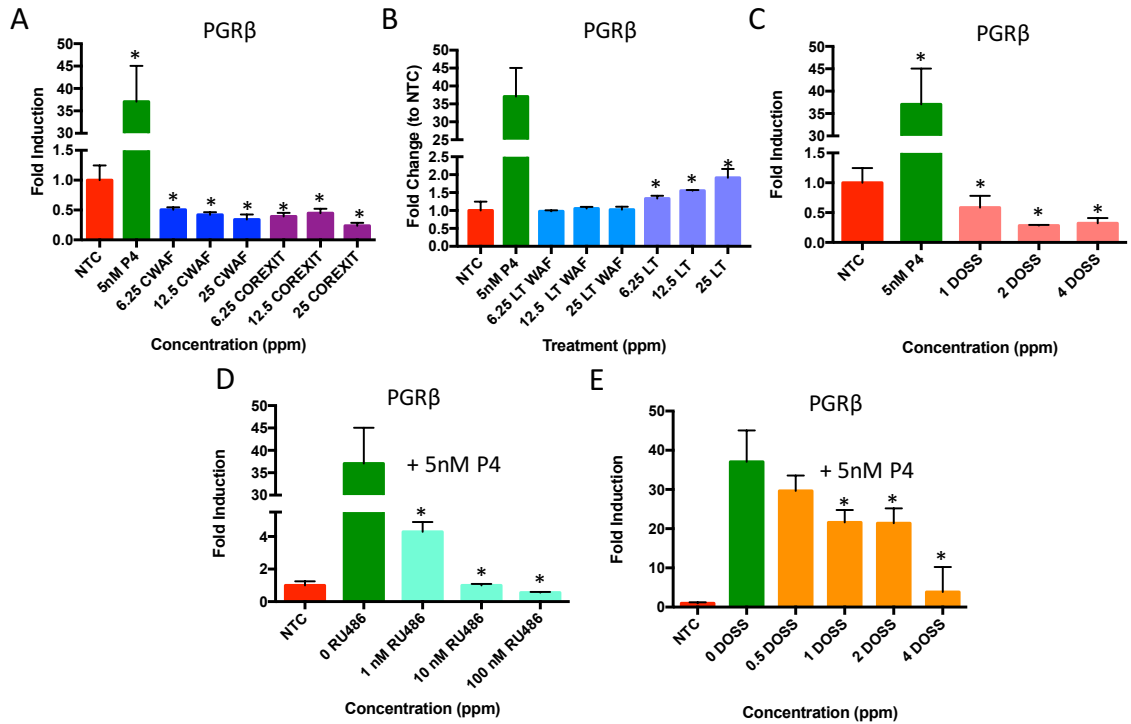


Figure 4. Potential antagonist activity of progesterone receptor beta by components of Corexit.

HEK293T/17 cells were transfected with full length human progesterone receptor beta, MMTV promoter luciferase reporter and *Renilla* luciferase transfection control. Cells were exposed A) CWAF and Corexit, B) LT WAF and LT, C) DOSS, D) 5nM P4 with 0, 1, 10, or 100nM of the antagonist RU486, and E) 5nM P4 with 0, 0.5, 1, 2, 4, ppm DOSS. Data are expressed as fold changed normalized to the non-treated/vehicle control. Data were analyzed using one-way ANOVA analysis $*=p<0.05$ compared to NTC (A-C) or 5nM P4 (D-E).

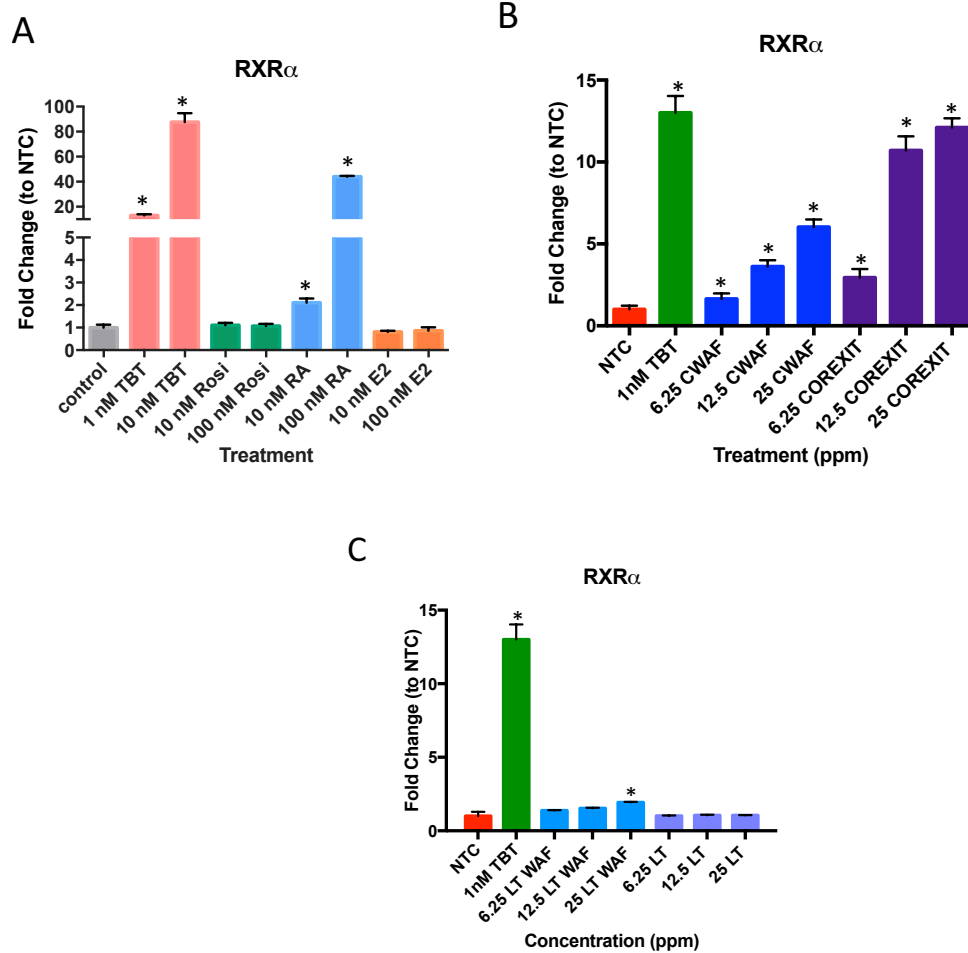


Figure 5. RXR α transactivation activity of the Corexit water accommodated fraction of MC252 crude oil (CWF), Corexit, the Lecithin/Tween 80 water accommodated fraction of MC252 Oil (LT WAF) and Lecithin/Tween80 (LT).

HEK293T/17 cells were transfected with vectors encoding the RXR α ligand binding domain – GAL4 DNA binding domain fusion protein and luciferase reporter constructs and exposed to A) positive and negative control ligands, B) 6.25, 12.5 or 25 ppm (vol/vol) CWF, Corexit and C) LT WAF or LT and luciferase activity was quantified as described in *Methods*. Data are expressed in Firefly luminescence normalized to Renilla luminescence as fold change over NTC: (* $p < 0.05$ versus control; error bars represent Mean \pm SD).

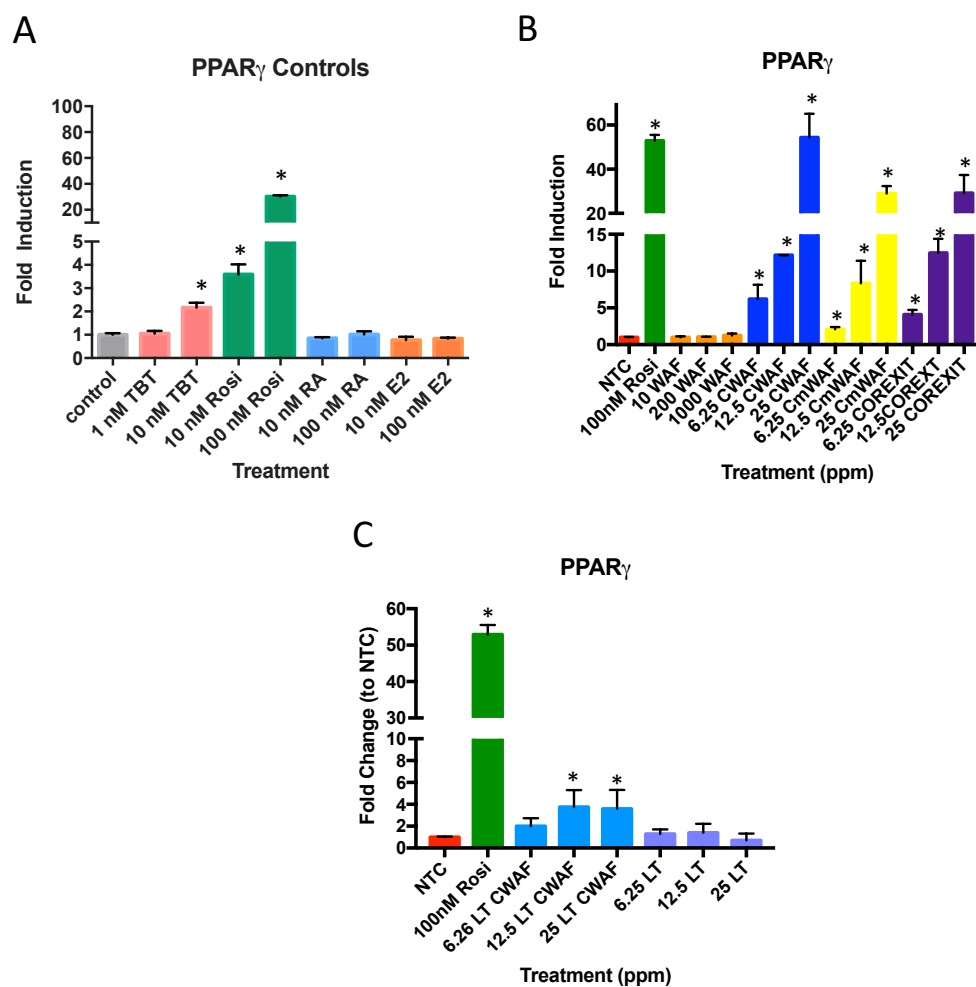


Figure 6. PPAR γ transactivation activity of the Corexit water accommodated fraction of MC252 crude oil (CWF), Corexit, the Lecithin/Tween80 water accommodated fraction of MC252 Oil (LT WAF) and Lecithin/Tween80 (LT).

HEK293T/17 cells were transfected with vectors encoding the PPAR γ ligand binding domain – GAL4 DNA binding domain fusion protein and luciferase reporter constructs and exposed to A) positive and negative control ligands, B) WAF, CWF, CmWAF, Corexit and C) LT WAF or LT and luciferase activity was quantified as described in *Methods*. Data are expressed in Firefly luminescence normalized to Renilla luminescence as fold change over NTC: (* $p < 0.05$ versus control; error bars represent Mean \pm SD).

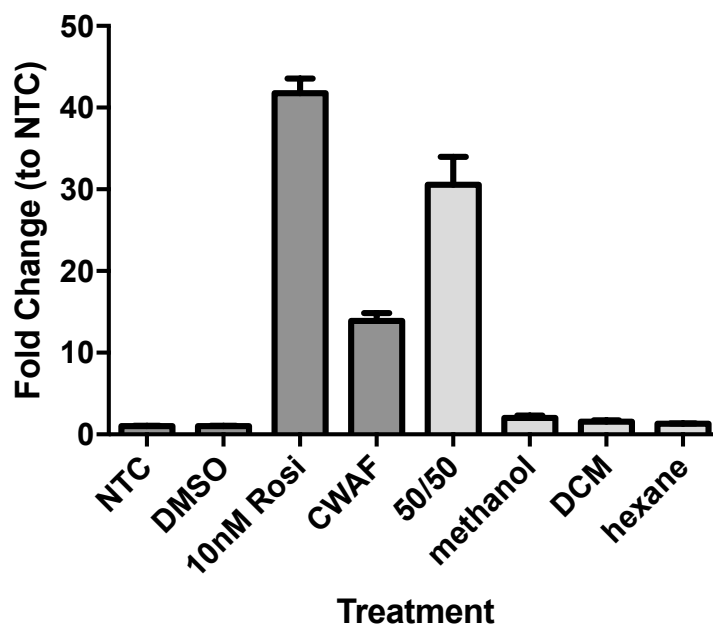


Figure 7. PPAR γ transactivation by the 50/50 ethanol:water CWAF volume fraction.

CWAF mixtures were fractionated using solid phase extraction methods and four solvent types to identify fractions containing PPAR γ activity. PPAR γ activity was observed only in the 50:50 ethanol:water volume fraction but not for methanol, DCM or hexane fractions. Data are expressed as Mean \pm SD; n = 3 per group (* p < 0.05 versus no treatment control).

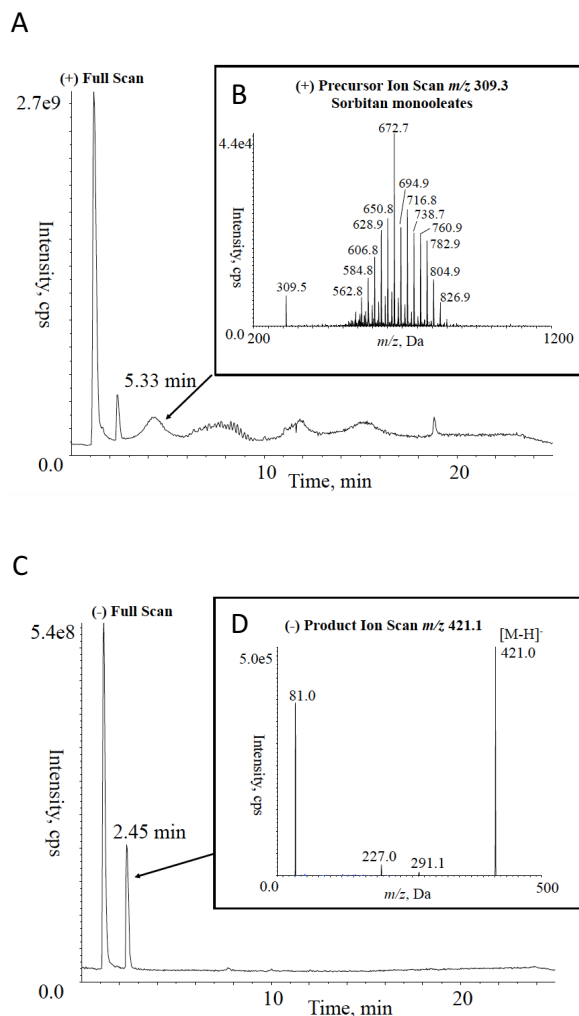


Figure 8. Tween 80 and DOSS are present in the 50/50 ethanol:water fraction.

A) Total ion chromatogram in full scan positive mode of the CWF ethanol/water SPE extractable fraction. B) corresponding to peak at 5.33 min, displays a positive mode precursor ion scan of m/z 309.3 that produces a mass spectral pattern (sorbitan monooleates with 16 – 27 polyoxyethylene units) present in Tween 80. C) Total ion chromatogram in full scan negative mode of the CWF ethanol/water SPE extractable fraction. D) Corresponding to peak at 2.45 min, displays a product ion scan for m/z 421.0. Examining the fragmentation profile, noting the fragment ion m/z 81.0, indicates the presence of DOSS.

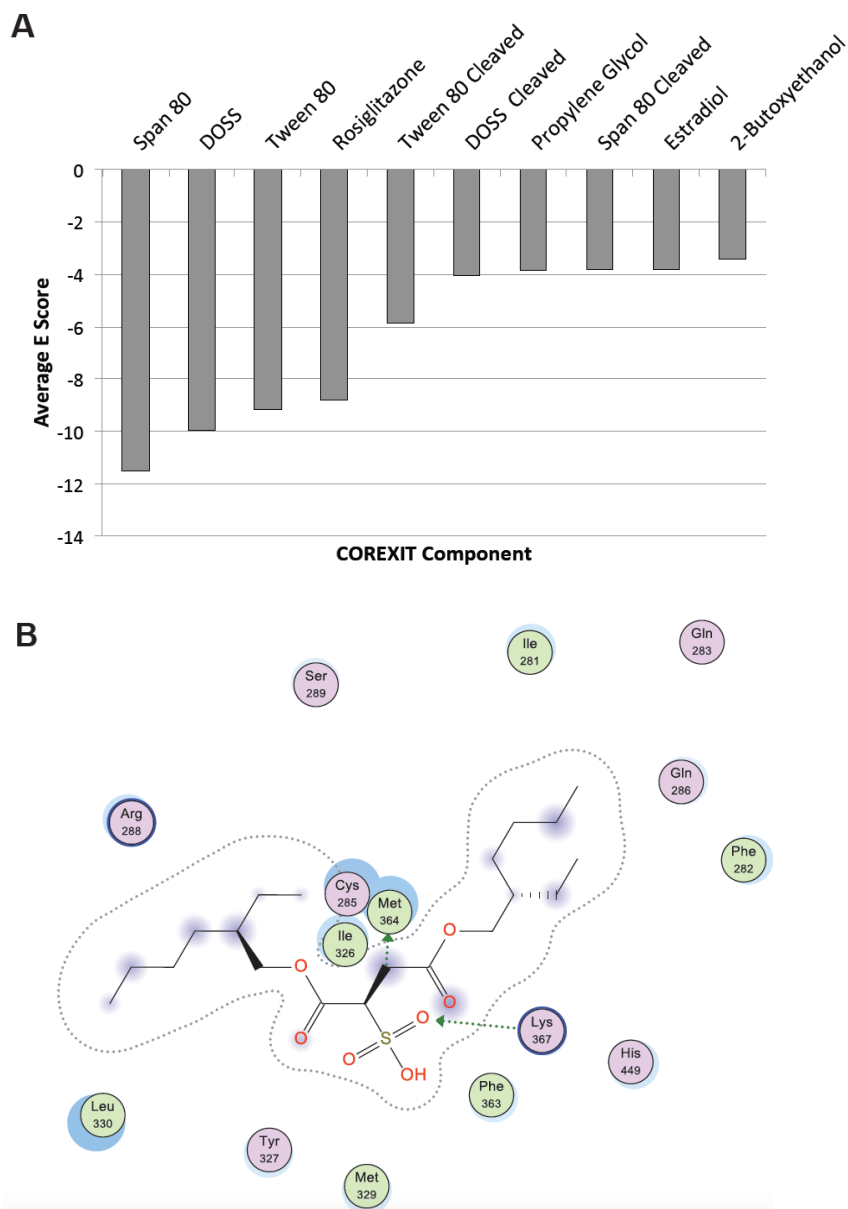


Figure 9. Molecular modeling suggests that Span 80, Tween 80 and dioctyl sodium sulfosuccinate (DOSS) components of Corexit have predicted PPAR γ ligand binding activity.

A) Average E Score for COREXIT components analyzed for PPAR γ ligand binding using MOE as in *Materials and Methods*. B) DOSS modeled in the PPAR γ ligand binding pocket.

2.4. Discussion

The work described in this chapter utilized mixtures of MC252 oil and Corexit dispersant to test the hypothesis that components of MC252 oil would contain endocrine disrupting activities as measured by PPAR γ receptor and other nuclear receptor transactivation assays. Here we provide evidence that the complex mixture of MC252 oil (derived from the DWH source) and Corexit 9500 dispersant can activate several nuclear receptors. Contrary to our hypothesis, the data indicate that components of Corexit, not MC252 oil, primarily activate PPAR γ and RXR α , and thereby identify Corexit components as potentially obesogenic. This was accomplished using a series of dispersant-solvent-oil mixtures to determine where the origin of specific activities was derived. This type of effects-based method can be used in the future when screening oil and dispersant mixtures and other matrices for endocrine disruption activities. Additionally, this can help inform the safety of dispersant used during oil spill remediation through consideration of multiple endpoints together with available toxicity data.

Our results for estrogen receptor transactivation assays are consistent with published studies on the estrogenic activity of oil discussed as follows. Collectively, it appears that the components of oil are primarily estrogenic, and that they transactivate ER β more strongly than ER α (Figure 2 and ref [165]). The implications of this result are less well understood than results on ER α agonists, and warrant further investigation. Rodent models suggest exposure to petroleum products and PAHs can induce reproductive toxicity and disease and obesity via ER α [134-136]. Additionally, the type and origin of oil have been shown to result in varied responses[139]. Williams, et al.,

studied the estrogenic effects of MC252-derived CWAF and estrogen receptor sequences of the American Alligator (*Alligator mississippiensis*) and similarly found that the ER β isoform to be more sensitive than ER α [191]. Although we did not interrogate the anti-estrogenic activity in MC252 oil and Corexit, others have identified this response in WAFs prepared from other oil types [138].

We also observed low but significant estrogenic activity in Corexit, which was not observed by others [140]. Thesis research by McNabb et al. (College of Charleston) studied the estrogenic activity of Corexit in the American Alligator and found no functional estrogenic effect as measured by male to female sex reversal after treatment during development and analysis of gene expression markers indicative of estrogen exposure indicated the observed weak estrogenic activity of Corexit may not be biological relevant [192]. Estrogenic activity was also observed in an alternative, food-grade dispersant (composed of lecithin and Tween 80). This is consistent with others who have tested lecithin for its estrogenic activity, given that it is a common food additive, and found it to be strongly estrogenic [193].

To my knowledge this is the first investigation into the progestin and anti-progestin effects of oil and dispersants. Here we identify potential anti-progestin effects of DOSS, a component of Corexit, but also a common stool softener taken by pregnant women. Given that anti-progestins, such as RU486, are pharmaceuticals used to terminate pregnancies [194], it may be of critical importance to further study the effects of DOSS on pregnancy and progesterone receptor signaling at the doses and frequencies taken. Initial studies of women taking DOSS during pregnancy have not report increased

rates of preterm births, although these studies primarily focused on identifying risk for birth defects and malformations associated with DOSS use [151, 152].

RXR α forms a heterodimeric complex with PPAR γ and many other nuclear hormone receptors to regulate gene expression [195]. Therefore, identifying compounds that activate RXR α might be important in several pathways. The PPAR γ pathway in particular is of interest as a master regulator of adipogenesis and fat metabolism [196]. Environmental chemicals that interact with the RXR α and PPAR γ receptors have been labeled as environmental ‘obesogens’ since they can lead to increases in adipogenesis, fat accumulation and overall metabolic disruption in vivo [92]. TBT is a well-studied obesogen that activates both RXR α and PPAR γ [94, 197]. Here we demonstrated both RXR α and PPAR γ transactivation activity by Corexit dispersants, suggesting Corexit exposure may lead to obesogenic effects by multiple pathways. Although we tested mammalian receptors in this study, there is high conservation among the nuclear hormone receptor super family among vertebrates and invertebrates, as well [198, 199]. It has been shown that environmental obesogens can alter lipid homeostasis in *Daphnia* [200] and piscine hepatocytes [201]. These results indicate the relevance and unintended yet widespread potential consequences of oil spill clean-up efforts, including marine organisms and humans exposed to Corexit during the DWH spill. Therefore, identifying specific compounds in Corexit that activate RXR α and PPAR γ is a worthwhile endeavor to pursue.

To help narrow the search *in silico* modeling was used to assist with prediction of compounds in Corexit that exhibit potential RXR α and PPAR γ binding. *In silico* modeling revealed Span 80, Tween 80 and DOSS as potential PPAR γ ligands. Given that

DOSS and Tween 80 were detected in the 50:50 water:ethanol fraction of CWAF, these data are consistent with the concept that one of these two compounds (or both) may bind PPAR γ . The fatty acid moiety of Tween 80 is oleic acid. While fatty acids are endogenous ligands of PPAR γ , oleic acid shows weak affinity for PPAR γ and the large hydrophobic head of Tween 80 would likely interfere with binding [104]. On the other hand, DOSS contains a methyl branched hydrocarbon chain similar to that observed in the chemical structure of MEHP and MiNP, the metabolites of the phthalate esters DEHP and DiNP respectively, both of which are EDCs known to activate PPAR γ [202]. This suggests DOSS is the more likely PPAR γ agonist.

The ability of Corexit components to interact with the PPAR γ receptor, *in silico* modeling prediction of DOSS as a PPAR γ ligand and the presence of DOSS in fractions of CWAF that activate PPAR γ , all indicate that additional studies to validate the hypothesis that DOSS is a PPAR γ ligand and obesogen are requisite. More focused aspects of this hypothesis are therefore explored in the subsequent two chapters.

CHAPTER 3: VALIDATION OF DOSS, A COMPONENT OF THE DISPERSANT COREXIT 9500A, AS A PROBABLE OBESOGEN *IN VITRO*

3.1 Introduction

The past three decades have witnessed a remarkable increase in the prevalence of obesity, a condition which contributes to the development of several chronic medical problems including type II diabetes, hypertension, cardiovascular and neurological diseases and several cancers [203-205]. While an imbalance in caloric intake and expenditure is the root cause of obesity, body weight regulation is a complex process involving interactions between genetics, behavior, diet and other environmental factors [206]. Increased industrial production of chemicals and increased consumption of processed foods containing food additives have coincided with increases in obesity rates [66, 207]. In addition, emulsifiers that are widely used in processed foods have been shown to induce inflammation, obesity and metabolic syndrome in mice [208]. Interestingly, domesticated animals living within proximity to humans and industrialized areas also demonstrate increased weight gain over the last several decades [70].

Mounting evidence suggests that endocrine disrupting chemicals (EDCs) termed "obesogens" may contribute to the development of obesity by driving fat cell differentiation from multipotent progenitors (adipogenesis), reducing metabolism or increasing appetite [206, 209]. PPAR γ , along with members of the C/EBP family of transcription factors are master transcriptional regulators of adipogenesis [103]. PPAR γ functions as a heterodimer with RXR α in this process [98, 210]. Bone-marrow derived stem cells and adipose derived stem cells are the progenitor cell types for fully differentiated adipocytes *in vitro* and *in vivo* [211-213]. PPAR γ is a member of the nuclear receptor super family, a ligand activated transcription factor which binds to

PPAR response elements (PPRE) regulating insulin sensitization, energy homeostasis and metabolic disease [108]. Endogenous ligands for PPAR γ , and RXR α , have been identified and include fatty acids (e.g., arachidonic acid [104]) and arachidonic acid-derived eicosanoids (e.g., 9-hydroxyoctadecadienoic acid and 15-deoxy-delta 12, 14-prostaglandin J2 [180, 214]).

Obesogens also can function as ligands of this pathway, activating PPAR γ or RXR α or both. The extensively well characterized obesogen, tributyltin (TBT), is an organotin compound that was used as a biocide in anti-fouling marine paint prior to being banned in all sites other than those known as “convenient ports of call” [92]. TBT acts as an agonist for the nuclear receptors PPAR γ and RXR α and increases adipocyte differentiation [94, 197, 215]. Other PPAR γ agonists that have been investigated as obesogens include phthalate metabolite monoesters [202, 216], perfluorinated chemicals [217], some pesticides [159], and flame retardants [218]. Two anionic sulfonyle surfactants, SDS and SDBS have also been identified as PPAR γ ligands and to increase adipogenesis in preadipocyte cell lines [219].

In Chapter 2, the endocrine disrupting and obesogenic potential of DWH oil and Corexit 9500A dispersant was investigated using nuclear receptor transactivation assays. Through that investigation and analysis, it was determined that Corexit is likely to contain obesogenic compounds, as PPAR γ and RXR α activity was observed in mixtures containing Corexit. DOSS is hypothesized to be the most likely component to activate PPAR γ based on *in silico* and LC MS/MS analysis of CWF and fractionated CWF. The primary objective of this current study was to test this hypothesis by validating DOSS as a PPAR γ activator and describing the functional role of DOSS as an obesogen

in vitro. Additionally, RXR α ligands present in Corexit were investigated to determine the obesogenic potential of Corexit as a whole. Lastly, oleic acid was investigated for PPAR γ and RXR α activity since it is a dietary fatty acid that shares structural similarity with the Corexit components Span80 and Tween80.

3.2. Materials and Methods

3.2.1 Cell viability assays

AlamarBlue® cell viability reagent was used for the viability assay. The cell's ability to reduce resazurin (active ingredient in AlamarBlue®) was measured as fluorescence with excitation wavelength at 530 nm and emission wavelength at 590 nm using a TYPHOON scanner or BioTek Luminometer. Cells were treated with indicated test compounds for 18 hours and data was normalized to the non-treated control (NTC) representing 100% viability. Wells with no cells were used as a background control. *Renilla* luciferase expression was also used as a viability marker. Cells were transfected with the *Renilla* PRL (constitutive expression) plasmid in a solution using Lipofectamine® 2000 (Invitrogen) according to the manufacturer's guidelines and described in Section 2.2.1. The day after transfection cells were exposed to various dilutions of DOSS for 18hrs in serum free conditions. Luciferase was quantified using the Promega Dual Luciferase kit (Promega), and BioTek Luminometer. Data were normalized to the NTC as 100% and compared to results obtained from Alamar Blue assay (Figure 1A).

3.2.2. Receptor transactivation and ligand-induced activation assays

PPAR γ and RXR α GAL4/UAS ligand-induced activation assays were performed as described in Chapter 2. For transactivation assays employing native RXR α , a vector

encoding full-length human RXR α and a vector employing the RXR α binding element from the ApoA1 gene driving firefly luciferase expression were used with pRL in a ratio of 1:5:0.1, respectively [214]. These vectors were kindly provided by B. Blumberg; UC Irvine. Additionally, GAL4/UAS ligand-induced activation assays using human PPAR γ , PPAR α and PPAR β/δ LBD-GAL4 fusion receptors were also performed as described in section 2.2 using Lipofectamine 2000 (Invitrogen) according to the manufacturer's instructions. These additional plasmids were kindly donated by Dr. Barbara Abbott, EPA as described in Bility et al 2004 [202]. Interrogated ligands included Corexit components petroleum distillates (ICP; CAS 64742-47-8), propylene glycol (PG), dioctyl sodium sulfosuccinate (DOSS), Span80 and Tween80 (Sigma Aldrich), the PPAR γ agonist Rosiglitazone (Rosi), the PPAR γ inhibitor T007907, and Wy14643 the PPAR α agonist (Cayman Chemical).

3.2.3. TR-FRET RXR α and PPAR γ binding Assays

For time-resolved fluorescence resonance energy transfer (TR-FRET) based assays, SelectScreen[®] Biochemical Nuclear Receptor profiling was employed (Life Technologies). Specifically, the LanthaScreen[®] TR-FRET coactivator protocol was used for RXR α . Briefly, a GST-tagged ligand binding domain (LBD) of RXR α was incubated with terbium labeled anti-GST antibody (excitation/emission 340/495 nm), test ligands, and a fluorescein labeled coactivator peptide (excitation/emission 495/520). A TR-FRET ratio of 520:495 was calculated to determine percent ligand binding and coactivator recruitment since energy transfer from the terbium labeled LBD to the fluorescein coactivator can occur when the two are in close proximity to one another. The LanthaScreen[®] TR-FRET competitive binding assay was used for PPAR γ . Briefly, a

terbium labeled GST-tagged PPAR γ LBD domain (excitation/emission 340/495 nm) was incubated with test ligands and a fluorescein labeled tracer ligand (excitation/emission 495/520). Loss of FRET signal between the antibody and tracer indicates displacement of high affinity labeled ligand by the test ligands since the complex is no longer intact and energy transfer cannot occur.

3.2.4. 3T3 L1 adipocyte differentiation assays

For triacylglycerol staining assays to quantify adipogenic differentiation 3T3 L1 preadipocyte cells (Zenbio; Research Triangle Park, NC) were plated in 48-well plates at a density of 10,000 cells per well in Preadipocyte Growth Medium (PGM); DMEM (Gibco by Life Technologies) supplemented with 10% Hyclone Defined fetal bovine serum (ThermoScientific), 2mM glutamax, 100 μ M nonessential amino acids and antibiotic/antimycotic (all from Invitrogen) and grown until confluence. Two days post-confluence the media was changed to differentiation media (minimal induction media, MIM) with test ligands or 1 μ M Rosiglitazone (positive control). MIM was determined to be 0.25X PDM (preadipocyte differentiation media) from serial dilutions with 1X PDM; PGM supplemented with 0.25 μ M dexamethasone, 0.5 mM IBMX and 1 μ g/mL insulin, 1X. After 72 hrs of induction, the media was switched to PGM containing 1 μ g/mL insulin. Cells were differentiated for four more days (7 days total) and fixed with 4% PFA. Triacylglycerol staining with AdipoRed (Lonza) and nuclear counter-staining with NucBlue (Hoechst; Invitrogen) was conducted according to the manufacturers' recommendations. Relative adipogenesis is expressed as fold change of MIM. Data are represented from mean fluorescence of 42 fields per well with five replicates used for each treatment. Fluorescence was quantified using a HERMES high content screening

scanner (WiScan, IDEA Bio-Medical Ltd., Rehovot, Israel). Hoechst fluorescence was quantified using excitation 390/18nm, emission 440/40nm (light intensity: 50%, exposure: 30ms, gain: 30%) and AdipoRed was quantified using excitation 485/20nm, emission 525/30nm (light intensity: 90%, exposure 58 ms, gain: 30%).

3.2.5. Mouse and human bone marrow derived mesenchymal stem cell adipogenesis assay

Murine (C57BL/6) BM-MSCs were obtained from Dr. Phinney's lab at The Scripps Research Institute (Jupiter, FL) in line with the NIH policy on resource sharing. Human BM-MSCs were obtained from Texas A&M University Institute of Regenerative Medicine. Both types of BM-MSCs were maintained in complete culture medium (CCM), alpha-MEM (Gibco by Life Technologies), supplemented with 16% Hyclone Defined FBS (ThermoScientific), 2mM glutamax and antibiotic/antimycotic (all from Invitrogen). Murine MSCs and human MSCs were plated at a cell density of 2×10^4 cells/well in CCM and grown until 90% confluence. Media was then changed 0.5X PDM (determined to be optimal based on serial dilutions) differentiation media (described in 3.2.3) alone, or with different concentrations of DOSS or 1uM Rosiglitazone as a positive control. Media was changed every three days for 14 days (mouse MSCs) or 18 days (human MSCs) at which point cells were fixed with PFA, stained with AdipoRed and NucBlue and quantified as described in 3.2.3. The settings on the Hermes were optimized at each run.

3.2.6. mRNA gene expression by qPCR

3T3-L1 preadipocytes, human BM-MSCs, and mouse BM-MSCs were exposed or not to differentiation media or differentiation media supplemented with test ligands as described in 3.2.3 and 3.2.4. Three wells of cells from each treatment group were pooled

from each of two experiments for mRNA expression analyses. RNA was isolated using the RNeasy Kit (Qiagen) or Trizol with the PureLink RNA Minikit (Invitrogen) following the manufacturer's instructions with addition of *DNaseI*. RNA quality was assessed using Nanodrop absorbance ratios 260/280 (2.0-2.2) and 260/230 (>1.5). Two types of gene expression analysis were used. For 3T3 L1 cells gene expression was assessed in triplicate using 25 ng of RNA per qPCR reaction and the iTaq Universal SYBR Green One-Step Kit following the manufacturer's instructions (BioRad). For mouse and human BM-MSCs, 250ng to 1µg RNA was reverse transcribed to cDNA using SuperScriptIII (Invitrogen) following the manufacturer's instructions. cDNA was then diluted appropriately so that ~10-20 ng of cDNA was used per qPCR reaction with Roche FastStart Essential DNA Green Master mix (Roche). The same touchdown PCR cycle program was used for all primer pairs: 95°C 10 sec, 66°C-56°C 20 sec dropping a degree each cycle for 10 cycles, then remaining 35 cycles at 56°C, 72°C 20 sec for a total of 45 cycles. Results were normalized to the reference gene *Hprt* using the $\Delta\Delta C_t$ method. *Hprt* was used as the reference gene, however *Gapdh* and *18S* rRNA were also analyzed and determined to be more variable with treatment (stdev Ct value, 0.44, 0.85 and 0.94 respectively). Calibration curves were prepared to ensure equal PCR efficiencies between test and reference genes (+/- st. dev. <1.01%). Data are expressed as a fold change compared with the MIM/PDM-only control. Queried genes and primer sequences are listed in Table 1.

Table 1. Genes and corresponding primers used for qRT-PCR analysis.

Gene	Species	Forward Primer	Reverse Primer
<i>Hprt</i>	Mouse	AGGCCAGACTTTGTTGGATTTG	TTCAACTTGCCTCATCTTAGG
<i>Dlk1/ Prefl</i>	Mouse	CCTGGCTGTGTCAATGGAGT	CAAGTTCCATTGTTGGCGCA
<i>AdipoQ</i>	Mouse	G TTCCTCTTAATCCTGCCCA	G TTCCTCTTAATCCTGCCCA

<i>Fabp4</i>	Mouse	ATGTGTGATGCCTTTGTGGGA	GATGATCATGTTGGGCTTGGC
<i>HPRT</i>	Human	TGACACTGGCAAAAACAATGCA	GGTCCTTTTCACCAGCAAGCT
<i>ADIPOQ</i>	Human	GCTGGGAGCTGTTCTACTGC	CGATGTCTCCCTTAGGACCA
<i>FABP4</i>	Human	TCACTGCAGATGACAGGAAAGT	GTGACGCCTTTCATGACGCA
<i>EZH2</i>	Human	AATCAGAGTACATGCGACTGAGA	GCTGTATCCTTCGCTGTTCC

3.2.7. Statistical analysis

All data analyses were performed using GraphPad Prism software (GraphPad Software Inc.). Prior to statistical analysis, data represented as fold change or percentages that did not meet Gaussian distribution and equivalency of variance conditions for ANOVA analysis were log transformed. Normality and equal variance was assessed via graphical display and confirmed using the Shairo-Wilk or Kolmogorov-Smirnov test and Brown-Forsythe test respectively. P-values < 0.05 were deemed significantly different using one-way ANOVA with Dunnett's, Tukey or Sidak's multiple comparisons post-hoc tests. Two-way ANOVA was used for multiple comparison analysis with Sidak's test and significant p-value < 0.05. GraphPad Prism software was used to calculate EC50 data using sigmoidal, 4PL curves. Similarly, LC50 was calculated using log (inhibitor) vs. normalized response – variable slope.

3.3. Results

3.3.1. DOSS activates PPAR γ

The results from Section 2.3 implicated a Corexit component(s) in the PPAR γ transactivation observed in the CWAF prepared from MC252 oil. Mass spectrometry indicated that Tween 80 and DOSS are present in the 50:50 water:ethanol fraction of CWAF, which exhibits activity in the GAL4-UAS assay system, and molecular modeling predicts that Span 80, Tween 80 and DOSS can bind to the PPAR γ ligand binding domain (Section 2.3). Therefore, these compounds were tested for PPAR γ activity. We

used assay conditions optimized in Chapter 2 to test Corexit components for PPAR γ activity. Prior to testing, we obtained LC50 values for test compounds using AlamarBlue cell viability assay as a marker for metabolic activity which also validated *Renilla* luciferase values as a proxy for cytotoxicity to monitor assay to assay (Figure 1A). The LC50 for DOSS was determined to be 10 ppm in HEK 293 cells under serum free conditions (Figure 1A and B). We determined the LC50 value for Span 80 and Tween 80 to be approximately 500 μ M (about 200 ppm) and 150 μ M (about 200 ppm), respectively (Figure 1E and F). It should be noted that DOSS is more cytotoxic than Span 80, with the same cytotoxicity at approximately 10-fold lower concentration than that of Span 80.

We observed that Span 80 and Tween 80 both demonstrate weak PPAR γ activation, even at the highest concentrations tested, reaching only about 10% of maximal induction (based on 100nM Rosi) at 128 μ M (Figure 2A and B) for both compounds. We observed no activities for these compounds at the concentrations used in Corexit. Furthermore, a mixture of petroleum distillate (ICP) and propylene glycol (PG), other major components of Corexit, does not demonstrate PPAR γ activation (Figure 3C). We next tested DOSS for PPAR γ activation. Unlike Span 80 and Tween 80, DOSS alone elicits a dose-dependent increase in PPAR γ activity in the low ppm range (Figure 3A, B and C). Significant activation was observed at 2, 4 and 8 ppm, reaching approximately 50% maximal induction compared to Rosi (Figure 3A). When using water or DMSO as DOSS solvents, we observed comparable activities, with DOSS dissolved in water being slightly more efficacious (Figure 3B). Under control conditions, when cells were transfected with the reporter plasmids but no receptor plasmid and treated with DOSS, no response was observed (Figure 3B), indicating DOSS specificity. As described above,

ICP:PG mixtures do not activate PPAR γ , however, when this mixture is supplemented with increasing concentrations of DOSS, robust PPAR γ activity is now observed (Figure 3C). Thus, DOSS has PPAR γ ligand induced activity in this assay whereas Span 80, Tween 80, ICP, and PG do not. Since Corexit 9500 is approximately 10-30% DOSS [162], it is likely that the PPAR γ agonist activity observed following treatment with CWAF, C_MWAF or Corexit (Section 2.3) is largely due to DOSS.

Curiously, only slight reductions in PPAR γ activation were observed when cells were treated with 75ppm DOSS and 1 μ M of the PPAR γ inhibitor T007907, using serum containing conditions (Figure 3D). Conversely, activity observed with 100 nM Rosi was reduced ten fold in the presence of 1 μ M T007907 inhibitor. Interestingly, when preadipocyte differentiation media (PDM) containing DOSS was tested for PPAR γ activation with and without inhibitor, the activity was decreased by about half in the presence of the inhibitor (Figure 3E). However, the greatest reduction was always observed in the Rosi with inhibitor treatments suggesting that DOSS and Rosi may not interact with the ligand binding and/or other domains of PPAR γ in the same way.

DOSS interaction with the ligand-binding domain of PPAR γ was validated using a TR-FRET competitive binding assay. Using this assay, DOSS was able to displace a high-affinity ligand bound to the LBD of PPAR γ with an EC₅₀ of 1.38 μ M, similar to that of the endogenous PPAR γ ligand arachidonic acid (Figure 3E). In the same assay, EC₅₀ values for Span 80 and Tween 80 were much higher, at 315 μ M and 45.14 μ M, respectively (Figure 5C and D). This is consistent with the concept that DOSS is largely responsible for PPAR γ activation observed in CWAF and Corexit.

Given the structural similarity of the PPAR isoforms with each other as well as between species, we tested human PPAR γ , PPAR β/δ and PPAR α for DOSS ligand induced activity as well using the GAL4/UAS system (Figure 6). DOSS was able to activate human PPAR γ in a dose-dependent manner, although this assay was not as sensitive as for mouse PPAR γ , with 100nM Rosi producing only a 4-fold response and 4ppm DOSS producing a 3-fold response using the human PPAR γ LBD-GAL4 assay (Figure 6A). We observed approximately a 1.2-fold induction of PPAR α activity by DOSS, but no trend relating to dose was observed, suggesting that DOSS has extremely low if any affinity for PPAR α (Figure 6B). Interestingly, and worth further investigation, we observed a strong dose response in PPAR β/δ activity by DOSS, with 7-fold induction at 4ppm DOSS (Figure 6C). While PPAR β/δ is a widely-expressed isoform, it is also arguably the least studied PPAR isoform, but has been implicated as an essential mediator of COX-2/PGE2-driven inflammation in colorectal carcinogenesis [220].

3.3.2 Span 80 exhibits RXR α activity

Since Corexit was able to activate both PPAR γ and RXR α (section 2.3), several Corexit components were interrogated specifically for RXR α ligand induced activity including DOSS, Span 80 and Tween 80 using the GAL4/UAS system. While we observed weak PPAR γ activation by Span 80 and Tween 80, these compounds had stronger RXR α activity, particularly Span 80 (Figure 2A and B).

Corexit components DOSS (Figure 4A), petroleum distillates and propylene glycol mixed 50/50 (ICP/PG; Figure 4B) demonstrated no significant RXR α activity. Conversely, Tween 80 modestly (Figure 2B), and Span 80 markedly (Figure 2A) activated RXR α , reaching 20% maximal induction (relative to TBT) at 64 μ M (~30 ppm)

and 40% maximal induction at 128 μM (~60 ppm), respectively. Collectively, these results suggested that the RXR α activity present in CWF and Corexit (section 2.3) derives primarily from Span 80, with a lesser contribution from Tween 80. To further confirm Span 80 in a true RXR α transactivation assay (requiring ligand binding and DNA binding domain transactivation), HEK 293T cells were transfected with a full-length human RXR α expression vector and with a reporter vector containing the validated RXR α binding element of the ApoA1 gene driving luciferase reporter expression [214]. As shown in Figure 5D, Span 80 exhibited robust, dose-dependent RXR α transactivation in these assays, which was very similar to that observed with the RXR α ligand-binding domain – Gal4-DNA binding domain UAS luciferase system (Figure 5C).

Lastly, to verify that Span 80 can displace a high-affinity ligand for RXR α , the TR-FRET coactivator assays for Span 80 and Tween 80 was used. EC50s for Span 80 and Tween 80 in this assay were in the low micromolar range, 6.65 and 2.84 μM respectively. However, it should be noted that Tween 80 only reached a maximum percent activation of roughly 45% in this assay, supporting the concept that Span 80 is a higher affinity activator of RXR α than Tween 80.

3.3.3. *Oleic acid has stronger activity for RXR α than PPAR γ*

Oleic acid (C18:1 cis-9), is a fatty acid component of both Span 80 (a sorbitan monoester) and Tween 80 (an ethoxylated sorbitan ester) and represents a naturally occurring dietary fatty acid. As Span 80 and Tween 80 showed greater activation of RXR α than PPAR γ (Figure 2A and B), we sought to directly compare Span 80, Tween 80 and their fatty acid component oleic acid in the ligand induced (GAL4/UAS) activity

assays. As with all other dosing experiments, treatments were in the sub lethal range; LC50 values for HEK 293 cells were 319 μM for oleic acid; Figure 1). As shown in Figure 7A, oleic acid was more potent than either Span 80 or Tween 80 with significant RXR α activity at 16 μM versus 64 μM for Span 80 and Tween 80. From these data, EC50s for oleic acid, Span 80 and Tween 80 were 33 μM , 33 μM and 70 μM , respectively. Oleic acid was also more efficacious, eliciting approximately 60% of maximal activation at 128 μM compared to approximately 45% activation for Span 80 and approximately 20% for Tween 80 (100% activation is that achieved with 10 nM TBT).

For PPAR γ , all three compounds behaved similarly, eliciting only 12-15% maximal activation at 128 μM (Figure 7B). When these compounds were assessed using the TR-FRET assays for both receptors, similar results were obtained. As described above, EC50s for Span 80 and Tween 80 were in the low micromolar range for RXR α but an order of magnitude higher for PPAR γ (Figure 7C, D). As predicted by transactivation assays, oleic acid elicited the lowest EC50 for RXR α at 1.6 μM (Figure 7C) and was roughly 50 times greater for PPAR γ at 90 μM (Figure 7D). In sum, oleic acid and Span 80 are more potent and efficacious agonists for RXR α than PPAR γ with oleic acid eliciting the strongest response, suggesting that the sorbitan group of Span 80 and ethoxylated sorbitan group on Tween 80 may interact with the RXR α ligand binding domain to dysregulate signaling.

3.3.4. DOSS increases adipogenesis in preadipocytes and BM-MSCs

To functionally test the obesogenic potential of DOSS, murine 3T3-L1 preadipocytes, murine BM-MSCs and human BM-MSCs were exposed to low-level

adipocyte differentiation inducers with and without a dosage series of DOSS and then adipogenesis was quantified by measuring triacylglycerol content (Figure 8). To ensure test concentrations of DOSS were in the sublethal range, viability tests were performed (as above). The LC50 of DOSS in 3T3 L1 cells was determined to be approximately 90 ppm, which was well above the highest doses applied in adipogenesis experiments (Figure 1C). Cells were treated with minimal induction media (MIM) and DOSS, or 1 μ M Rosi as a positive control. Triacylglycerol accumulation was quantified and visualized using AdipoRed staining (Lonza; green) and normalized to cell number (Hoechst nuclear counter-staining). MIM with and without DOSS was tested for PPAR γ activity to coordinately demonstrate increases in PPAR γ activation with increases in triglyceride accumulation (Figure 3E). A dose-dependent increase in adipogenesis was observed with increasing concentrations of DOSS (Figures 8 and 9). Significant increases in adipogenesis in 3T3 L1 cells were observed at 20, 25 and 50 ppm DOSS exposure compared to MIM alone (Figure 8A). Additionally, murine BM-MSCs were exposed to MIM alone or MIM with increasing concentrations of DOSS (and Rosi as a positive control) to see if DOSS increased adipogenesis in undifferentiated progenitor primary cells. Significant induction was observed in 50 ppm DOSS and 1 μ M Rosi treated cells only with 3 fold and 40 fold induction over MIM respectively (Figure 8B), suggesting that mouse primary BM-MSCs are responsive to DOSS treatment, but less so than the 3T3 L1 cell line.

Human primary BM-MSCs were also used to assess the ability of DOSS to increase adipogenesis in an undifferentiated progenitor cell type, and to validate DOSS as an agonist for not only mouse PPAR γ but human PPAR γ as well. For human BM-MSCs,

similar results were observed (Figure 8C). Adipogenesis was quantified using the same methods as described for 3T3 L1 cells. Human BM-MSCs were treated with MIM alone, increasing concentrations of DOSS or 1 μ M rosiglitazone as a positive control for 18 days. Significant increases in adipogenesis relative to the MIM alone control were observed at 30, 40 and 60 ppm DOSS (Figure 8C), further supporting a role for DOSS as a driver of adipogenesis *in vitro* not only for the murine preadipocyte cell line and primary cell progenitors but also for the human primary cell progenitors as well.

Lastly, because results indicated that Span 80 is capable of activating RXR α and weakly activating PPAR γ , and that these receptors are known to regulate adipogenesis through dimerization, the potential of Span 80 to promote adipocyte differentiation *in vitro* was tested using the 3T3 L1 preadipocyte differentiation assay. Span 80 addition at 250, 500 or 1000 ppm to minimal induction media (MIM) caused a dose-dependent increase in adipocyte differentiation over basal levels; at 500 ppm Span 80 there was an approximately 2-fold and at 1000 ppm an approximately 3-fold increase in triacylglycerol levels (Figure 9A and B). Comparable to results described above, treatment with 12.5, 25, or 50 ppm DOSS in the presence of MIM also resulted in a dose-dependent increase in adipocyte differentiation (Figure 8A and Figure 9B; Ref. [13]). These results are also consistent with the concept that DOSS is more potent than Span 80, increasing adipogenic differentiation at concentrations over an order of magnitude lower than that of Span 80.

3.3.5. DOSS increases expression of adipogenic genes

To extend triglyceride data and validate that adipogenesis was occurring in differentiation assays, changes in gene expression of adipogenic genes resulting from DOSS treatment was investigated. For analysis in 3T3 L1 cells qPCR mRNA analysis

was performed on day three of differentiation. Significant dose dependent increases in gene expression was observed for two adipogenic gene markers, *AdipoQ* and *Fabp4* (Figure 10A and B). Decreases in the preadipocyte marker, *Pref-1/Dlk-1* (preadipocyte factor 1/delta like kinase 1) mRNA levels are an accurate and precise measure of adipocyte differentiation by preadipocytes [221]. Consistent with this, a significant dose-dependent decrease in *Pref-1/Dlk-1* in DOSS and Rosi treated 3T3 L1 cells was observed (Figure 10C). These data further support the conclusion that DOSS increases adipogenesis (and not merely triglyceride levels) in 3T3 L1 preadipocytes. Similarly, for mouse primary BM-MSC progenitors increases in *AdipoQ* and *Fabp4* expression were also observed (Figure 10D and E). However, similar to the results observed in the differentiation assays, these changes were only significant at the highest concentration of DOSS tests (50ppm), suggesting that primary progenitor cells are not as responsive as a mouse preadipocyte cell line.

The same adipogenic markers were also investigated in human BM-MSCs at day 16 of adipogenesis. Similarly, dose-dependent increases in gene expression for both *ADIPOQ* and *FABP4* were observed (Figure 11A and B). Notably, Rosi increased expression of these genes 100 fold more than the highest concentration of DOSS tested, suggesting that the adipocytes produced by DOSS may be different than adipocytes derived from Rosi treatment even though their triglyceride accumulation is comparable (Figure 8C). In MSCs, the histone methyltransferase gene, *EZH2*, is an early adipogenic marker as its methyl marks are documented to repress genes involved in osteogenesis, another lineage fate of BM MSCs [222]. Indeed, significantly decreased *EZH2* expression was observed in terminally differentiated DOSS and Rosi treated cells relative

to MIM (Figure 11C), suggesting that DOSS differentiated populations have fewer non-committed cells and more terminally differentiated adipocytes.

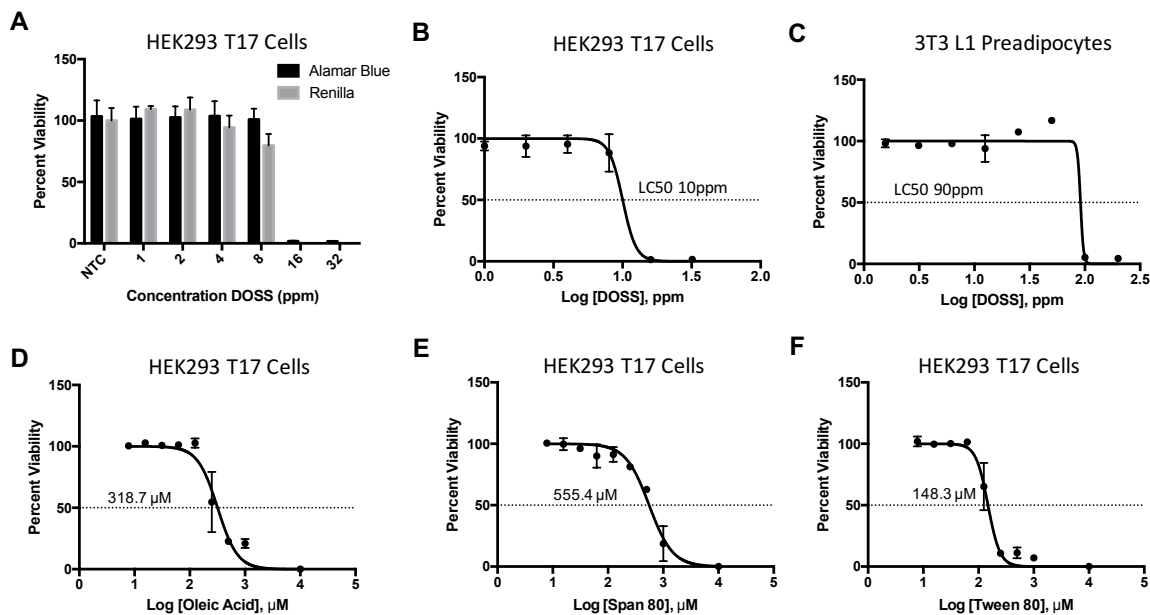


Figure 1. Cytotoxicity of DOSS, Span 80 and Tween 80 in HEK 293 T17 Cells and 3T3 L1 murine preadipocytes.

Percent viability of HEK293 T17 cells and 3T3 L1 preadipocytes was calculated for test compounds used in transactivation and adipogenesis assays. Cells were treated with test compounds in triplicate for 18hrs, AlamarBlue reagent was added and mitochondrial activity was measured based on the colorimetric assay. A) Comparison of percent viability of HEK 293 cells exposed to 1, 2, 4, 8, 16 and 32 ppm DOSS in serum free conditions measured by AlamarBlue and Renilla luciferase. B) LC50 for DOSS in HEK293 cells as measured by AlamarBlue. C) LC50 for DOSS in 3T3 L1 preadipocytes as measured by AlamarBlue. LC50 for D) Oleic Acid, C) Span80 and D) Tween80 in HEK293 T17 cells measured by AlamarBlue.

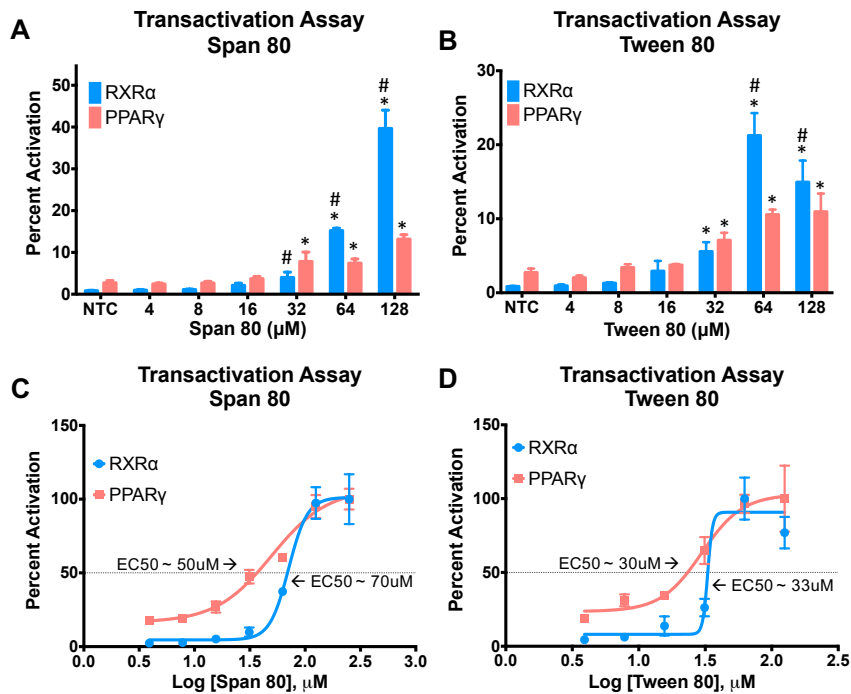


Figure 2. Comparison of Span 80, and Tween 80 potency and efficiency for RXR α and PPAR γ using receptor transactivation assays.

HEK293T/17 cells were transfected with RXR α and PPAR γ GAL4-LBD, UAS-luciferase and renilla luciferase reporter plasmids. Dilutions of mixtures were prepared and cells were exposed in triplicate for 18 h, luciferase activities were measured and firefly to renilla luciferase ratios were calculated. Data are expressed as percent activation relative to 100% activation by 10nM TBT for RXR α and 100nM Rosiglitazone for PPAR γ . Percent activation of RXR α and PPAR γ by A) Span80 and B) Tween80. Calculated EC50 values for RXR α and PPAR γ activation by C) Span80 and D) Tween80.

N=3 replicates for a given representative experiment. *P<0.05 compared to non-treated control (NTC). #P<0.05 between receptors at the concentration indicated using Two-Way Anova with Dunnet's multiple comparisons test.

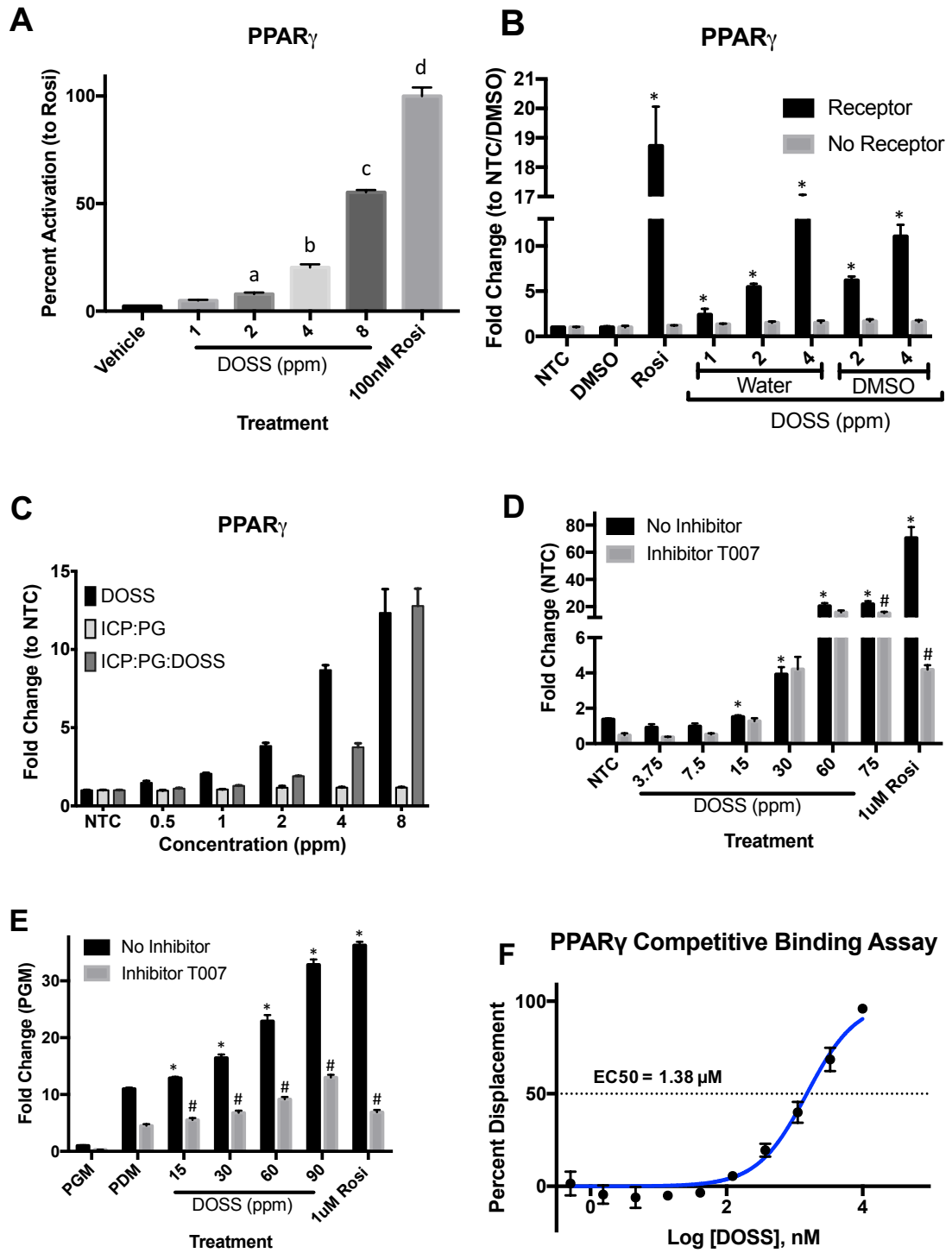


Figure 3. DOSS activates PPAR γ .

HEK293T/17 cells were transfected with PPAR γ GAL4-LBD, UAS-luciferase and renilla luciferase reporter plasmids. Dilutions of mixtures were prepared and cells were exposed in triplicate for 18 h, luciferase activities were measured and firefly to *Renilla* luciferase ratios were calculated. Data are expressed as percent activation relative to 100% activation by 100nM Rosiglitazone for PPAR γ or as fold change over the non treated control (NTC). A) DOSS activation of PPAR γ . B) Comparison of PPAR γ activation by DOSS in water or DMSO. C) PPAR γ activation by DOSS, ICP:PG and ICP:PG supplemented with DOSS. D) Effect of the PPAR γ inhibitor T007907 on the ability of DOSS to activate PPAR γ . E) Validation of PDM media with DOSS to activate PPAR γ with and without inhibitor F) Competitive binding of DOSS to PPAR γ measured by percent displacement in TR-FRET assay.

N=3 replicates for a given representative experiment. *P<0.05 by One-Way ANOVA compared to non-treated control (NTC). #p<0.05 for inhibitor compared to no inhibitor for a given concentration, Two-Way ANOVA with Sidak's multiple comparisons tests.

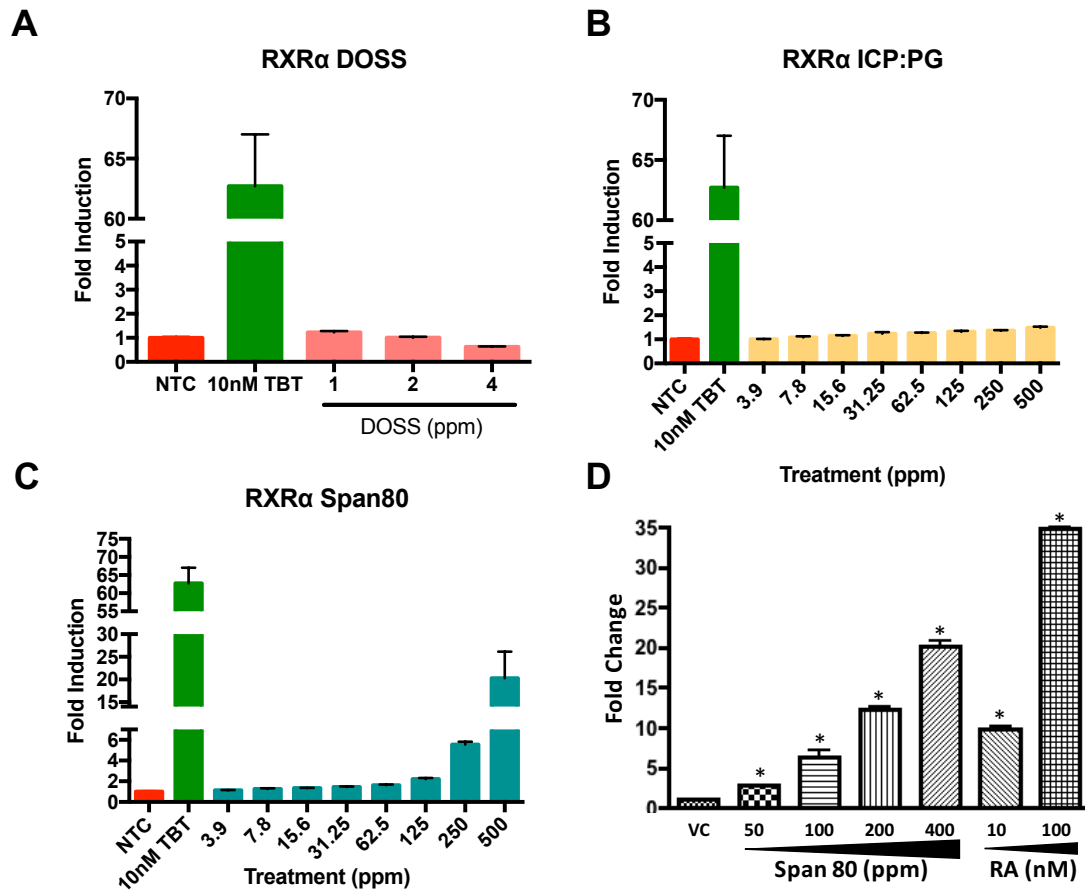


Figure 4. Span80, but not other components of Corexit, activate RXR α .

HEK293T/17 cells were transfected with RXR α GAL4-LBD (A-C) or full length RXR α receptor (D), UAS (A-C) or ApoA1 promoter (D) luciferase, and luciferase reporter plasmids. Dilutions of mixtures were prepared and cells were exposed in triplicate for 18 h, luciferase activities were measured and firefly to *Renilla* luciferase ratios were calculated. Data are expressed as Fold Change over the non treated control (NTC). RXR α transactivation activity by A) DOSS, B) ICP:PG and Span80 in C) and D).

N=3 replicates for a given representative experiment. *P<0.05 by One-Way Anova compared to non-treated control (NTC).

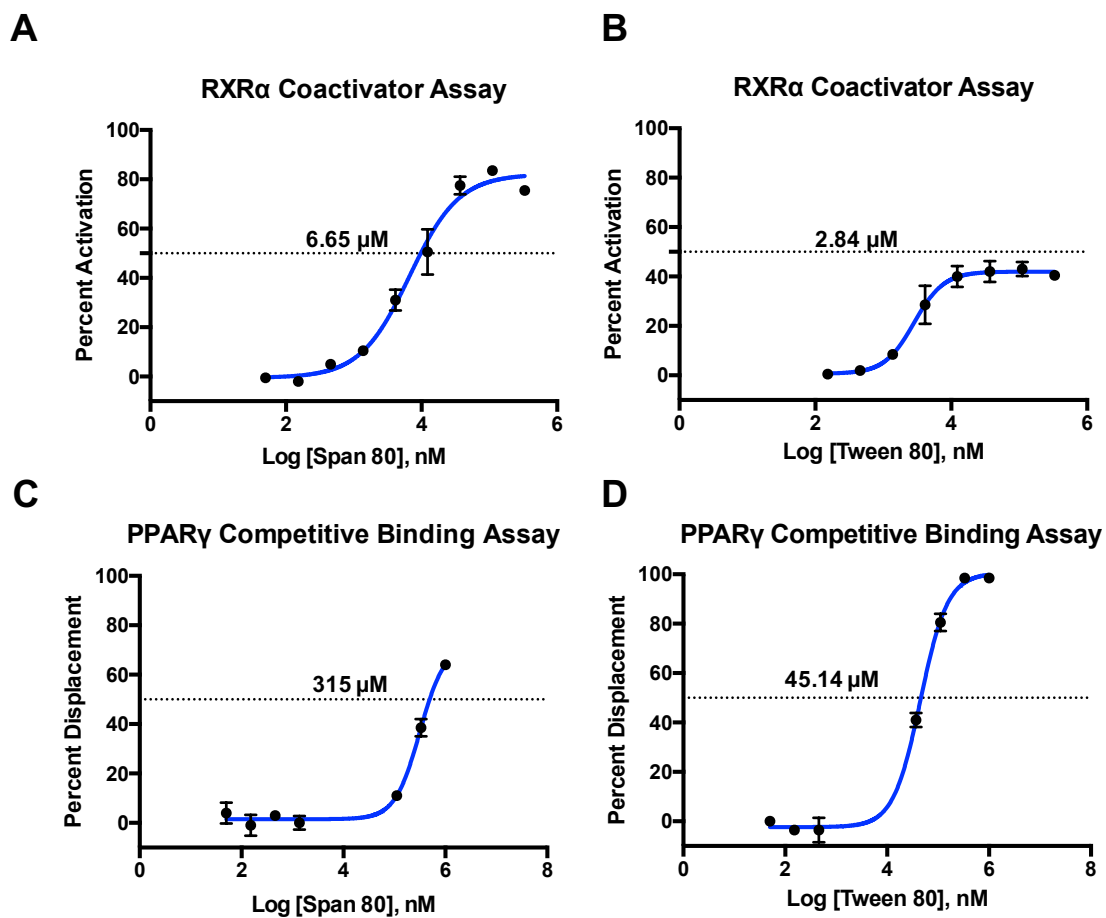


Figure 5. Span 80 and Tween 80 binding affinity for RXR α and PPAR γ using TR FRET assays.

Three-fold serial dilutions of test compounds were assessed for binding affinity to RXR α (A and B) and PPAR γ (C and D) and EC₅₀s were calculated for Span80 (A and C) and Tween80 (B and D) using LanthaScreen TR-FRET assays.

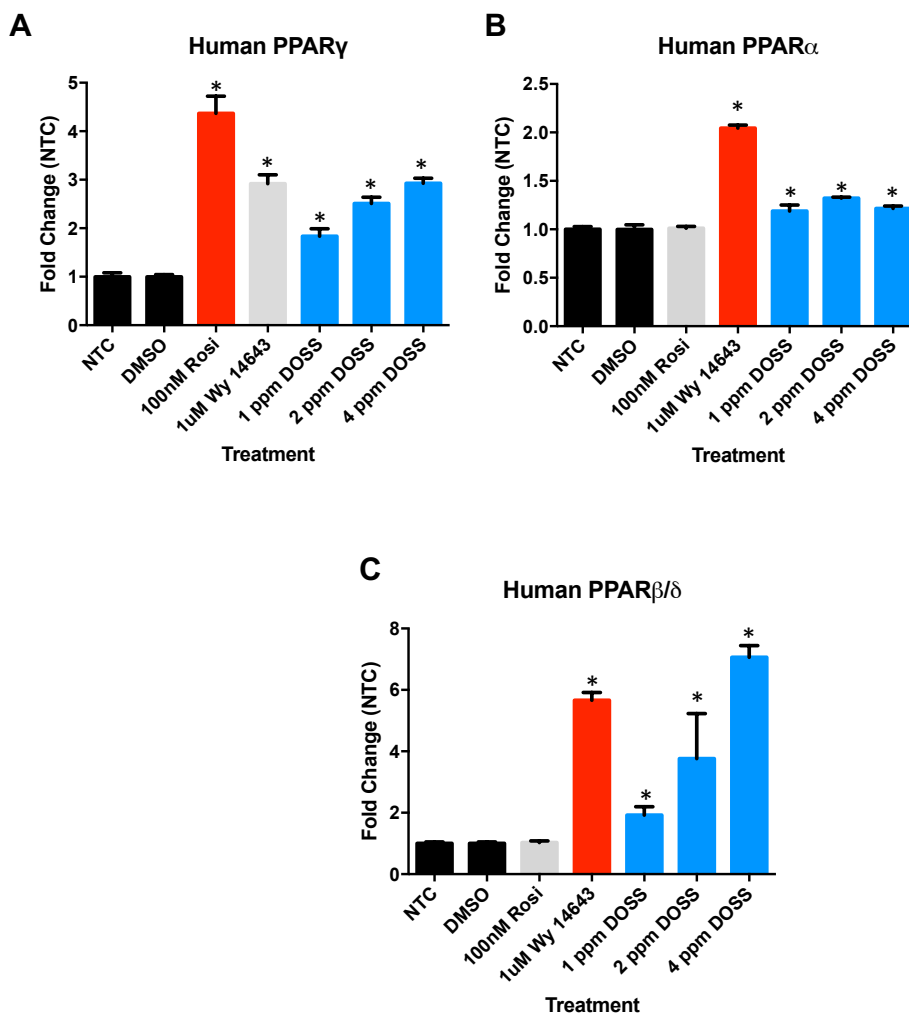


Figure 6. Potential activation of other PPAR isoforms by DOSS.

HEK293T/17 cells were transfected with each of three human PPAR isoform GAL4-LBD, UAS-luciferase and *Renilla* luciferase reporter plasmids. Dilutions of mixtures were prepared and cells were exposed in triplicate for 18 h, luciferase activities were measured and firefly to renilla luciferase ratios were calculated. Data are expressed as fold change over the non treated control (NTC). DOSS activation of human A) PPAR γ , B) PPAR α , and C) PPAR β/δ .

N=3 replicates for a given representative experiment. *P<0.05 by One-Way ANOVA compared to non-treated control (NTC).

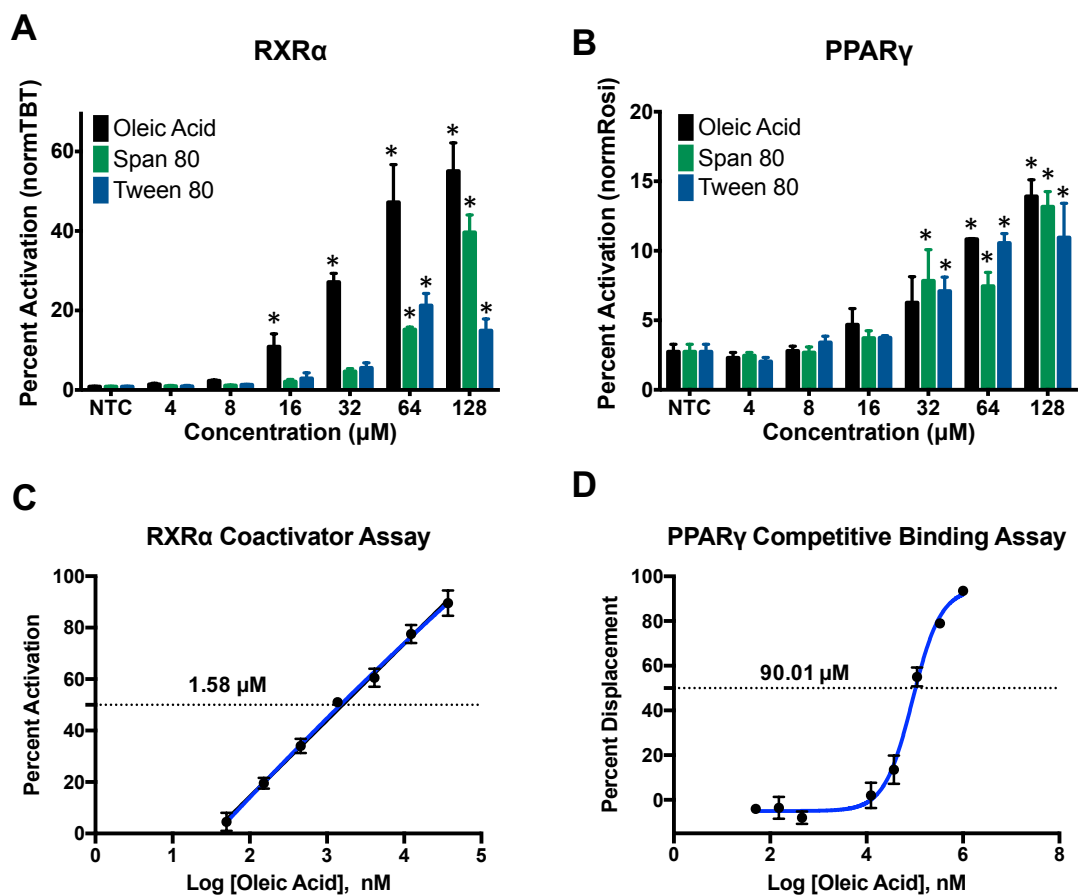


Figure 7. Oleic acid has stronger transactivation activity for RXR α than PPAR γ .

HEK293T/17 cells were transfected with RXR α and PPAR γ GAL4-LBD, UAS-luciferase and *Renilla* luciferase reporter plasmids (A and B). Dilutions of mixtures were prepared and cells were exposed to Oleic Acid, Span80 and Tween80 in triplicate for 18 h, luciferase activities were measured and firefly to *Renilla* luciferase ratios were calculated. Data are expressed as percent activation relative to 100% activation by 10nM TBT for RXR α and 100nM Rosiglitazone for PPAR γ . *p<0.05 compared to NTC. Three-fold serial dilutions of Oleic Acid were assessed for binding affinity to RXR α (C) and PPAR γ (D) and EC50s were calculated using LanthaScreen TR-FRET assays.

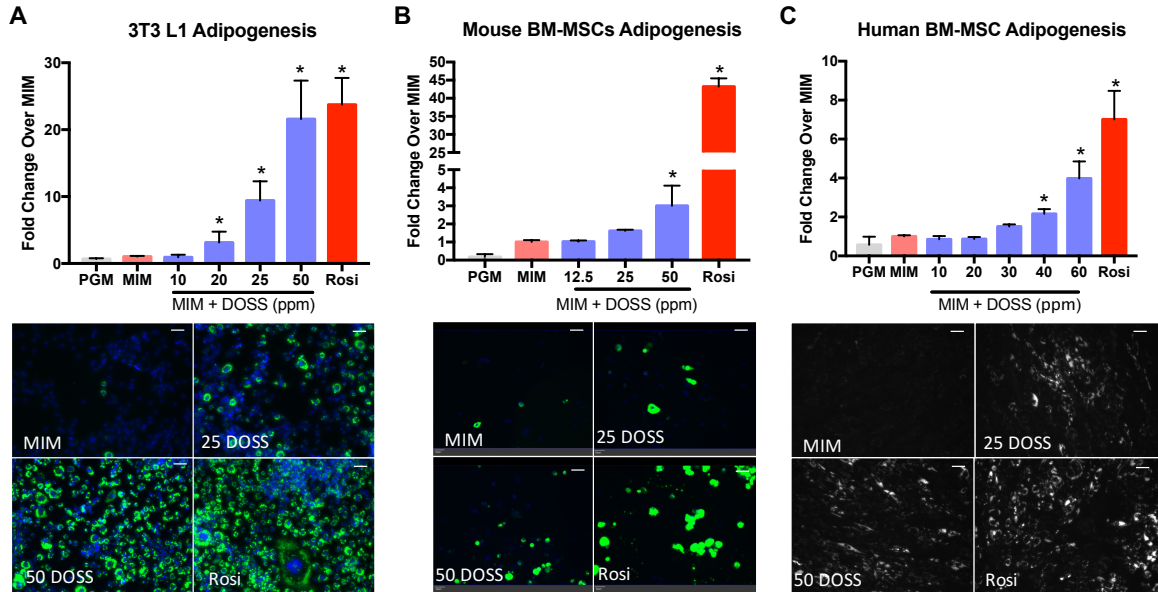


Figure 8. DOSS increases adipogenesis in preadipocytes and bone marrow derived mesenchymal stem cells.

3T3-L1 cells and mouse and Human BM MSCs were cultured as described in methods.

Cells were either maintained in PGM or treated with MIM (Minimal Induction Media) alone or supplemented with increasing concentrations of DOSS or 1 μ M Rosiglitazone.

Triglyceride/lipid accumulation was measured using AdipoRed fluorescent staining as depicted in representative images. Data are represented as fold change over MIM alone.

AdipoRed lipid quantification for A) day 7 3T3L1 cells, B) day 16 mouse BM-MSCs and C) day 18 human BM-MSCs.

N=3-6 replications of representative experiments. * $p < 0.05$ vs. MIM control by One-

Way ANOVA. Scale bar = 50 microns

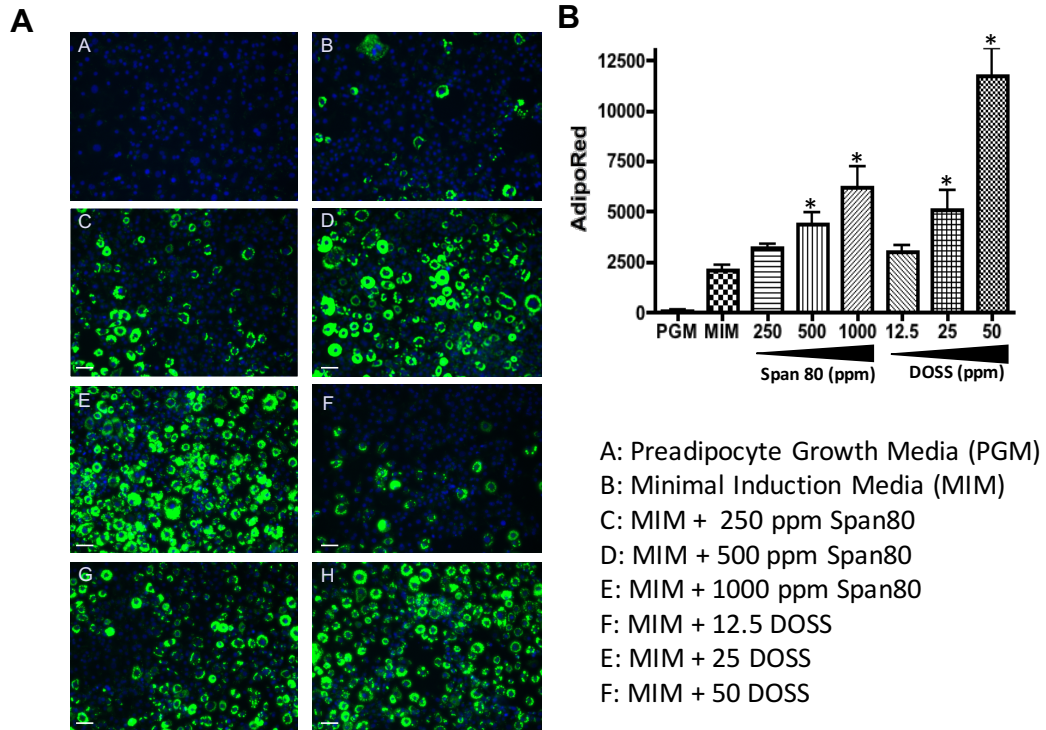


Figure 9. DOSS and Span80 increase adipogenesis in 3T3 L1 preadipocytes.

3T3-L1 cells were cultured as described in methods. Cells were either maintained in PGM or treated with MIM (Minimal Induction Media) alone or supplemented with increasing concentrations of DOSS, Span80 or 1 μ M Rosiglitazone. Triglyceride/lipid accumulation was measured using AdipoRed fluorescent staining as depicted in A) representative images and quantified B) as fold change over MIM alone.

N=3-6 replications of representative experiments. * $p < 0.05$ vs. MIM control by One-Way ANOVA. Scale bar = 50 microns

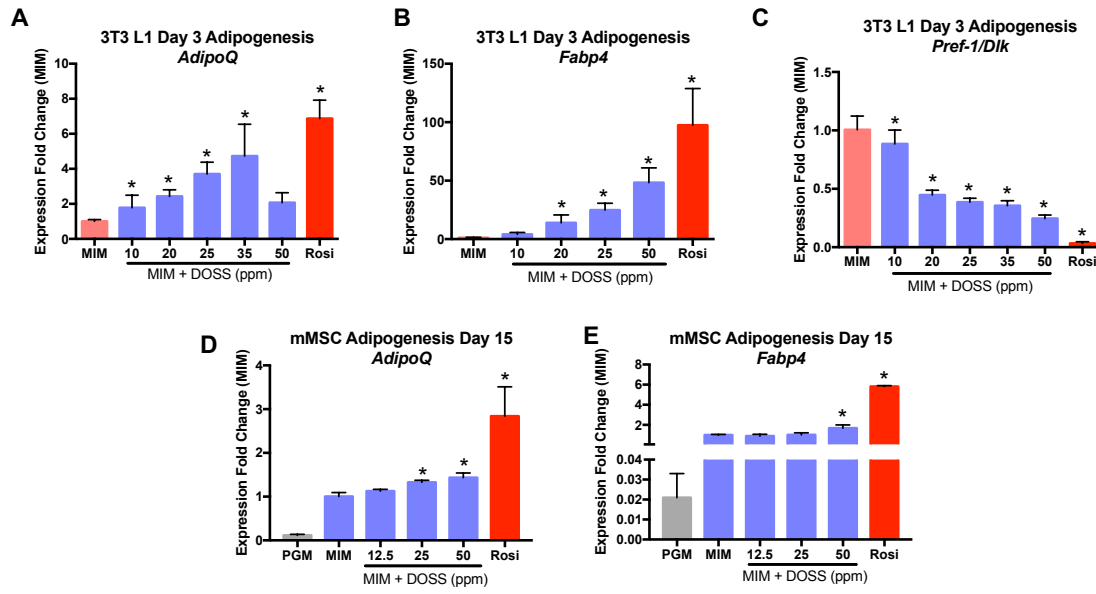


Figure 10. DOSS increase expression of adipogenic genes murine cell lines.

3T3-L1 cells and mouse BM MSCs were cultured as described in methods. Cells were either maintained in PGM or treated with MIM (Minimal Induction Media) alone or supplemented with increasing concentrations of DOSS or 1 μ M Rosiglitazone. RNA was isolated on day3 of adipogenesis for 3T3L1 cells or day15 from mouse BM-MSCs. Gene expression was measured using qRT-PCR and the $\Delta\Delta$ Ct method normalized to the housekeeping gene *Hprt*. Data are represented as fold change over MIM alone for A) *AdipoQ*, B) *Fabp4*, and C) *Pref1/Dlk* in 3t3L1 cells and D) *AdipoQ* and E) *Fabp4* in mouse BM-MSCs.

n= 3-6 replicates. *P<0.05 One-Way ANOVA compared to MIM.

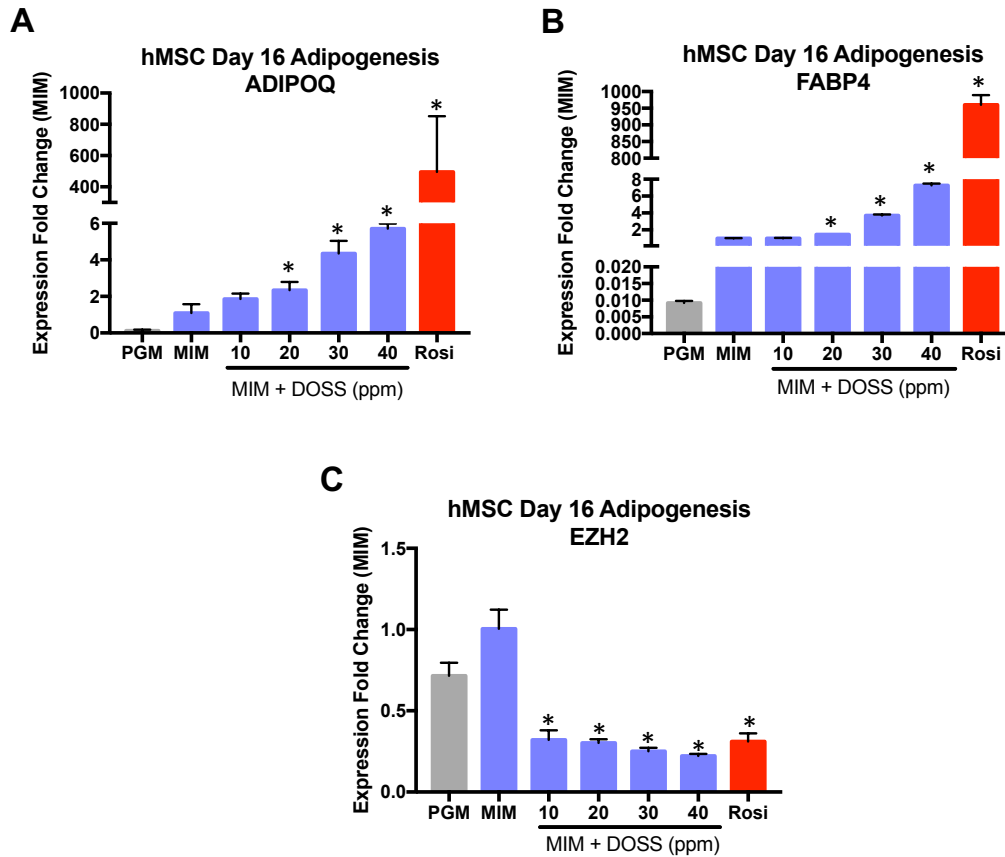


Figure 11. DOSS increase expression of adipogenic genes in human BM-MSCs.

Human BM MSCs were cultured as described in methods. Cells were either maintained in PGM or treated with MIM (Minimal Induction Media) alone or supplemented with increasing concentrations of DOSS or 1 μ M Rosiglitazone. RNA was isolated on day 16 of adipogenesis. Gene expression was measured using qRT-PCR and the $\Delta\Delta$ Ct method normalized to the housekeeping gene *HPRT*. Data are represented as fold change over MIM alone for A) *ADIPOQ*, B) *FABP4*, and C) *EZH2*.

n= 3 replicates. *P<0.05 One-Way ANOVA compared to MIM.

3.4 Discussion

PPAR γ is often referred to as the gate keeper or master regulator of adipogenesis. Once PPAR γ is activated via ligand binding, it translocates to the nucleus and regulates gene expression to promote adipogenic differentiation, lipid uptake and even autoactivation or induced expression of itself. Thus, PPAR γ ligand-binding and transactivation assays serve as convenient *in vitro* surrogates to identify potential *in vivo* obesogen. Since 2006, investigators have been exploring the obesogen hypothesis, investigating the role of exogenous compounds to promote obesity in wildlife and humans. Naturally, identification of PPAR γ ligands is an extremely active area of investigation, given the role of this receptor in promotion of obesity through adipogenesis [92]. Of note, the use of pharmaceutical PPAR γ agonists in the clinic to treat diabetes have been shown to cause weight gain and bone loss [223, 224]. PPAR γ has been used as a tool to identify obesogens, including the antifouling agent tributyltin, perfluorinated compounds and several flame retardants [111, 206].

Here evidence is provided in support of the hypothesis that DOSS, an anionic surfactant widely used as a food-additive and stool softener taken by pregnant women, is a probable obesogen *in vitro* via activation of PPAR γ in GAL4/UAS transactivation assays and increases in adipogenic differentiation of a murine preadipocyte cell line and murine/human primary stem cells. Additionally, we identified Span 80 and oleic acid as RXR α activators and showed that high concentrations of Span 80 can also promote adipogenic differentiation.

Other investigators have shown that surfactants with similar structures as DOSS, including SDS and SDBS can also act as ligands of PPAR γ , using receptor

transactivation assays and adipogenic differentiation assays like the ones describe herein [219]. It is hypothesized that the hydrocarbon chains of these anionic surfactants resemble the endogenous PPAR γ ligands (fatty acids and eicosanoids). Additionally, the extremely polar sulfonyl group of these compounds is likely to have interaction capabilities with residues in the ligand binding domain of PPAR γ . In the case of SDS and SDBS, they most closely resemble lauric acid, which has been shown to activate PPAR γ [104]. The hydrocarbon chain of DOSS is a branched fatty acid, a class of molecules which are also produced by bacteria in the gut, and which have also been shown to activate PPAR γ [225].

In this Chapter a fatty acid moiety of Span 80, oleic acid, was shown to act as an RXR α activator and weak PPAR γ activator, further supporting the idea these types of compounds can interact with PPAR γ and RXR α via their hydrocarbon chains. Our data agrees with studies suggesting that oleic acid can bind to and activate both RXR α and PPAR γ with low micromolar affinity, as demonstrated using *in vitro* transactivation assays. While Fan and coworkers report very modest RXR α activation by oleic acid, using a GAL-4-UAS *in vitro* system [226], Lengqvist and coworkers report results of oleic acid RXR α activation very similar to those described herein, and the authors noted that reported EC50s may be conservative estimates as reagent dilution in plastic tubes may affect apparent ligand concentration [214].

Currently, human exposure to and the metabolism and circulating/intracellular levels of Span 80 and DOSS *in vivo* are unknown. Toxicity data for Span 80 is presented here and by others [227, 228], however the work presented is its first evaluation of either compound as a potential endocrine disruptor. Circulating levels of oleic acid in healthy

adults range between 179 μM and 3.2 μM [229], and liver levels are between 100 μM and 500 μM [230, 231]. These levels are much greater than our reported EC50s for oleic acid activation of RXR α , while intracellular levels of free fatty acids may be impacted by the expression of fatty acid binding proteins, which are expressed at millimolar levels, they can bind to free fatty acids only in the low nanomolar range [232]. Thus, intracellular concentrations of oleic acid may be in the low micromolar range, and capable of activating RXR α . Additionally, given that RXR α and PPAR γ are ubiquitously expressed throughout the human gastrointestinal tract, dietary consumption of Span 80 may alter endogenous fatty acid absorption and signaling [233].

Comparable levels of triglyceride accumulation was observed in 50ppm DOSS treated 3T3 L1 cells and human BM-MSCs when compared to Rosi treated cells, suggesting that DOSS might function as a PPAR γ agonist *in vitro* and facilitate adipogenesis. This is supported by our observation of increases in proadipogenic genes and decreases in antiadipogenic genes, however their expression levels, particularly in the MSCs, were orders of magnitude lower than their rosiglitazone counterparts. These data might suggest that DOSS may produce a functionally distinct adipocyte when compared to Rosi, as has been shown with the obesogen TBT, or may be more potent as an inhibitor of osteogenesis. While TBT increases adipogenesis, it has been shown that the resulting adipocyte produces less adiponectin and has altered glucose uptake when compared to equivalently differentiated adipocytes from Rosi treatment [234]. These may have deleterious effects *in vivo* resulting in systemic metabolic disruption. Similarly, adipocytes differentiated in the presence of DOSS seem to produce less adiponectin

mRNA and could potentially be less sensitive to insulin stimulated glucose uptake than their Rosi counter parts.

Contrary to the anticipated mode of action, DOSS activation of PPAR γ in ligand induced activation assays was not inhibited by the PPAR γ competitive inhibitor T007907. Gene expression data suggests that DOSS is acting through a PPAR γ dependent mechanism to increase adipocyte differentiation and promote gene expression changes in PPAR γ target genes (Figures 7, 8, 9 and 10). However, and in support of the receptor activation assay results, there is a new body of research that support the concept of alternate binding sites in the PPAR γ ligand binding domain. Like DOSS, ligands for this alternate binding site are not inhibited by T007907 in transactivation assays but still result in conformational changes leading to DNA binding and downstream gene transcription [235]. Determining how DOSS interacts with the ligand binding domain of PPAR γ warrants future investigation.

Human exposure to DOSS is likely to be wide-spread given its ubiquitous use [236]. Apart from its use as a crude oil dispersant, DOSS is approved by the FDA as a food additive and is used in certain types of food at up to 1% total weight [148, 237]. Additionally, 38% of pregnant women suffer from constipation, and DOSS is approved for use as a stool-softener to treat such symptoms [238, 239]. Studies on the pharmacokinetics of DOSS suggest that some of it is excreted through the GI tract but also absorbed into the blood stream and excreted via biliary metabolism, suggesting that DOSS enters circulation and reaches multiple target organs. However, there are gaps in knowledge and insufficient information concerning DOSS metabolism and/or impacts of DOSS exposure on infant and adult health. To the best of our knowledge, DOSS

detection in breast milk has not been investigated. However, a study on women taking DOSS while breast feeding did not detect increase bowel movements in the exposed infants [154]. Given the ability of DOSS to activate PPAR γ , increase adipogenic differentiation in multiple cell types, its wide use in consumer products, as a food additive, and use as a stool softener by pregnant women, the evaluation of DOSS as an obesogen *in vivo* is essential to fully evaluate the safety of its use, as pursued in Chapter 4.

CHAPTER 4: CHARACTERIZATION OF DOSS AS AN OBESOGEN AND METABOLIC DISRUPTOR *IN VIVO*

4.1 Introduction

Obesity and diabetes are chronic diseases effecting human populations worldwide. In the last 30-50 years, rates of occurrence of these metabolic disorders have increased to unprecedented levels. In the United States, 37.7% of adults are obese and 7.7% are extremely obese, based on the most recent data from 2013-2014 [1]. This epidemic effects children and adolescents as well with 17% of children ages 2-19 obese and 5.8% extremely obese [2]. Rates of diabetes and metabolic syndrome have also increased and are often coupled with the presence of obesity [4, 240]. Additionally, despite increased efforts in nutrition and fitness education, rates of obesity and diabetes have not subsided or declined and are expected to continue to increase with an estimated 51% of the population obese by 2030 [241]. Genetics and heritability are important factors in obesity cases accounting for roughly 50-90% of disease based on studies from obesity discordant twins and 20-80% based on familial heritability studies [242, 243]. However, while genome-wide association studies have identified several polymorphisms as contributors to obesity rather than single deleterious mutations, these SNPs only account for roughly 2% of the variance associated with BMI [244]. Even when genetic loci are analyzed in an additive manner via complex trait analysis only 30-37% of variance is explained [245]. This indicates that the remaining cases or “missing heritability” can likely be attributed to environmental/epigenetic factors and gene by environment interactions, the most accepted being lifestyle choices influencing caloric intake and expenditure [246, 247].

In recent years, research has focused increasingly more on understanding how the environment may play a role in the development of obesity and metabolic syndrome [248]. In particular, the environment in which an individual is exposed to during development and how it relates to later life health trajectories has been investigated and broadly classified as the exposome [249] and historically classified as the fetal/developmental origins of adult disease due to the more long lasting epigenetic impacts [250, 251]. Environmental exposures can include stress, diet, exposure to pollutants, as well as exogenous pharmaceuticals and chemicals used during pregnancy, all of which interact with the systemic chemical environment to elicit a biological response [252]. For example, children of women who experienced severe malnutrition during pregnancy as a direct result of the Dutch famine, have higher BMIs and display glucose intolerance [73]. Additionally, recent epidemiological studies have identified positive correlations with several chemicals measured during pregnancy, such as phthalates and persistent organic pollutants, and obesity in the children [253-255]. Exogenous chemicals that can promote the development of obesity and metabolic syndrome have been deemed environmental obesogens, a class of endocrine and metabolic disruptors [66, 256].

There are multiple mechanisms of action by which obesogens could act to drive obesity including nuclear hormone receptor interaction, neuroendocrinology effects on hunger and satiety signaling, interference with coactivator and corepressor recruitment, membrane receptor signaling, cell membrane and organelle lipid bilayer destabilization (e.g. mitochondrial membrane potential), epigenetic programming and commitment of stem cells towards adipogenic lineages. The most well studied mechanism of action is via

compounds that act as agonists for the nuclear receptor PPAR γ [92, 166, 257]. Primarily, these obesogenic activities have been identified and evaluated *in vitro* using methods described in Chapter 2 and Chapter 3 such as transactivation assays and adipogenic differentiation assays, respectively. Published work described in these chapters identified DOSS as a probable obesogen using molecular modeling, receptor transactivation assays and adipogenic differentiation of murine preadipocytes and human bone marrow derived mesenchymal stem cells [258]. Using similar assays, other groups have identified similar molecules, the anionic surfactants SDS and SDBS, as PPAR γ agonists as well, suggesting a previously unidentified and unexplored mechanism of action for this class of molecules [219]. The hydrocarbon chains of many anionic surfactants resemble hydrocarbon chains of fatty acids (such as arachidonic acid and oleic acid), one class of endogenous ligands for PPAR receptors.

However, to the best of our knowledge, these molecules have not been evaluated for their obesogenic effects *in vivo*, especially using and considering *in utero* development as vulnerable and a critical window for exposure. Studies of obesogen exposure *in vivo* have primarily evaluated the obesogenic effects in the offspring of exposed dams and mothers using markers of adiposity and metabolic syndrome such as a combination of morphometrics, glucose tolerance, body composition, circulating adipokines and cytokines, tissue gene expression and epigenetic marks like DNA methylation. Obesogens that act as ligands to activate PPAR γ and have currently been evaluated *in vivo* include MEHP [158], tributyltin [93], PFOA[156], and triflumazole [159].

Approximately 11- 38% of pregnant women experience constipation during pregnancy due to physiological and anatomical changes directly impacting the gastrointestinal tract including increased progesterone levels, water absorption, and increased blood volume associated with anemia [238]. Common practice to treat pregnancy related constipation is via prescription of stool softeners, specifically Colace/docusate sodium, comprised of DOSS and iron-supplemented vitamins containing DOSS [153]. Given the widespread use of docusate sodium stool softeners during pregnancy at up to 500mg a day during gestation as well as postpartum, human exposure to DOSS is evident especially during vulnerable times of development. While levels and duration of Colace use vary among women, the highest levels and longest duration are associated with African Americans and underserved populations (personal comm. DDS). Therefore, it is essential to fully understand the use and safety of DOSS during pregnancy.

The aim of this study was to use a mouse model to evaluate DOSS as an obesogen *in vivo* with a dose and exposure scenario relevant to pregnant women. The offspring of exposed dams were analyzed for multiple established obesogenic endpoints to test the hypothesis that developmental DOSS exposure promotes adult onset of obesity associated symptoms (metabolic syndrome).

4.2. Materials and Methods

4.2.1. Animal husbandry and treatment

C57BL/6J mice were housed in the MUSC DLAR facilities in accordance with IACUC standards. This strain of mice (and especially males of this strain) are susceptible to diet and environmental induced obesity and metabolic syndrome [259-261]. Animals

were fed a standard chow diet of Envigo/Teklad 2918 containing 18.6% crude protein, 6.2% fat, and 44.2% carbohydrates. Sterile corncob bedding was used in cages, except when mice were fasted (see 4.2.2). Room temperature was maintained between 68-74⁰F and relative humidity between 30-70%. Light was controlled to 12hr:12 hr light:dark cycle. Two females and one male were placed in a cage together to initiate breeding at D0. At D7, females were weighed to determine if they were pregnant based on weight gain. It was determined that a 5.5g weight gain correlated with E11.5, at which point females were housed individually with water bottles containing water and either vehicle control or DOSS. The automatic watering system was inactivated by either disconnecting the water supply hose or by removal of Lixit sipper tubes.

Pregnant dams (n=3-4 per group [159]) were exposed to either vehicle control (0.5% carboxymethylcellulose; CMC) or 31.25 µg/mL DOSS from E11.5 through weaning. The dose we chose to use is representative of a dose received by a pregnant woman (88.5 kg) taking 500mg of DOSS in the form of Colace stool softener daily (5.6mg/kg) given that a mouse drinks about 4mL per day and weighs around 25g. The timing of exposure was based on the incidence of constipation in women rising up through mid-gestation [262]. CMC was used to increase palatability of the DOSS solution and had been used as a vehicle control in other studies on obesogens [94]. Stock bottles of each solution were prepared as needed (usually weekly). A 1% CMC solution in autoclaved water and a 62.5µg/mL solution of DOSS in autoclaved water were prepared and then mixed together in a ratio of 1:1 to achieve the final desired concentration for treatment. Autoclaved water was used to dilute the 1% CMC solution 1:1 to achieve the desired concentration of 0.5% CMC for the vehicle control.

Only litters with 5-7 pups were used for analysis to control for nutrient availability *in utero*. Due to this criterion, some litters had to be eliminated resulting in decreased sample size for certain groups. Therefore, the first “Cohort A” experiment was repeated in a second cohort approximately five to six months later. In figures and discussion of results, data from this second group of animals is referred to as Cohort B and are represented by open black circles (controls) and open blue squares (DOSS treated). Solid black circles (controls) and solid blue squares (DOSS treated) are used for animals of Cohort A.

4.2.2. *Oral glucose tolerance test*

At 12 weeks of age, animals were assessed for glucose tolerance using an oral glucose tolerance test (oGTT). Animals were fasted for 5-6 hours before administering the test by changing animals to cages containing alphasadri bedding with no food but access to water. At T0 animals were weighed and a baseline blood glucose measurement was taken by making a 0.5-1mm cut at the base of the tale with a razor blade. A glucose bolus (2mg/g body weight) was administered via oral gavage followed with blood glucose measurements at 15, 30, 60, 90 and 120 minutes. TRUEBalance glucose meter and strips were used for all measurements. If a “HI” error was obtained, the value was assigned as 600 (mg/dL), the maximum output of the detector. If other errors occurred, the measurement was taken again using a new test strip.

4.2.3. *Body composition assessment*

Dual-Energy X-Ray Absorptiometry (DXA) was used to assess body composition at 12 weeks of age. Mice were anesthetized using isoflurane, placed into the DEXA instrument and scanned individually, ventral down. Data were collected for bone mineral

density (BMD; g/cm²), bone mineral content (BMC; grams), bone area (cm²), lean mass (grams), fat mass (grams) total mass (grams) and percent fat. BMD is defined as the ratio of BMC to bone area and is primarily used for assessment and prediction of osteoporotic associated fractures. The amount of BMC present in the bone will influence the amount of energy absorbed. Denser bones absorb more energy and a relative energy/pixel can be calculated as a density [263]. BMD and BMC are tightly correlated with one another while BMD and bone area correlations are weaker possibly due to variations in bone size in different regions [264]. Both BMD and bone area are associated with stronger bones although some studies suggest bone size and not density is a better measure for stiffness [265]. DXA data was only collected on the first cohort of mice due to instrument availability. At 16 weeks of age, mice were sacrificed and the reproductive fat pads (epididymal or EWAT; and ovarian or OWAT) and inguinal fat pads (IWAT) were dissected and weighed. Percent fat was calculated as total fat pad weight relative to total body mass at time of sacrifice.

4.2.4. Animal sacrifice and tissue collection

Animals were sacrificed and exsanguinated at 16 weeks of age after being anesthetized (freshly prepared tribromoethanol solution; 125 mg/Kg; 15 µL of 2.5% Avertin per gram of body weight, i.p.) and cervically dislocated. Reproductive fat pads (EWAT and OWAT), inguinal fat pads (IWAT) and liver were dissected, weighed, and a 200mg piece was homogenized in 1mL Trizol for subsequent nucleic acid isolation. Remaining fat pads were fixed over night at 4⁰C in 4% PFA in PBS. The following day, fixed tissues were washed 2X with PBS then stored in 70% ethanol until further analysis.

4.2.5. Circulating adipokine and cytokine levels

At time of sacrifice (16 wks), plasma was collected from each mouse. Blood was collected via cardiac puncture into EDTA coated tubes and incubated at room temperature for at least 15 minutes. Blood was then transferred to Eppendorf tubes and centrifuged at 2,000 x g for 10 minutes at 4⁰C. Plasma was collected (about 500uL), aliquoted and stored at -80° C until analysis.

Adiponectin, leptin, insulin, IL-6 and TNF-alpha were measured using commercially available kits from Meso Scale Discovery (MSD) following the manufacture's protocol and MESO QuickPlex SQ 120 instrument. Specifically, the Mouse Adiponectin Kit (K152BXC-1), the Mouse Metabolic (leptin and insulin) Kit (K15124C-1) and mouse Proinflammatory Panel (IL-6 and TNF-alpha) V-PLEX Kit (K15048D) were used. This method is similar to standard sandwich ELISA immunoassay protocols in that it utilizes a capture antibody pre-coated onto a plate, followed by addition of the sample in which the target of interest binds to the capture antibody. A detection antibody is then added, binds to the analyte and emits a measurable and detectable signal. These MSD assays utilize detection antibodies labeled with electroactive (rhenium-based) compounds that emit light in the presence of a redox-sensitive compound when voltage is applied to the plate. This allows for more sensitivity, a broader dynamic range, less signal to noise background, the ability to multiplex samples and fewer washing steps than standard ELISA methods. Specific protocols differ slightly for each metabolite. Plates were pre-coated with capture antibodies and provided by the manufacturer. An eight-point standard curve was prepared with provided calibrators and buffers each time the assays were run. Plasma samples were then diluted

as suggested by MSD with supplied diluent before measurement. Calibrator or diluted sample were added to the plate in duplicate and incubated at room temperature with shaking for two hours. The 96-well plate was then washed three times with 150 μ L of wash buffer (0.5% Tween20 in PBS) per well. Supplied detection antibody was added to each well and incubated at room temperature with shaking for two hours. The plate was then again washed three times with wash buffer, 150 μ L of 2X Read buffer was added per well and the plate was read on the MSD SECTOR instrument. Discovery Workbench 4.0 Software (Meso Scale Discovery) was used to determine analyte measurements using standard curves.

4.2.6. Gene expression

At time of sacrifice, approximately 200mg of tissue was homogenized in Trizol reagent and stored at -80°C. RNA was isolated using Trizol Reagent following the manufacturer's protocol. For adipose tissue extractions, an additional chloroform wash step was performed to minimize phenol contamination typically associated with lipid rich tissues. RNA concentration and quality was assessed using Nanodrop ND 1000 (Thermo Fisher Scientific) absorbance ratios 260/280 (2.0-2.2) and 260/230 (>1.5). One μ g of RNA was reverse transcribed to cDNA using Superscript III First-Strand Synthesis Super Mix (Invitrogen) following the manufacturer's instructions. qPCR was performed using the FastStart Essential DNA Green Master Kit (Roche). All primers were designed to be intron spanning to ensure no DNA contamination could be amplified. The same touchdown PCR cycle program was used for all primer pairs: 95°C 10 sec, 66°C-56°C 20 sec dropping a degree each cycle for 10 cycles, then remaining 35 cycles at 56°C, 72°C 20 sec for a total of 45 cycles on the LightCycler 96 system (Roche). Results were

normalized to the reference gene *Hprt* using the $\Delta\Delta C_t$ method as it showed minimal variation between samples across treatment (Ct +/- 0.34 SD). Calibration curves were prepared to ensure equal and high PCR efficiencies (90-110%) between test and reference genes. Data are expressed as a fold change in treated animals compared with control animals. Primers used are listed in Table 1.

Table 1. Genes and corresponding primers used for qRT - PCR analysis

Gene	Forward Primer	Reverse Primer
<i>Hprt</i>	AGGCCAGACTTTGTTGGATTTG	TTCAACTTGCGCTCATCTTAGG
<i>AdipoQ</i>	G TTCCTCTTAATCCTGCCCA	CTCCTGTCATTCCAACATCTC
<i>Leptin</i>	CCTGTGTCGGTTCCTGTG	CCTGTTGATAGACTGCCAGAG
<i>IL-6</i>	AGCCAGAGTCCTTCAGAGAGAT	GAGAGCATTGGAAATTGGGGT
<i>Cox2</i>	TTCAACACACTCTATCACTGGC	AGAAGCGTTTGCGGTACTCAT
<i>Nox4</i>	CCTTTTACCTATGTGCCGGAC	CATGTGATGTGTAGAGTCTTGCT

4.2.7 DNA Methylation Analysis via Targeted Bisulfite Sequencing DNA Isolation

After RNA was isolated from samples, residual interphase and organic material was stored at 4°C (Section 4.2.6) until DNA isolation was performed. Samples were centrifuged at 15,000 x g at 4°C for 15 minutes. Any remaining aqueous phase containing RNA was removed. An equal volume (about 600µL) of Back Extraction Buffer (4 M guanidine thiocyanate, 50 mM sodium citrate and 1 M Tris) was added to interphase-organic phase mixture. The sample was vigorously mixed by inversion and incubated at room temperature for 10 minutes. Samples were centrifuged at 15,000 x g at 4°C for 15 minutes and 420µL of the aqueous phase was transferred to a separate tube. At this point samples were processed following a modified protocol for Qiagen Blood and Tissue

DNeasy Kit. Briefly, 200uL of ethanol was added to the sample, mixed well and pipetted onto a provided spin column, centrifuged and flow through discarded. The column was washed 1x with 500uL Buffer AW1, then 1X with 500uL Buffer AW2. Care was taken to ensure the column was completely free of ethanol before eluting DNA with 75uL Buffer AE. DNA concentrations were quantified using Nanodrop ND 1000 (ThermoFisher Scientific).

Bisulfite Conversion and PCR Amplification

Genomic DNA (500ng) from IWAT of 16 week-old mice was bisulfite converted for methylation analysis using the Methylamp DNA Modification Kit (Epigentek) following the manufacturer's protocol. Eight control samples (4 from Cohort A and 4 from Cohort B) and all 12 treated samples were used. Target genes for PCR were selected based on previous studies that identified methylation or expression changes in these genes as a result of obesity, glucose intolerance and diabetes, or obesogen exposure (referenced in Table 2). Studies from both human and mice were utilized. For targets where primers were listed in publications, these primers were used with conditions optimized in house. For new targets, primers were designed using MethPrimer in promoter regions of genes flanking CpG islands. For PCR amplification, 12.5 ng of converted DNA was used with EpiMark HotStart Taq DNA polymerase following the manufacturer's recommendations. Primer sequences, PCR conditions and references are listed in Table 2. Amplification of single products was validated using gel electrophoresis. PCR products were purified using GenCatch PCR Clean Up Kit (Epoch) and quantified using Nandrop equipment (Thermo Fisher Scientific). All products from a

single individual were then pooled using equal nanomoles using volumes adjusted based on nM concentration (based on lowest concentration) for sequencing.

Illumina Library Prep, Next Generation Sequencing and Analysis

The MUSC Cancer Genomics core was used for next generation sequencing of products. The sequencing library was prepared using the TruSeq Kit, following the manufacturer's protocol beginning at "End Repair". Adapters were ligated so each individual was barcoded. Samples were then paired end sequenced on an Illumina MiSeq. All data analysis was performed in BaseSpace. Raw sequences were trimmed using Trimmomatic [266]. Methylation analysis was performed in Methyl Seq v1.0 (Illumina, Inc.). Methyl Seq aligns generated sequences to a bisulfite converted genome using Bowtie 2 [267]. Sequences were aligned to Mouse mm9 using a targeted manifest specifically for targeted amplicons based on chromosomal locations for start and end sites. CpG methylation status was obtained for each CpG in an amplicon using BisMark [268]. If a sample didn't have at least 12 reads per CpG site it was dropped from analysis. No correlation was observed between read count and methylation status (data not shown).

4.2.8 Plasma lipidomic profiling

Lipids were extracted from blood plasma samples using Bligh-dyer extraction [269]. Thirty microliters of plasma were spiked with lipid internal standards (36 μ L), and 4mL of 1:1 chloroform:methanol, followed by the addition of 1.8mL water. Samples were then incubated on ice for 30 minutes, vortexed for 20 seconds and centrifuged at 2000 rpm for 10 min to separate organic and aqueous layers. The organic layer was collected and the aqueous layer was re-extracted with 1mL 1:1 chloroform:methanol. The

organic layers were combined, transferred to a new tube then dried down under nitrogen and reconstituted in 50uL isopropanol.

All lipid extracts were analyzed by ultra-high performance liquid chromatography coupled to high-resolution mass spectrometry (UHPLC-HRMS). Samples were de-identified and individuals performing extractions and running samples were blinded to sample conditions. Mass spectra were acquired on a Thermo Scientific Orbitrap Fusion Lumos Tribrid mass spectrometer equipped with a heated electrospray ionization (HESI II) probe in positive and negative ion mode. HESI and mass spectrometric parameters for lipid extracts were as follows in positive/negative ion mode, respectively: spray voltage: 3.5/2.5 kV, sheath gas: 40/35 AU; auxiliary nitrogen pressure: 15 AU; sweep gas: 1/0 AU; ion transfer tube and vaporizer temperatures: 325 and 300/275 °C, respectfully; and RF lens level: 30. Full scan, data-dependent MS/MS (top10-ddMS2), and data-independent acquisition mode data were collected at m/z 150-2000, corresponding to the mass range of most expected cellular lipids. External calibration was applied before each run to allow for LC-HRMS analysis at 120,000 resolution (at $m/z=200$).

A Thermo Scientific Vanquish UHPLC system (Thermo Scientific, San Jose, CA) was coupled to the Orbitrap Fusion Lumos Tribrid for the chromatographic separation of lipids. The autosampler temperature was maintained at 4 °C for all experiments. Solvent extraction blanks and quality control samples were jointly analyzed over the course of a batch (10-15 samples). A Waters Acquity™ C18 BEH column (2.1 × 100 mm, 1.7 μm particle size, Waters, Milford, MA) maintained at 60 °C was used for all lipidomic studies. The injection volume was 5 μL in positive and negative ion mode with a mobile phase flow rate of 450 μL/min. The gradient program consisted of mobile phase C [60:40

v/v acetonitrile/water] and mobile phase D [90:8:2 v/v/v isopropanol/ acetonitrile/water], each containing 10 mM ammonium formate and 0.1% formic acid. The gradient included 32% D at 0 min, 40% D at 1 min, a hold at 40% D until 1.5 min, 45% D at 4 min, 50% D at 5 min, 60% D at 8 min, 70% D at 11 min, 80% D at 14 min, 100% D at 16 min, and a hold at 100% D until 17 min. The total run time was 22 min, including a 5 min equilibration

Full scan raw data files acquired from Xcalibur™ (Thermo Fisher Scientific), centroided and converted to a useable format (mzXML) using MSConvert. Data processing and peak area integration was performed using MZmine, resulting in a feature intensity table. The resulting feature table was filtered using extraction blank samples in FRAMe (Feature Reduction Assistant for Metabolomics v1.0). Only features with a signal/noise ratio greater than 10 times that of the blank were included. LipidSearch™ (Thermo Scientific) and LipidMatch were used to identify features [270]. Peak areas were normalized to plasma weight for each sample.

4.2.9 Statistical analysis

For oGTT data, area under the curve (AUC) was calculated for each individual in GraphPad Prism. Means for AUC from treated and control groups were then compared using unpaired student's t-test. Additionally, means for blood glucose were compared at each time point between treated and control groups using two-way ANOVA.

Since data were collected from two different cohorts and grouped together for graphical display, significant differences were tested between controls from each group and treated animals using students t-test and reported in the text. Normality and equal variances was assessed by Shapiro-Wilks test and Brown-Forsythe or F test respectively,

before proceeding with mean comparisons. If data did not pass the assumptions, data were log transformed to increase normality or Welch's correction was used to account for differences in variance. Results are discussed in each section and statistical tests are specified in Figure legends. Two-way ANOVA was also used to assess differences between treatment and cohorts and is described in text. For DNA methylation analysis, average methylation results are presented for each CpG site in an amplicon. Two-way ANOVA was used to assess overall treatment effect and differences observed at specific CpG sites.

4.3 Results

4.3.1 DOSS treatment induces glucose intolerance in male mice

Glucose tolerance tests are used to assess metabolic function clinically in humans at risk for diabetes and can be used in mouse models of diabetes and obesity, as well. To determine if DOSS treatment during development altered glucose tolerance in F1 mice, oral glucose tolerance tests were performed at 12 weeks of age on control and animals treated with DOSS *in utero*. Male, but not female animals exposed to DOSS during development display marked glucose intolerance compared to animals receiving vehicle control (Figures 1 and 2). Data are represented with cohorts grouped together as well as for each Cohort separately. When grouped and analyzed together all male data indicates DOSS induces impaired glucose tolerance via significantly higher blood glucose levels at 15 min, 30 min, and 60 min when compared to control males using a repeated measures ANOVA (Figure 1A). Similarly, treated animals show a significantly increased area under the curve, indicative of glucose tolerance impairment (Figure 1B $p=0.0012$). For animals in Cohort A only, significant increase in blood glucose was observed at 15 and

30 min only (Figure 1C). Significant increases in area under the curve were also observed in treated animals from this cohort (Figure 1D $p=0.0004$). For cohort B, higher levels of blood glucose were observed at all time points, although this trend did not reach significance (Figure 1E). Similarly, DOSS treated animals in Cohort B displayed increased area under the curve, although these values did not achieve significance (Figure 1F $p=0.0898$).

For female animals, the data indicate DOSS did not significantly alter normal glucose homeostasis (Figure 2). For Cohort A, increases in blood glucose, although not significant, were observed at T15 and T30 only, however basal levels were reached by T60 in both control and treated animals (Figure 2C). No differences between control and treated females were observed in the second group on animals (Figure 2E and F).

Of note, in the second cohort, male and female control animals had higher levels of blood glucose compared to cohort A. This is likely attributed to the test being performed by different individuals and successful and accurate delivery of the glucose bolus, since animals do not show significant differences in basal glucose levels.

4.3.2. DOSS treatment increases body mass, fat grams, fat percentage and reduces bone area in male mice

By definition, *bona fide* obesogens have been shown to increase overall body weight as well as fat percentage in treated animals [256]. At 12 and 16 weeks of age, F1 males from treated dams weighed significantly more than females (Figure 3A and B $p<0.0001$). No significant cohort differences in males were observed between controls at 12 and 16 week ($p=0.1480$ and $p=0.2044$) and 12 and 16 week treated animals ($p=0.2012$ and $p=0.1510$) from each cohort so they were grouped together for analysis (unpaired t-test with Welch's correction for unequal SD).

F1 males from treated dams were slightly but significantly heavier than control males at 12 ($p=0.015$) and 16 weeks ($p=0.0181$) of age with mean/median values of 27.44/27.14 g and 29.42/28.25 g for treated animals and 26.28/25.9 g and 28.27/28.00 g for control animals respectively (Figure 3A; two-tailed Mann Whitney non-parametric test was used because a non-Gaussian distribution was observed). No significant differences were observed between control and treated females at either 12 or 16 weeks of age (Figure 3B).

For a subset of animals (Cohort A), DXA scans were used to assess body composition including percent body fat, fat mass, lean mass, bone area, bone mineral density and bone mineral content at 12 weeks of age (Figure 2). In male mice, DOSS treatment increased total body fat percentage analyzed by DXA with mean fat percentages of 14.5% and 16.6% for control and treated males, respectively (Figure 2A, $p=0.0476$). There was also a significant increase in fat grams for male mice with mean fat mass values of 3.2g and 3.9g for control and treated male mice respectively (Figure 2B, $p=0.0200$). Importantly, there were no differences observed in lean mass (Figure 2C), indicating that overall body weight gain was due to increase in fat mass. Additionally, a significant reduction in male bone area, 8.30 and 8.83 cm² for treated and control animals respectively, and a decrease, although not significant in bone mineral density and bone mineral content were observed (Figure 2D $p=0.0014$ and E). No significant differences were observed in female mice. Based on the nature of the equation to calculate BMD ($BMD = BMC/BoneArea$), a reduction in bone area would not influence a reduction in BMD given constant BMC. Bone Area as measured by DXA is calculated based on a 2D planar image and is not a complete representation of total bone volume. Bone area can

also be influenced by different regions of the body, suggesting BMC and BMD are better indicators of bone strength although some studies in human suggest bone size is a better determinant for stiffness than density [264, 265].

At 16 weeks of age, all animals (Cohort A and B) were sacrificed and gross tissue weight for liver, inguinal (IWAT) and reproductive white adipose tissue (male EWAT and female OWAT) was recorded. Fat percentage was calculated for each fat pad individually and combined for a representative total fat percentage ((Total WAT weight/16wk body mass) X 100). When all animals were analyzed together, F1 males from treated dams showed significant increases in grams adipose tissue for IWAT ($p=0.0099$), EWAT ($p=0.0205$) and total WAT ($p=0.0101$) (Figure 4C). Graphically display of these data, suggest this result may be driven by Cohort differences with F1 males from treated dams in Cohort B exhibiting more adiposity than those from Cohort A. In fact, F1 males from treated dams in cohort B, but not Cohort A, showed a significant increase in grams adipose tissue for IWAT ($p=0.0001$), EWAT ($p=0.0008$) and total WAT ($p<0.0001$) relative to grouped controls. No significant differences were observed between control animals in different cohorts and were therefore grouped together for statistical analyses. Body fat percentage as well as fat pad specific fat percentage also significantly increased in treated animals (Figure 4E), primarily driven by Cohort B DOSS-treated animals. No significant differences were observed in female mice for adipose tissue weight or percent (Figure 3D and F). Similarly, no differences were observed between treated and control animals for liver weight in both males and females (data not shown).

Bone density measurements were not performed on the second group of animals. Although an increase in percent body fat measured by tissue weight at 16 weeks was not observed in Cohort A, the DXA scans of Cohort A at 12 weeks did provide a comprehensive indication of increased body fat percentage due to DOSS treatment. This could indicate that overall body adiposity measured by DXA is more likely to detect significant differences than IWAT/EWAT weight measurements alone, which represent only a portion of overall adiposity. This could also indicate that differences in adiposity decrease from 12 week to 16 weeks of age. That said, Cohort B did result in a larger increase in body fat observed in tissue weight suggesting that IWAT/EWAT weight measurements alone can suffice and that the effects of DOSS treatment on body composition can be variable and in this case were more pronounced in the second group. These data demonstrate variability in cohort or individual susceptible to the effects induced by DOSS exposure during development.

4.3.3. DOSS treatment alters circulating adipokine levels

In both human and mouse studies, obesity and metabolic disorders are often associated with differences in multiple circulating adipokines and cytokines that are either increased or decreased based on their given disease state. For example, a decrease in adipose tissue-derived circulating adiponectin and an increase in circulating leptin are hallmarks of obesity and metabolic syndrome [271]. Also, obesity can be characterized as a chronic low-grade inflammatory disease [51]. Thus, to further characterize the level and type of metabolic disruption observed in animals treated with DOSS, adipokine (adiponectin and leptin), proinflammatory cytokine (IL-6 and TNF-alpha) and insulin levels were chosen for analysis in plasma. Multiple diet-induced obesity studies focus on

male C57BL/6 mice [272] [273]. Also, due to limited resources and since male C57BL/6 animals displayed a significant phenotype while females did not, adipokine and cytokine levels were measured in control and DOSS males only.

Adiponectin is a signaling molecule exclusively produced by adipose tissue and plays a role in insulin sensitization and glucose homeostasis [274]. In both cohorts, there were significant differences in adiponectin levels in treated animals compared to controls (Figure 5). To account for increases in adiposity in treated animals (Figure 3), adiponectin levels were normalized to gram weight of adipose tissue (IWAT + EWAT) for all individuals, a method that has been previously utilized [115]. After correcting for adiposity, no differences were observed between controls or treated animals between cohorts and therefore both cohorts were grouped together for each controls and treatment groups (data represented as $\mu\text{g adiponectin/mL plasma} \times \text{gram adipose tissue}$). Relative (normalized per gram fat) circulating adiponectin levels were significantly lower in F1 males from treated dams than in control males with means of $9.51 \mu\text{g/mL} \times \text{g}$ and $13.30 \mu\text{g/mL} \times \text{g}$ respectively (Figure 5A $p=0.0029$). Primarily glucose intolerance and adiponectin, but also obesity and adiponectin have previously been described to have an inverse relationship [275], although positive correlations between circulating adiponectin and adipose fat mass have been observed [276, 277]. In fact, in our animals adiponectin is positively correlated with adipose tissue weight in both control and treated mice (Figure 5B). However, in cohort A treated animals displayed lower mean circulating levels of adiponectin ($12.7 \mu\text{g/mL}$) compared to controls ($15.17 \mu\text{g/mL}$), while in cohort B, treated animals displayed higher circulating levels of adiponectin ($20.66 \mu\text{g/mL}$) compared to controls ($17.43 \mu\text{g/mL}$). This observation might be expected given that

treated animals from Cohort A exhibit more severe glucose intolerance than those from Cohort B (Figure 1). The increase in adiponectin in treated animals from Cohort B (open blue squares) is likely driven by increases in body fat percentage even though these animals also display mild glucose intolerance.

The significant reduction in normalized adiponectin levels observed in treated animals could be due to significant changes in white adipose tissue gene expression, specifically of the inguinal adipose depots (IWAT), since *AdipoQ*, the gene encoding adiponectin, is down regulated in treated versus control animals in IWAT (Figure 5C $p=0.0153$) regardless of cohort. Although not significant, a trend for lower *AdipoQ* expression was observed in female animals (data not shown). Similarly, decreased gene expression of *AdipoQ*, although not significant, was observed in the gonadal (EWAT) adipose tissue as well (data not shown). These data further support the hypothesis that prenatal DOSS treatment can result in decreased adiponectin in C57BL/6J male mice relative to control males.

Leptin is an adipokine that regulates satiety and control of appetite and positively correlated with adiposity and obesity [278]. When animals from both cohorts were group together significant increases in leptin were observed (Figure 5D, $p=0.0332$ Mann Whitney). As expected, leptin levels were positively correlated with fat grams in our animals (Figure 5E), as a positive relationship between leptin and adiposity markers is well documented in both humans and mice [279, 280]. Circulating mean leptin levels for Cohort A control and treated animals were 2.91 ng/mL and 2.91 ng/mL, respectively and for Cohort B were 4.50 and 11.28 ng/mL, respectively. Thus, no significant difference in leptin was observed between control and treated animals in Cohort A ($p=0.99$) or between

controls from either group ($p=0.2275$) even though there was an increased trend. However, treated animals from Cohort B showed increase circulating levels of leptin compared to combined controls ($p=0.0002$ Mann Whitney). Notably, the cohort effects for circulating leptin levels were much more pronounced than for adiponectin (Fig. 5B, E) as expected due to the increase in fat mass in Cohort B treated animals. While some individuals from Cohort B displayed high leptin expression relative to controls, no significant differences were observed between control and treated animals (Figure 5F). Other fat depots may produce and secrete more leptin than IWAT which was investigated here.

While we also measured circulating insulin levels to determine if the glucose intolerance observed in our treated animals was due to insulin desensitization marked by hyperinsulinemia, we observed no significant differences between any of the groups (Figure 5G, $p = 0.8507$). However, the data for insulin were not taken after fasting, which would be more indicative of insulin desensitization. In future experiments plasma for insulin measurements should be collected after fasting and prior to gavage in oGTT tests.

4.3.4. DOSS treatment is associated with a persistent inflammatory state

IL-6 is a proinflammatory cytokine secreted by immune cells. Obesity and type 2 diabetes (T2D) are often accompanied by an inflammatory state driven by infiltration of adipose tissue with macrophages [281]. To determine if DOSS treated animals showed indication of a proinflammatory state, we analyzed circulating IL-6 levels. We observed increased circulating levels of IL-6 in treated animals compared to controls without cohort differences and therefore cohorts were grouped together for analysis. The mean levels of IL-6 were 13.70 pg/mL and 48.12 pg/mL for control and treated animals

respectively, where treated animals had significantly higher levels of IL-6 than controls (Figure 6A, $p=0.0112$). However, unlike adiponectin and leptin, we did not observe a correlation between body fat percentage and circulating IL-6 levels in either treated or control animals (Figure 6B).

TNF α is another inflammatory cytokine secreted by immune cells positively correlated with obesity and T2D in some cases. We analyzed mouse plasma for levels of TNF α . In cohort B we observed non-detectable levels in four samples. These values were removed from the analysis and attributed to assay error given that the values were below the LOD for TNF α in this assay. Although mean circulating TNF α was higher in DOSS animals (8.44 pg/mL) compared to control animals (7.54pg/mL), it was not significant (Figure 6D). However, we did observe a cohort effect for TNF α levels. There was a slight but significant increase in circulating TNF α levels in DOSS treated animals for Cohort A only ($p=0.0277$). This was a notable result, as most other significant differences occurred in Cohort B, but not Cohort A.

We also investigated gene expression changes in adipose tissue associated with inflammation. Although a few individuals had elevated expression of IL-6, we observed no significant differences in IL-6 gene expression in IWAT tissue, despite increase circulating levels of IL-6 in treated animals (Figure 6C). However other fat depots could be contributing to overall circulating IL-6 levels. And within adipose tissue, the stromal vascular fraction accounts for 90% of the IL-6 expression in adipose tissue although it represents a small percentage of adipose tissue cells [52]. Other genes we investigated were cyclooxygenase 2 (*Cox2*) and NADPH oxidase (*Nox4*). Elevation in expression for both *Cox2* and *Nox4* are associated with the presence of reactive oxygen species and

systemic chronic inflammation [282, 283]. We observed significantly increased expression of both Cox2 and Nox4 expression in IWAT from DOSS exposed male mice (Fig. 6E, F). Interestingly, Cox2 expression was primarily significant in Cohort B (Figure 6E), while Nox4 (Figure 6F) expression was more significant in Cohort A.

4.3.5 DOSS treatment altered DNA promoter methylation of IL-6 and Cox2

Since we observed persistent changes in gene expression and circulating levels of adipokines and cytokines in 16 week-old F1 males of DOSS treated dams, we hypothesized that promoter methylation may be altered at these loci in IWAT. We investigated promoter methylation at several genes identified to be significant to DOSS exposure (adiponectin, IL-6 and Cox-2) and/or previously identified to be regulated by DNA methylation in response to high fat diet, obesity or T2D (*Leptin*, *Pparg*, *Glut4*, *Fasn*, *Irs1*, *Hmox1*, *Fabp4*). A complete list of loci interrogated, bisulfite primers used and references can be found in Table 2. Highlighted here are the most significant results.

We observed decreased levels of circulating adiponectin as well as decreased levels of gene expression in IWAT tissue, suggesting the adiponectin promoter may be hypermethylated, repressing gene expression. We performed targeted bisulfite sequences for 6 CpG sites in the adiponectin promoter, four sites which have been associated with gene expression in response to high fat diet (deemed adiponectin region 2) and two sites nearby which were not associated with gene expression (deemed adiponectin region 1) (Figure 7A). Unexpectedly, at region 1 significant hypomethylation was observed, particularly at CpG site 1 (Figure 7B) in tissue from treated animals. There was no significant difference in average region 2 promoter methylation between treated and control animals, although on average treated animals had slightly higher mean overall

methylation and at each CpG site in R2 (Figure 7C). Particularly interesting results were observed at CpG site 3 in which 58.33% of treated animals had over 80% methylation compared to 28.57% for controls. When CpG 3 methylation was correlated with gene expression, no significant positive or negative correlations were observed (Figure 7D).

Although changes in *Il-6* gene expression was not observed, there were significant increases in circulating levels of IL-6 in response to prenatal DOSS exposure. Therefore the promoter region of *Il-6* was investigated for changes in DNA methylation. Five CpG sites roughly 300bp upstream of the *IL-6* transcription start site that were previously identified as possible regulatory CpGs were evaluated for methylation status [284] (Figure 7E). DOSS treatment significantly reduced overall promoter methylation (Figure 7F $p=0.0042$ Two way ANOVA) and especially at CpG site 2 (Figure 7F $p=0.045$). As with adiponectin, no significant correlation between gene expression and DNA methylation was observed at this loci (Figure 7G). However, there was a significant inverse correlation between *IL-6* methylation and circulating *IL-6* levels (Figure 7H $p = 0.011$).

Since there were changes in *Cox2* expression relative to treatment and *Cox2* promoter hypermethylation has been linked to gene expression in other studies [285], 14 CpG sites about 500bp upstream of the *Cox2* transcription start site were evaluated for methylation status (Figure 7I). While treatment did not affect the overall *Cox2* promoter methylation for the region (Figure 7J $p=0.1277$), average DNA methylation at CpG site 1 was significantly reduced in treated animals (Figure 7K $p=0.0052$ outlier removed). While increased *Cox2* gene expression for IWAT was observed there were no significant correlations between CpG site 1 methylation and *Cox2* expression (Figure 7L).

No significant differences in promoter methylation were observed for *Leptin*, *Fasn*, *Pparg*, *Glut4*, *Irs1*, *Fabp4*, or *Hmox1*. Specific average methylation results for all loci are displayed in Table 3.

4.3.6 DOSS treated animals have elevated circulating phospholipids associated with high fat diet induced obesity and diabetes

Due to advances in mass spectrometry and ultra high performance liquid chromatography, untargeted lipidomics has been employed to survey for changes in circulating lipids associated with obesity and diabetes [270, 286, 287]. Targets identified may potentially be used as diagnostic biomarkers as well as to elucidate cellular mechanisms associated with disease states. We used an untargeted lipidomics approach to identify significant changes in circulating lipids associated with DOSS exposure. We were able to identify 664 features in positive mode and 171 features in negative mode. One treated individual was excluded from analysis due to outlier behavior as identified by random forest test. Multiple lipids were significantly increased in 16 week-old F1 male offspring of dams exposed to DOSS, including several phosphatidyl choline species, two phosphatidylethanolamine species, one cholesterol ester and one oxidized phosphatidyl choline species. We observed significant or near significant increases in relative peak area for PC(34:3) (p=0.0433), PC(36:1) (p=0.0053), PC(18:0_20:1) (p=0.0179), PC(18:0_20:3) (p=0.0383), PC(38:4) (p=0.0125), PE(18:0_20:1) (p=0.0149), PE(18:0_20:3) (p=0.0444), CE(20:3) (p=0.0583), and OxPC(24:1) (p=0.0224) as shown in Figure 8A-I. Visual inspection of the data suggests that for PC(34:3), PC(18:0_20:1), PC(38:4), and PE(18:0_20:3) the relative increase in F1 males prenatally exposed to DOSS is driven by animals from Cohort B. Several lipid species identified here have also been identified as associated with high fat diet induced obesity in C57BL/6J mice

including PC(36:1), PC(38:3), PC(38:4) and CE(20:3) [288]. Similarly, although not significant, we did observed reductions in several LPC species including 15:0, 17:0, 19:0, 20:0, 22:0, 22:1 and 24:1. These specific LPCs have not been described before but in general, LPCs are reduced in response to high fat diet, obesity and diabetes [289]. These results indicate that developmental exposure to DOSS promotes a persistent dyslipidemia akin to long-term high fat diet induced obesity in adult mice.

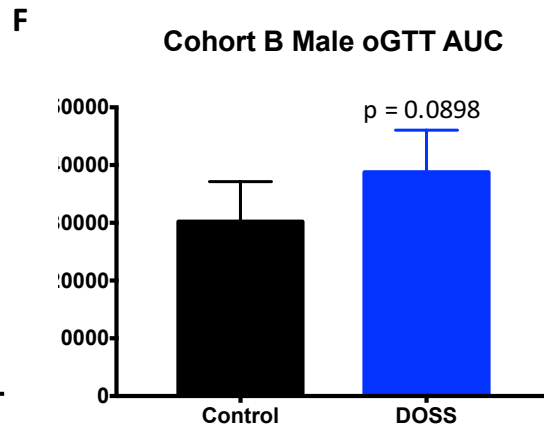
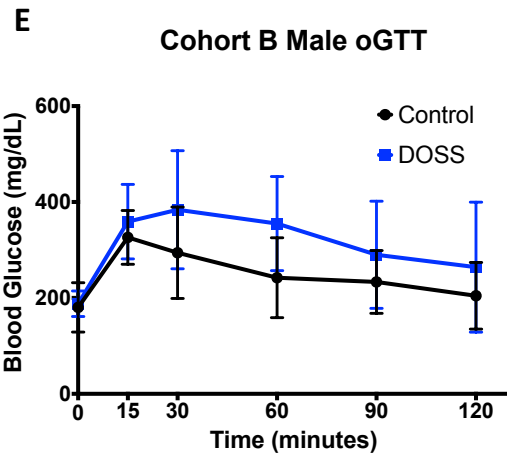
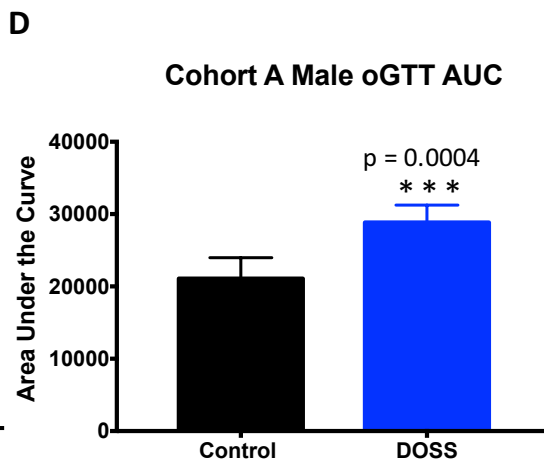
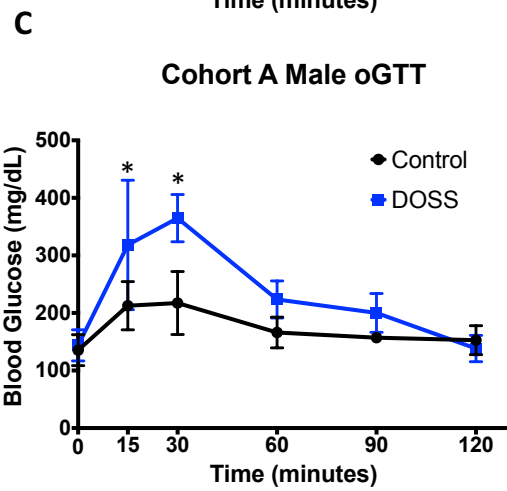
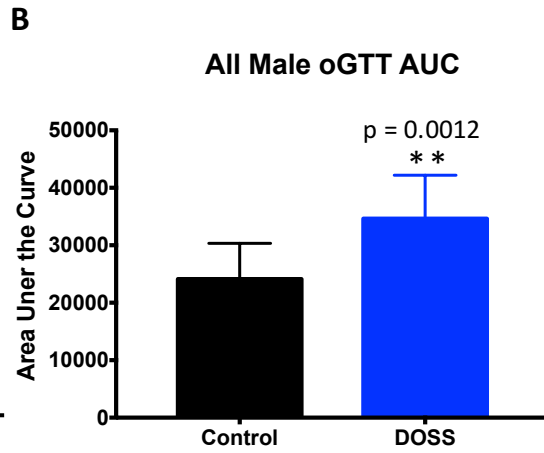
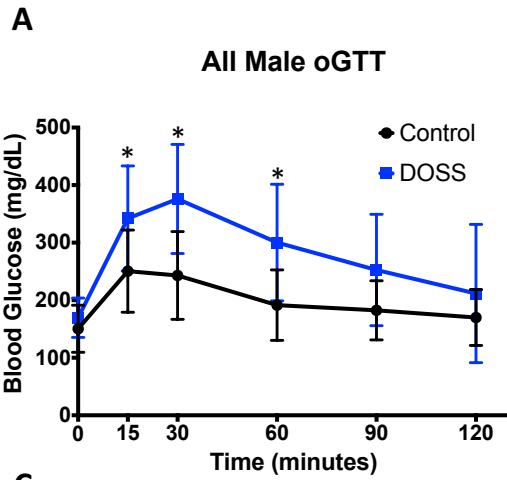


Figure 1. Developmental DOSS treatment promotes glucose intolerance in male F1 mice.

Pregnant C57BL/6J dams were treated with either vehicle control CMC or 31.25 µg/mL DOSS from E11.5 through weaning. F1 pups were assed for indications of metabolic syndrome at 12 weeks using oral glucose tolerance testing. Mice were fasted for 6 hours and basal glucose measurements were taken. Mice were then administered at 2mg/g bolus of glucose and blood glucose was measured at 15, 30, 60 and 120 minutes. Blood glucose measurements for all control and treated male mice are shown in A) with corresponding area under the curve values in B). Blood glucose values from male mice in Cohort A and area under the curve values are shown in C) and D). Blood glucose values and area under the curve values from male mice in Cohort B are shown in E) and F) respectively.

Two-Way Anova was used to determine significant difference in blood glucose at different time points (* $p < 0.05$ for a given time point). Area under the curve values were calculated for each individual mouse, pooled and students t-test was used to determine significance (** $p < 0.01$, *** $p < 0.0001$).

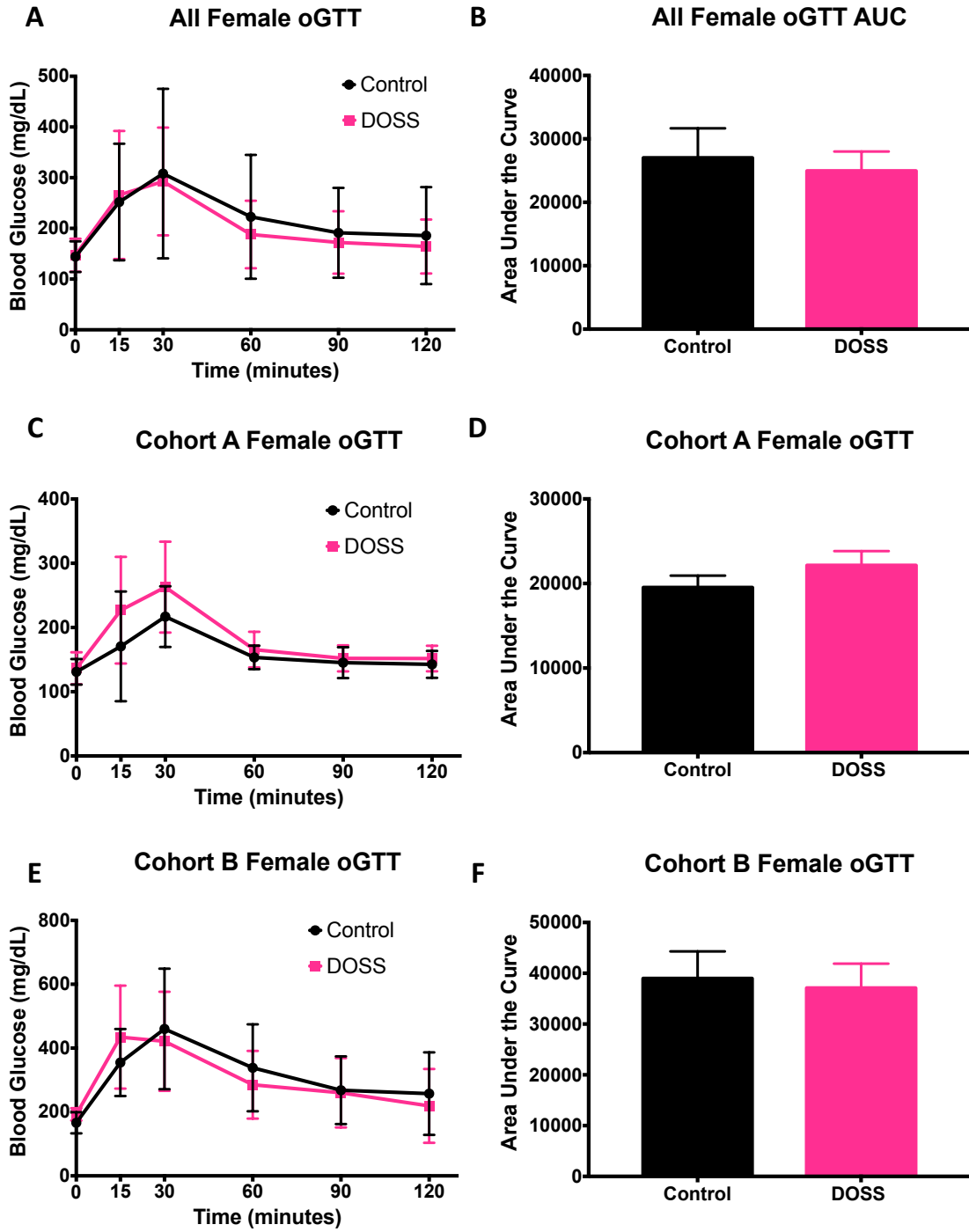


Figure 2. Developmental DOSS treatment does not promote glucose intolerance in female F1 mice.

Pregnant C57BL/6J dams were treated with either vehicle control CMC or 31.25 µg/mL DOSS from E11.5 through weaning. F1 pups were assed for indications of metabolic syndrome at 12 weeks using oral glucose tolerance testing. Mice were fasted for 6 hours and basal glucose measurements were taken. Mice were then administered at 2mg/g bolus of glucose and blood glucose was measured at 15, 30, 60 and 120 minutes. Blood glucose measurements for all control and treated female mice are shown in A) with corresponding area under the curve values in B). Blood glucose values from female mice in Cohort A and area under the curve values are shown in C) and D). Blood glucose values and area under the curve values from female mice in Cohort B are shown in E) and F) respectively.

Two-Way Anova was used to determine significant difference in blood glucose at different time points (* $p < 0.05$ for a given time point). Area under the curve values were calculated for each individual mouse, pooled and students t-test was used to determine significance (** $p < 0.01$, *** $p < 0.0001$).

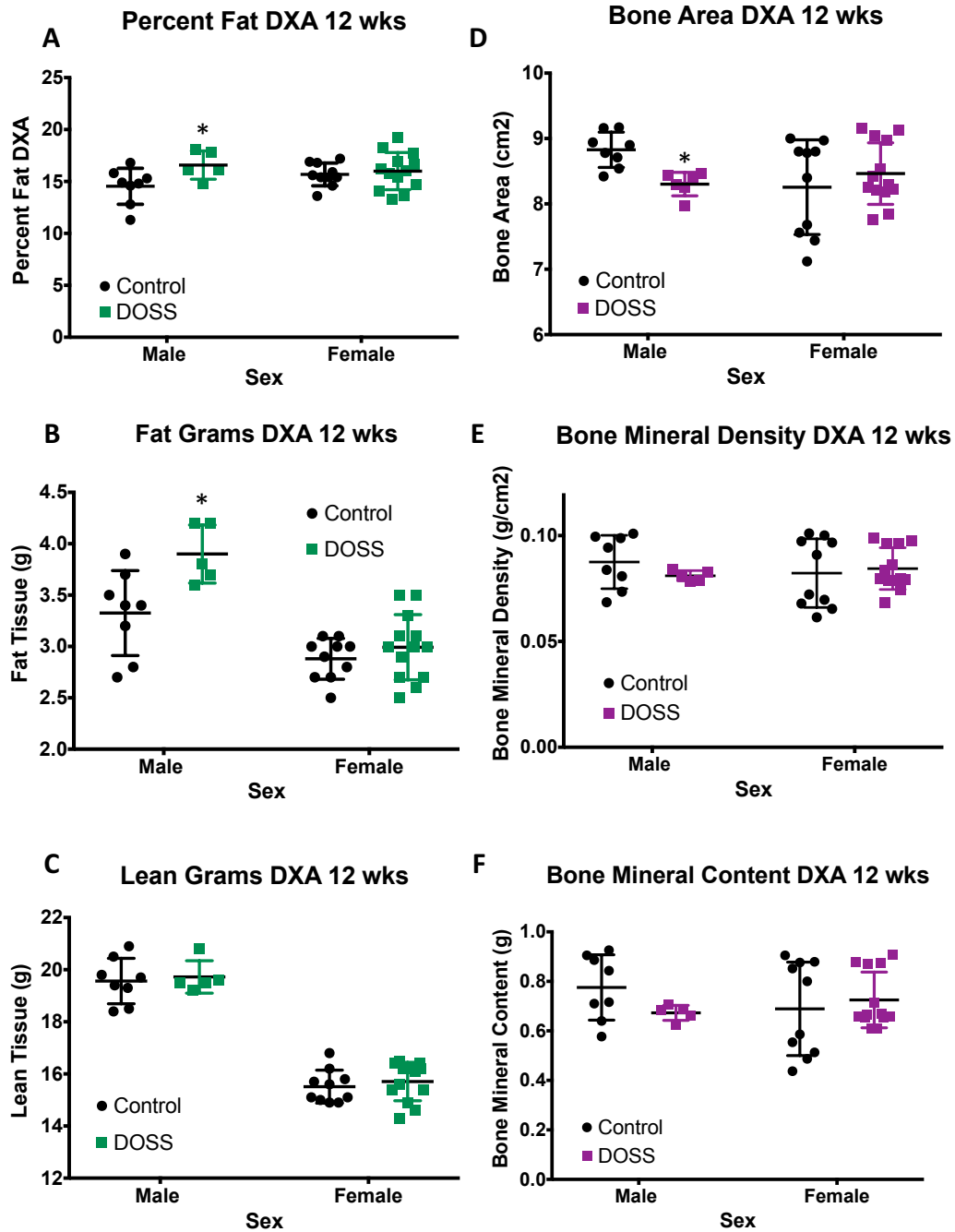


Figure 3. Body composition at 12 weeks of age in F1 male and female mice from dams treated with DOSS or vehicle control.

At 12 weeks of age, DXA scans were used to assess body composition in male and female mice from Cohort A. Measurements were obtained for A) percent fat, B) fat grams, C) lean grams, D) bone area, E) bone mineral density, and F) bone mineral content.

Male and Female mice were analyzed separately using unpaired t-test (* $p < 0.05$).

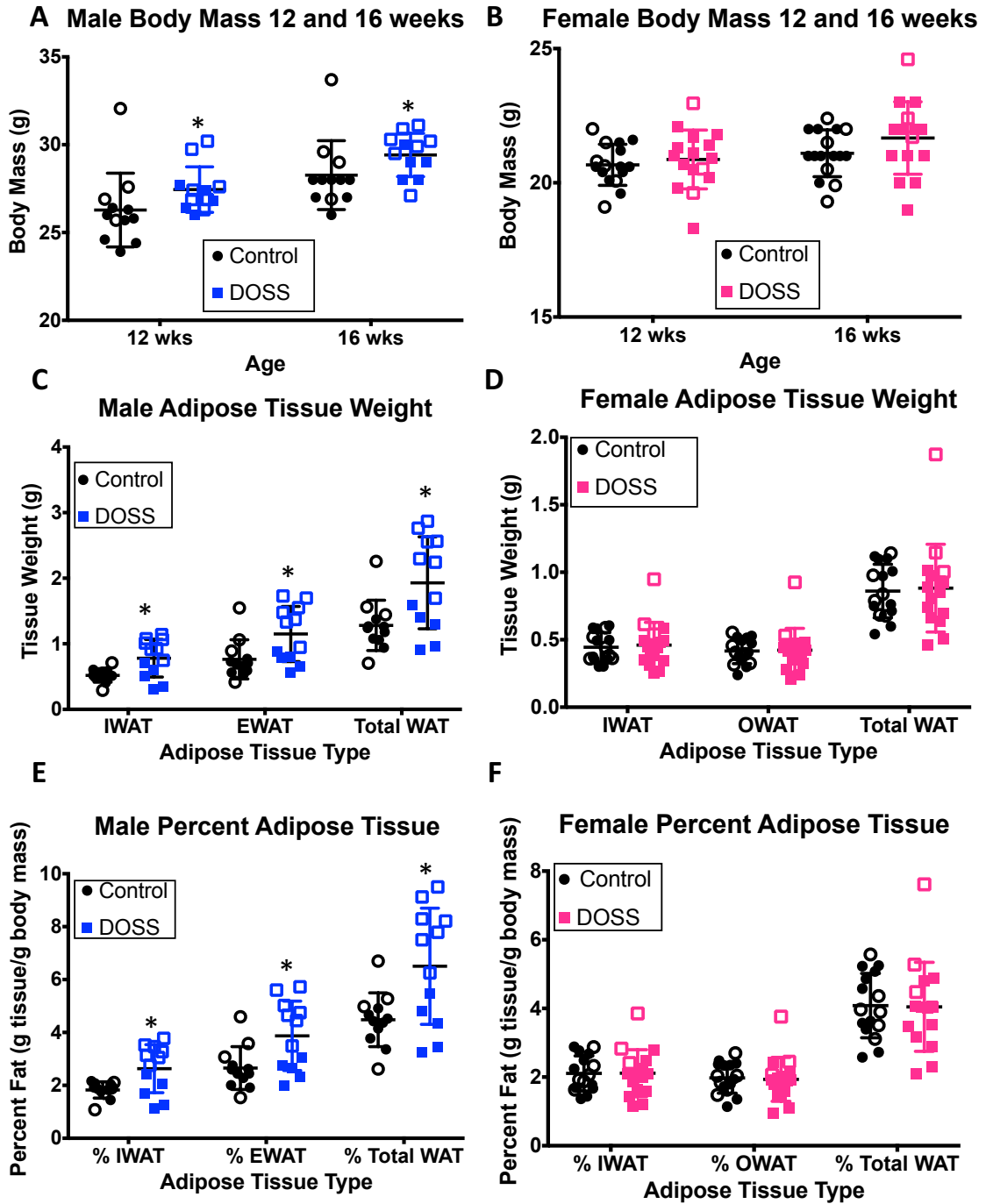


Figure 4. Effects of DOSS treatment on body mass, adipose tissue weight and percent adipose tissue and male and female F1 mice.

Body mass was measured at 12 and 16 weeks of age. At 16 weeks of age, F1 males and females were sacrificed and inguinal and gonadal adipose tissue was weighed and collected. Adipose tissue percent was calculated as grams adipose tissue/total body mass.

A) Male body mass, B) female body mass, C) male adipose tissue weight, D) female adipose tissue weight, E) male adipose tissue percent, F) female adipose tissue percent.

Data are represented as mean +/- SD and pooled from both cohorts with animals from Cohort A as closed shapes and animals from Cohort B as open shapes. Unpaired students t-test with Welch's correction for unequal variance was used for male mice (*p<0.05).

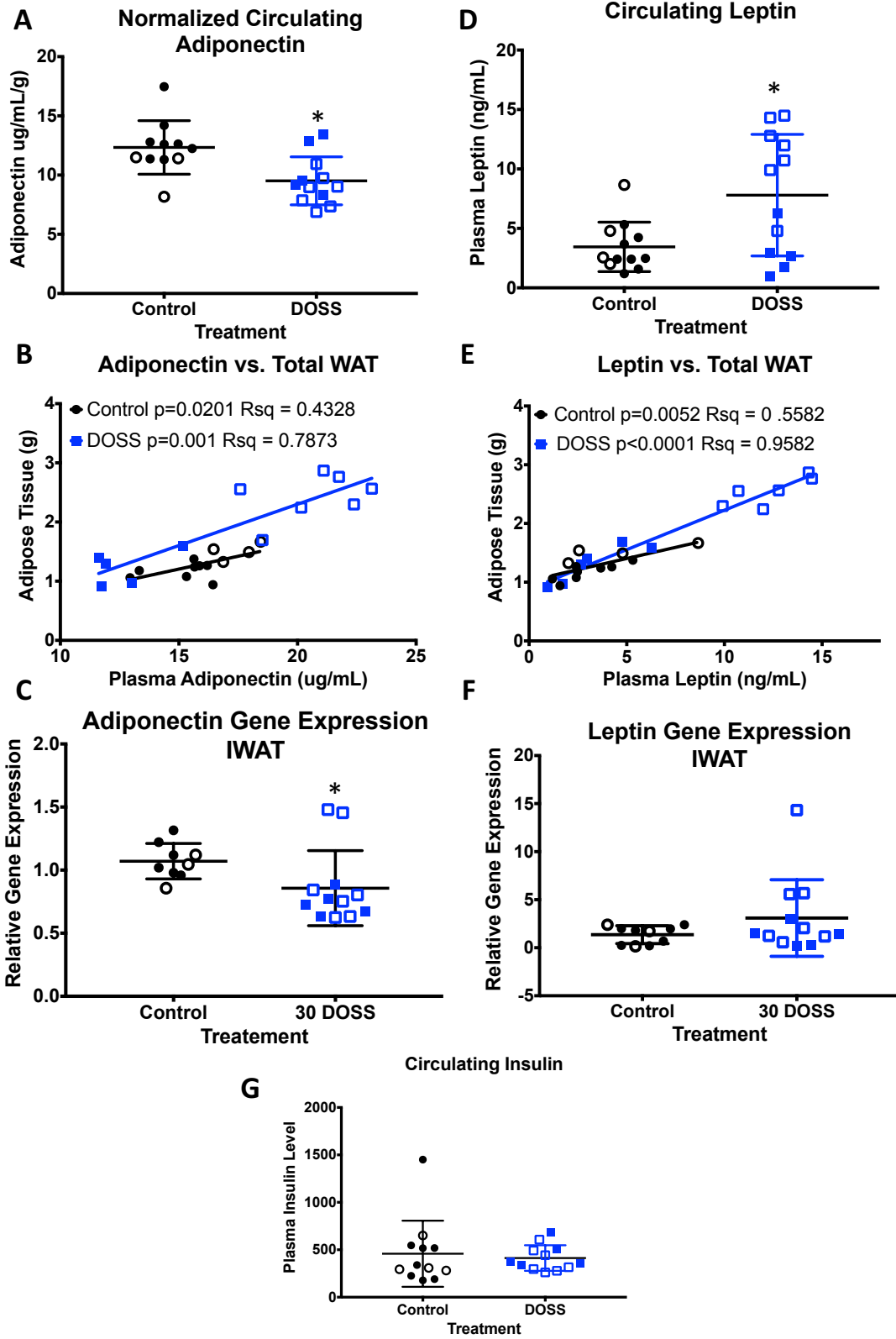


Figure 5. Developmental DOSS treatment alters expression and circulating levels of adipokines in male F1 mice.

At time of sacrifice (16 wks), plasma and adipose tissue was collected. Circulating levels of adiponectin and leptin were determined using MSD assays. Gene expression was determined via RNA isolation, cDNA conversion and qPCR using the deltadelta Ct method with *Hprt* as the housekeeping gene. A) normalized circulating levels of adiponectin, B) raw diponectin correlated with fat grams, C) *AdipoQ* gene expression in IWAT, D) circulating levels of leptin, E) leptin correlated with fat grams, F) *leptin* gene expression in IWAT and G) circulating insulin levels. Linear regression was used to determine correlations between adiponectin and leptin and fat grams. *p<0.05 Unpaired t-test

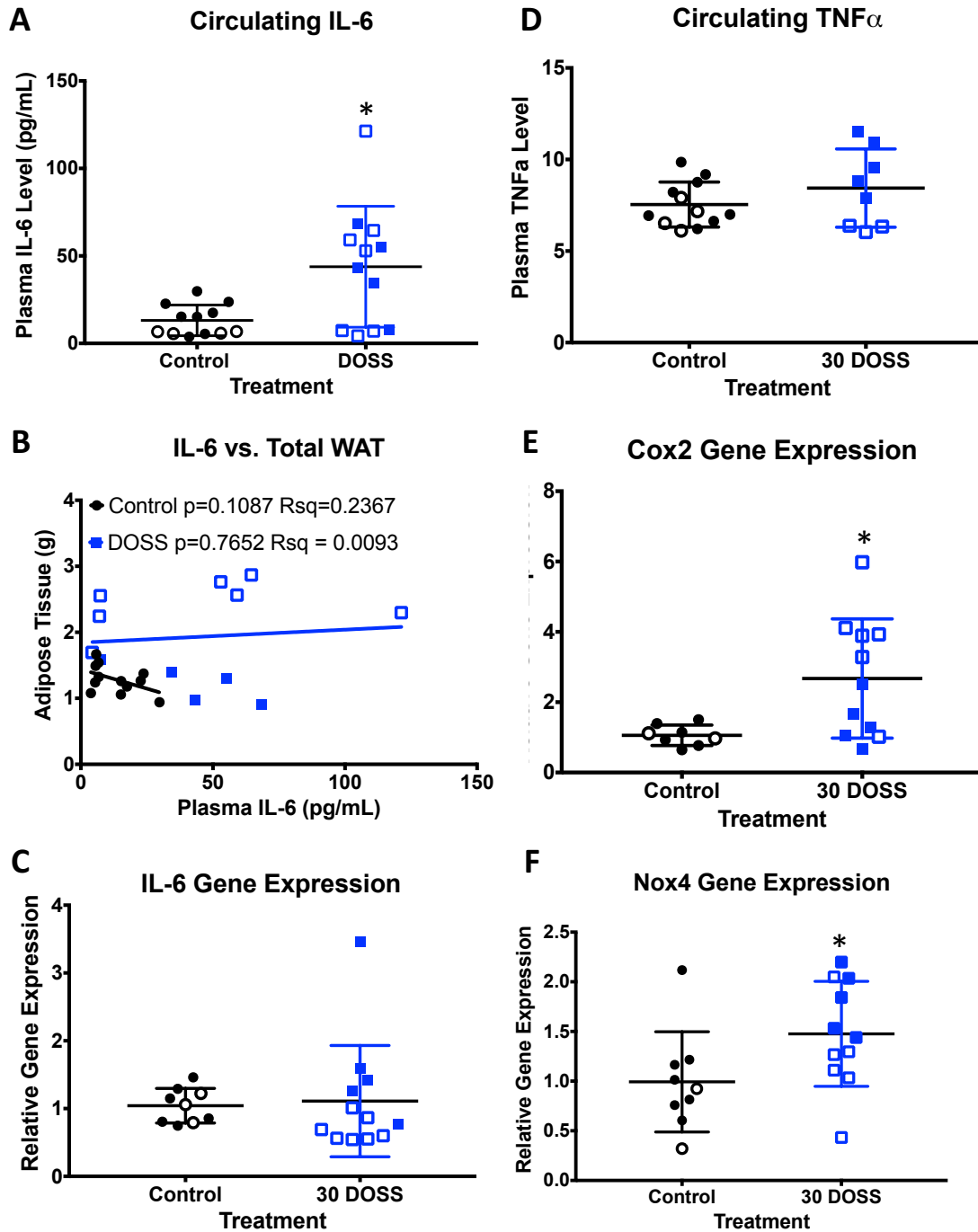


Figure 6. Developmental DOSS treatment promotes a proinflammatory state in male F1 mice.

At time of sacrifice (16 wks), plasma and adipose tissue was collected. Circulating levels of IL-6 and TNF- α were determined using MSD assays. Gene expression was determined via RNA isolation, cDNA conversion and qPCR using the deltadelta Ct method with *Hprt* as the housekeeping gene. A) circulating levels of IL-6 in plasma, B) plasma IL-6 correlated with fat grams, C) IL-6 gene expression in IWAT tissue, D) circulating levels of TNF- α in plasma, E) Cox2 gene expression ion IWAT tissue, F) Nox4 gene expression in IWAT tissue.

*p<0.05 Unpaired ttest.

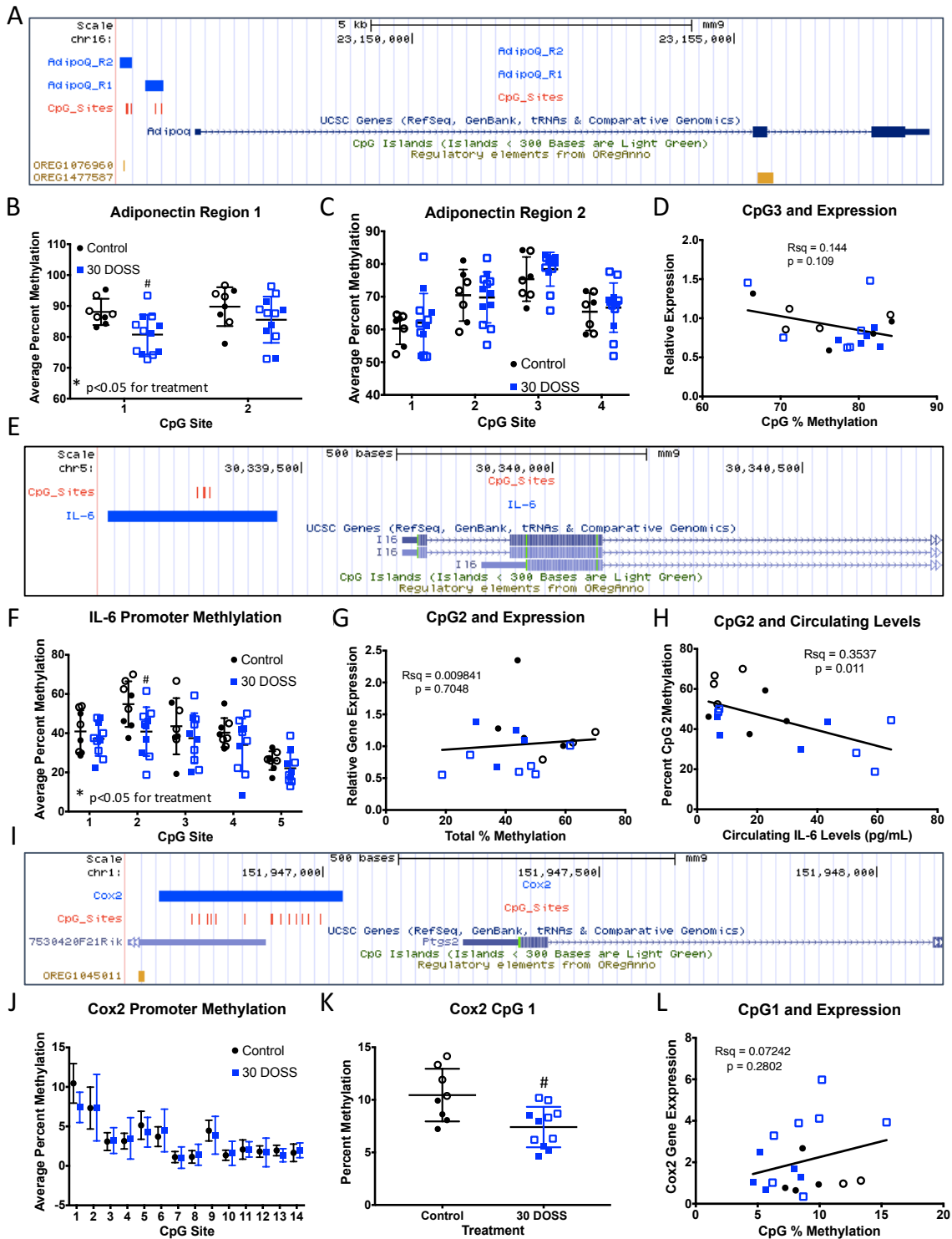


Figure 7. DOSS promotes changes in DNA methylation in promoter regions of inflammatory genes in IWAT.

Targeted bisulfite sequencing was used to assess promoter methylation in IWAT tissue for genes in which changes in gene expression and circulating protein levels associated with DOSS treatment were observed including adiponectin (A-D), IL-6 (E-H) and Cox-2 (I-L). A) Chromosomal location of promoter adiponectin regions investigated for CpG methylation. Average methylation for individual CpGs in B) region 1 and C) region two of the adiponectin promoter. D) Correlation between adiponectin region 2 CpG3 methylation and *AdipoQ* expression. E) Chromosomal location of the IL-6 promoter region investigated for CpG methylation. F) Average methylation for individual CpG sites in the IL-6 promoter. G) Correlation between CpG2 methylation and *Il-6* expression. H) Correlation between CpG2 methylation and circulating adiponectin levels. I) Chromosomal location of the Cox-2 promoter region investigated for CpG methylation. J) Average methylation for individual CpG sites in the Cox-2 promoter. K) Average percent methylation for CpG1 in the Cox-2 promoter. L) Correlation between CpG1 methylation and *Cox2* expression.

Two Way Anova was used to assess significant changes in DNA methylation based on treatment across the whole promoter region with Sidak's post-hoc test for individual CpG sites differences.

* $p < 0.05$ treated vs. control Two-Way Anova. Individual sites were then also compared using Sidak's post-hoc test ($\#p < 0.05$).

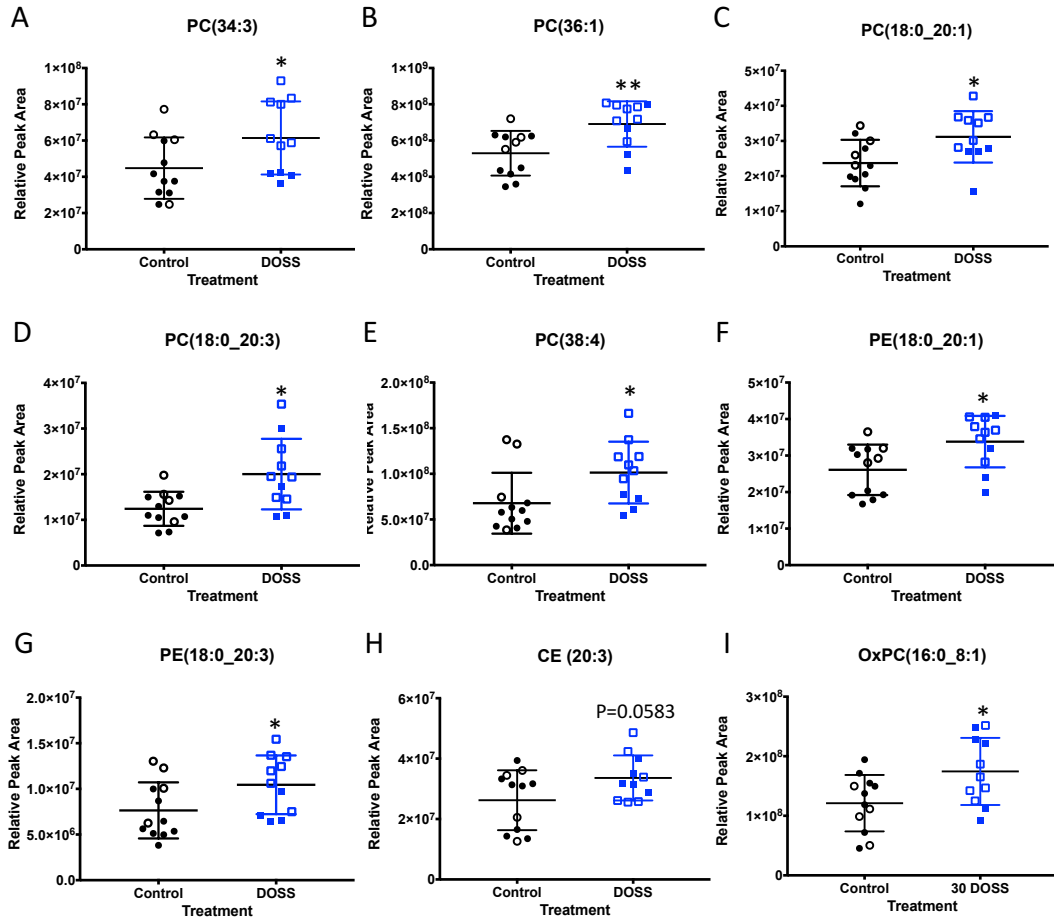


Figure 8. DOSS treatment promotes changes in circulating phospholipids.

At time of sacrifice plasma was collected from F1 animals. Untargeted lipidomics was used to determine the presence of circulating lipids. An in-house software called LipidMatch and LipidSearch™ was used to identify lipid species based on unique m/z ratios and retention times. Feature processing and peak area integration was performed using mzMine. The resulting peak area table was filtered using FRAMe. Relative peak areas between DOSS treated and vehicle control F1 males are shown for A) PC(34:3) (unpaired ttest equal SD, $p=0.0433$), B) PC(36:1) (unpaired ttest equal SD, $p=0.0053$), C) PC(18:0_20:1) (unpaired ttest equal SD, $p=0.0179$), D) PC(18:0_20:3) (unpaired ttest equal SD, $p=0.0373$), E) PC(38:4) (log transformed unpaired ttest equal SD, $p=0.0125$), F) PE(18:0_20:1) (unpaired ttest equal SD, $p=0.0149$), G) E(18:0_20:3) (unpaired ttest equal SD, $p=0.0444$), H) CE (20:3) (unpaired ttest equal SD $p = 0.0583$) and I) OxPC(16:0_8:1) (unpaired ttest equal SD, $p=0.0224$) * $p<0.05$, ** $p<0.01$

4.4. Discussion

From results of experiments delineated in this Chapter, evidence is presented in support of the hypothesis that DOSS has the potential to act as an obesogen *in vivo* via metabolic disruption indicated by impaired glucose tolerance, increases in adiposity (e.g. fat grams and fat percentage), and changes in gene expression and circulating levels of adipokines, cytokines and phospholipids consistent with obese, diabetic, and metabolic syndrome phenotypes. This phenotype was observed in C57BL/6J male mice, but not females. Sexually dimorphic metabolic and obesogenic effects have been observed in this strain of mice and others before. For instance, although female and male mice both gain weight when fed a high fat diet for 14 weeks, females are protected from metabolic syndrome [114, 290]. In a prenatal exposure model for MEHP in C57BL/6J mice, markers of obesity were observed in male offspring but not female offspring [158]. With regard to obesogen exposure, in studies by Blumberg et al., on TBT exposed C57BL/6 mice during development, the obesogenic phenotype is observed in both the female and male offspring. This phenotype persisted transgenerationally for TBT, supporting the concept that the obesogenic phenotype observed in offspring of DOSS-exposed dams could persist transgenerational as well although additional experiments would be needed to evaluate this hypothesis [93]. Similarly, triflumazole, another PPAR γ agonist induces obesogenic effects including MSC fate commitment in male mice, although this was tested in the CD1 mice not C57BL/6J background [159]. The recently identified metabolic disruptor, tolyfluanid, although not a PPAR γ agonist, similarly exerts its metabolic disrupting effects in adult male C57BL/6J mice, while the phenotype is not observed in females.

Results indicate that DOSS induces glucose intolerance and increases fat percentage, coupled with a reduction in adiponectin gene expression and circulating levels. This inverse relationship is well documented in the literature as a marker of metabolic syndrome in humans and mice [291]. Adiponectin signaling is involved in insulin sensitization and the observed reduction in adiponectin in treated animals may be a reason for the observed glucose intolerance. For instance, when T2D patients are treated with adiponectin their hyperglycemia symptoms are ameliorated and in adiponectin knockout mice the effects induced by a high fat diet are accentuated [292]. In general, human cohort studies have identified lower circulating levels of adiponectin in individuals with T2D compared to controls. In one study, a positive correlation between BMI and serum adiponectin was observed in a human cohort of obese and non-obese T2D described in a 2016 study by Chand and Silambanan [293]. Although all T2D individuals in this study had lower adiponectin levels than the control group. Given that we observed decreases in normalized adiponectin in all treated mice relative to controls, where as we only observed increases in leptin for mice with the threshold level of greater than 2 grams adipose tissue (Cohort B; Fig. 5A), adiponectin may serve as a better marker for understanding the phenotype associated with developmental DOSS exposure and mild metabolic syndrome.

Similarly, from one perspective, our two treatment cohorts may represent two classes of type two diabetics (T2D), that is, obese (Cohort B) and non-obese T2D (Cohort A) individuals since Cohort B treated animals displayed increased circulating leptin levels relative to controls and treated animals from Cohort A. Similarly, while non-obese T2D patients have reduced circulating adiponectin, data suggests they do not have

increased leptin as is the case with obese T2D patients [294]. As shown in Figure 5A, the 2 grams threshold could be used to distinguish these two cohorts, at least on the level of adiposity and circulating adiponectin and leptin levels with further characterization necessary to fully establish those populations.

Counter to our hypothesis, no significant increases in DNA promoter methylation for adiponectin were observed given the observation of decreased gene expression in treated animals, however not all control animals were analyzed for promoter methylation and only select promoter regions were interrogated. Others also have shown that a high fat diet induces adiponectin promoter hypermethylation and correlated with decreased adiponectin gene expression in region 2 of the adiponectin promoter [46]. Future studies should investigate other adiponectin promoter regions for regulatory CpG sites. For instance, 500bp upstream of the region investigated in this study, there is an *Ebfl* transcription factor binding site and *Ebfl* binding has been shown to be reduced at methylated sites [295]. In this study, there was significant hypomethylation in region 1 of the adiponectin promoter. It would be interesting to determine if CpG methylation in this region promotes recruitment of transcription factors as this mechanism has recently been described for other genomic loci [38].

Notably, no significant differences in insulin levels between F1 males from DOSS treated or control dams was observed. Hyperinsulinemia is commonly associated with impaired glucose tolerance, increased adiposity and reduced adiponectin levels, all of which are indicators of metabolic syndrome and were observed in treated animals from this study [296]. In this study, insulin was measured at time of sacrifice, not at time of oGTT and the values were not obtained from fasted animals. Future studies should

measure fasting insulin as well as insulin after glucose challenge (glucose stimulated insulin secretion) to get a more comprehensive view of insulin signaling in DOSS treated animals. Alternatively, the observed impaired glucose tolerance and elevated blood glucose could be a result of malfunctioning glucose transporters like Glut4 in skeletal muscle tissue, the tissue that first responds to insulin stimulation[297, 298].

Both cohorts of treated mice had higher circulating levels of IL-6 a cytokine commonly found to be positively correlated with diabetes and obesity [56]. Here, an increase in IL-6 gene expression in IWAT was not observed, although there were decreases in promoter methylation which negatively correlated with circulating IL-6 levels suggesting a function role for DNA methylation in the IL-6 promoter. Given that a hallmark of obesity is adipose tissue inflammation and adipose tissue is comprised of multiple cell types including adipocytes, mesenchymal stem cells, immune macrophage and lymphocytes, it is possible that the heterogeneity of the tissue is confounding the results, especially given that cells predominantly expressing IL-6 such as macrophage and preadipocytes are likely a small proportion of the total cell population. Future studies should separate the stromal vascular fraction from adipocytes and perform gene expression and DNA methylation in both cell fractions to gain a more comprehensive understanding of IL-6 regulation. Additionally, not all control adipose tissue samples were included in the methylation analysis and two samples were excluded from analysis due to low coverage. It is possible that some highly representative samples were missed in this analysis. IL-6 promoter methylation in adipose tissue has not been investigated with regards to obesity, but in humans IL-6 promoter methylation has been investigated in circulating white blood cells with differing results. In circulating white blood cells

Kirchner et al observed hypomethylation of IL-6 promoter with no correlation to circulating levels [299] while Kyung Na et al (2015) observed hypermethylation of the IL-6 promoter [300] without having determined circulating levels. Determining if white blood cell IL-6 methylation correlates with adipose tissue IL-6 methylation would strengthen the results observed human studies.

Increases in expression of two other genes commonly associated with a systemic inflammatory state and obesity, Cox2 and Nox4, were observed in IWAT tissues in F1 males from DOSS treated dams [282, 283]. Cox2 has been shown to be an essential mediator in obesity-induced adipose tissue inflammation and insulin resistance [301]. DOSS treatment of induced pluripotent stem cells (iPSCs) has been shown to increase Cox2 enzyme activity and gene expression (correspondence with Theresa Cantu), suggesting increased arachidonic metabolism to proinflammatory eicosanoids and a common role for DOSS promoted inflammatory response. Eicosanoid profiling focusing on products of Cox2 mediated reactions in adipose tissue or plasma from males prenatally exposed to DOSS would further elucidate the role of DOSS induced inflammation *in vivo*. Others have identified increased Cox2 expression in IWAT in response to maternal obesogen exposure, specifically PAHs [136]. In F1 males from DOSS treated dams from this study, upregulated transcription of Cox2 and hypomethylation of one CpG site in the promoter region of Cox2 in IWAT was observed. This site was the most upstream site interrogated and was more methylated than the other sites examined (Fig. 7I-L; sites 2-14). It is possible that the regulatory region associated with DOSS-mediated upregulation of Cox2 in adipose tissue may be located further upstream given the trend observed at CpG site 1. While Cox2 methylation has been

investigated in other tissue types and plays a role in progression of some cancers [301], to the best of my knowledge this is the first investigation into adipose tissue Cox2 methylation as it relates to obesity and diabetes. Given that indicators of low-grade inflammation were observed at the epigenetic (IL-6 and Cox2 hypomethylation), gene expression (*Cox2* and *Nox4*) and protein levels, (circulating IL-6) inflammation is likely a key mechanism by which developmental DOSS exposure can promote adult onset metabolic syndrome.

Cox2 activity is associated with a specific category of lipid mediators in inflammation. The broader field of lipidomics has emerged as a useful tool in identifying pathological pathways of diseases like diabetes and obesity as well as to serve in identifying biomarkers of disease states [302]. Using untargeted lipidomics analysis on plasma samples from F1 male offspring of DOSS exposed and unexposed dams significant differences in multiple circulating phospholipids was observed (Fig. 8). Difference were observed primarily in phosphatidylcholine species. There have been a few studies that independently performed untargeted lipidomics on blood samples from C57BL/6 male mice fed a high fat diet to determine lipid biomarkers of obesity while others have explored the associations in human cases of obesity and diabetes. Van Ginneken et al. identified CE(20:3) and PC(36:1) to be increased in animals fed a high fat diet, both of which were significantly increased in our DOSS treatment animals [303]. PC(36:1) has also been identified as a biomarker for T2D in a large human cohort study [304]. Of note, it will be important to determine the specific composition of this phosphatidylcholine species, since treatment of *db/db* mice with PC(18:0_18:1) improves glucose tolerance obesity and T2D. Similarly, Eisinger et al. also observed increases in

CE(20:3) along with PC(38:3) and PC(38:4), both of which were also significantly increased in our DOSS treatment animals [288]. Similarly, PC(38:3) was associated with an increased risk in diabetes in a human cohort [304]. While Barber et al. observed increases in PE(38:0), PE(36:1) and PE(38:4), DOSS treatment animals displayed increases in related, but different phosphatidylethanolamine species, PE(18:0_20:1) and PE(18:0_20:3). Importantly, the method used in this study was able to identify specific tail composition while Barber et al. did not [289]. Although not significant, a decrease in several LPC species in DOSS treated males was observed, which have been negatively correlated with diet induced obesity and T2D in mice and humans [288, 289, 305]. Although no significant differences were observed for sphingomyelin and ceramide species, these lipid classes have also been associated with obesity and T2D. Together these data suggest that DOSS treatment induces phospholipid changes similar to diet induced obesity models but that some distinct differences are still evident and identifiable.

A limitation of this study is low sample size. Due to criteria necessary for consistent litter numbers, several experimental and control litters had to be dropped from analysis, reducing sample size and power. There were also some observable differences in the effects of DOSS treatment in our two cohorts of animals (performed to increase sample size) with animals from Cohort B showing a more exaggerated effect with regard to fat accumulation and variables that correlate with adiposity including circulating leptin. This could be a result of natural individual variance, differences in maternal water consumption and therefore effective dose of DOSS, differences in food consumption and physical activity of pups, or seasonality of birth of offspring. Future experimentation

would be needed to determine the source of variation. Monitoring food, water consumption and activity would be good measures to take in future studies. Since treatment conditions did not vary between cohorts and even though mice are maintained in relatively controlled conditions, winter (Cohort A) versus summer (Cohort B) seasonal differences often remains a factor [306]. Siberian hamsters are an extreme example of rodent's changing adiposity based on season [307]. Thus, the season in which the dosing was administered may mask the ability to detect differences in adiposity in treated and control groups.

DOSS may elicit features in the syndrome of its obesogenic effects (glucose and lipid metabolism, inflammation and adiposity) through alternative mechanisms not explored here. While DOSS has been shown to act as a ligand activator of PPAR γ , (described in previous publications by our group [258] and Chapter 2/3), DOSS is also likely to alter fundamental properties of lipid bilayers associated with cell membranes and organelles given it's molecular structure and function [308]. Additionally, DOSS may alter the microbiome of pregnant dams, thereby influencing maternal nutrition and transfer to pups, which could also explain some of the variation observed in treated animals. In humans, it has been documented that the composition of the maternal microbiome, as well maternal nutrition, can impact the onset of obesity and diabetes in offspring [309]. Furthermore, other food additives and emulsifiers like DOSS have been evaluated for their impact on the microbiome and subsequent adverse health effects including obesity and inflammatory bowel disease were observed [208, 310]. In cows, DOSS exposure was shown to alter microbial communities, increased circulating blood glucose and changed the fatty acid composition of their milk [311]. Given that many

EDCs have multiple mechanisms of action, it is likely that DOSS can simultaneously act as a PPAR γ agonist and through other mechanisms that we have yet to explore.

Given the observed indication of metabolic disruption in male offspring from dams treated with DOSS compared to controls, the use, safety and prescription of docusate (Colace) stool softener during pregnancy should undergo further study. Interestingly, several studies have evaluated the effectiveness of DOSS to treat constipation with similar results suggesting it is not very effective and that there are missed opportunities to reduce prescription or use this medication [312, 313]. This indicates that Colace use perhaps presents unintended risks that could easily be ameliorated through changes in standard of care practices. A standard protocol for measuring DOSS in biological samples like blood and breast milk is currently nonexistent. While protocols for DOSS exist for seawater and fish tissue, they are not directly transferable to human biological samples due to differences in matrix composition and their high limits of detection [185, 314]. Development of such protocols in conjunction with data provided herein may significantly aid in understanding how the use of docusate (Colace) during pregnancy may impact child metabolism, obesity and overall health later in life.

Table 2. Bisulfite sequencing primer sequences, chromosomal location, product size, CpG number and references.

Gene Loci	Forward	Reverse	Chromosome location mm9	Size(bp)	CpG #	Ref
<i>AdipoQ R1</i>	AGGTAAGTGTGTTTGTGATATTGGGT	ACACCCACAATAATTCCATAAAAATC	chr16:23145842+23146117	276	2	[46]
<i>AdipoQ R2</i>	TGGAGGAAGTAGATGTTTGGTTAGT	CAAAACAATACCTTAAAAACCTCTC	chr16:23145441+23145636	196	4	[46]
<i>IL-6</i>	TGTTTAGGTTGGGTGTTG	ACCCTAAAAAACATAAACACTCTTC	chr5:30339113+30339453	341	5	[284]
<i>Cox-2</i>	AGATGTGGATTTTGATAGAGGATATT	CTACCCTTAACTACCCCAAATAATAC	chr1:151946703+151947035	333	14	[315]
<i>Leptin</i>	GAGTAGTTAGGTTAGGTATGTAAGAG	TAATAACTACCCCAATACCACTTAC	chr6:29009816+29010194	379	19	[48]
<i>Fabp4</i>	AGGAATTGTTTTTTTGAAAAGTAG	AATAAACACCTCCAACACTATACC	chr3:10202723+10202992	270	5	[94]
<i>Glut4</i>	TGGGTATATGTATTTGTTAGGGTA	TATTAATCCCTTAAATCATCTCCTC	chr11:69761972+69762232	261	13	[316]
<i>Fasn</i>	TAGTAGGTAGGATAGGGAATATTGA	CAACCTCTCTAAACTCAAAAAAC	chr11:120686159+120686445	286	17	[317]
<i>Irs-1</i>	GTAGTGGGTTTAGGGTGAGTGTAGT	CCCCTACCCAAAAATATTTAATTTAC	chr1:82287290+82287526	237	15	[318]
<i>Hmox1</i>	GGGTTGGATGTTGTAATAGTAG	CATTCCCAAACAAAATAAAAAACAC	chr8:77617422+77617730	308	24	[319]
<i>Pparg2</i>	GATGTGTGATTAGGAGTTTAATTAAG	CAAACCTAAATTAATAACTACTATCCTAAC	chr6:115371595+115371953	259	4	[320]

Table 3. Average percent methylation of interrogated genes in IWAT tissue of F1 males from control and DOSS treated dams.

Gene Loci	Percent Methylation Control (Mean +/- SD)	Percent Methylation DOSS (Mean +/- SD)	P value - 2Way ANOVA Treatment/Post-Hoc CpG	Coverage (Mean +/- SE)
<i>AdipoQ R1</i>	88.93 +/- 4.8	83.13 +/- 6.6	0.008/0.032	121.5 +/- 45.3
<i>AdipoQ R2</i>	67.88 +/- 5.7	69.21 +/- 6.2	0.431/NA	155.6 +/- 44.3
<i>IL-6</i>	41.10 +/- 7.4	34.29 +/- 9.3	0.004/0.041	41.5 +/- 15.5
<i>Cox-2</i>	3.46 +/- 0.5	3.30 +/- 0.3	0.349/ 0.005	280.6 +/- 69.7
<i>Leptin</i>	64.08 +/- 4.8	65.06 +/- 6.4	0.240/NA	141.4 +/- 56.3
<i>Fabp4</i>	78.01 +/- 5.8	77.46 +/- 11.9	0.789/NA	128.6 +/- 32.3
<i>Glut4</i>	3.01 +/- 0.5	3.02 +/- 0.9	0.996/NA	136.0 +/- 41.5
<i>Fasn</i>	2.66 +/- 0.3	2.73 +/- 0.7	0.752/NA	113.2 +/- 41.6
<i>Irs-1</i>	3.37 +/- 0.5	2.28 +/- 0.5	0.631/NA	237.9 +/- 41.6
<i>Hmox1</i>	1.66 +/- 0.2	1.59 +/- 0.4	0.535/NA	211.4 +/- 38.7
<i>Pparg2</i>	63.83 +/- 6.7	61.69 +/- 12.4	0.412/NA	127.5 +/- 36.9

CHAPTER 5: CONCLUSIONS, LIMITATIONS, AND FUTURE DIRECTIONS

The work presented here describes a logical workflow designed to identify, validate and characterize metabolic disrupting compounds using several screening assays, functional *in vitro* validation assays and ultimately an *in vivo* exposure model to characterize phenotypic changes associated with metabolic syndrome as a result of exposure. In a time when industrial chemical production and usage is at its highest points and our environment and bodies are burdened with multiple exposures, this work helps identify a potentially unanticipated outcome of a commonly used chemical, dioctyl sodium sulfosuccinate (DOSS).

As presented and reported in a publication derived from the work of Chapter 2 and Chapter 3, receptor transactivation assays for multiple nuclear receptors were used to identify potential endocrine disrupting chemicals present in the Deepwater Horizon oil (MC252 Louisiana sweet crude) and/or Corexit 9500 dispersant used in the spill remediation process. Major research efforts have focused on understanding the role of exogenous compounds in the development of obesity, diabetes and metabolic syndrome given the alarming prevalence of these diseases [256]. Therefore, particular interest was put on identifying novel obesogens or metabolic disruptors, leveraging as a tool for identification, compounds capable of activating the PPAR γ /RXR signaling pathway. This search identified a compound present in Corexit 9500, likely dioctyl sodium sulfosuccinate (DOSS), as a PPAR γ agonist which was then validated *in vitro* and *in vivo* in subsequent aims and chapters (Figure 1).

This first required the generation and testing of a variety of oil and dispersant mixtures that led to an elegant set of experiments based on nuclear hormone receptor

activation helping to identify the component within the mixture that exhibited potential obesogenic activity. Since oil and dispersant are both complex mixtures in and of themselves, this was a critical and necessary step to efficiently and effectively evaluate transactivation assay results.

While responses of several nuclear hormone receptors were investigated, including PPAR γ , PPAR α , PPAR β/δ , RXR α , PR β , ER α and ER β it was not an exhaustive list. From this investigation DOSS activated mouse and human PPAR γ , human PPAR β/δ , weakly activated PPAR α , had no observed activity for RXR α or the estrogen receptors and possibly antagonized PR β . Other receptors of interest that were not investigated due to time and experimental limitations are thyroid hormone receptor, androgen receptor and glucocorticoid receptor. Glucocorticoid receptor would be particularly relevant for identification of other potential obesogens based on the work of Sargis et al., which concluded that activation of glucocorticoid receptor by exogenous chemicals induced adipogenesis in 3T3L1 cells [113].

Iida et al., investigated SDS and SDBS, molecules that are similar in structure and function to DOSS, and identified these compounds as PPAR γ agonists, but did not find activity for 19 other receptors tested, suggesting possible PPAR γ specificity for similar compounds like DOSS [219]. The Environmental Protection Agency has an assay screening program under the names of Toxcast and Tox21 that includes hundreds of assays (receptor transactivation assays, radio ligand binding assays, transcription assays) to help identify EDCs and other chemicals of concern[321]. Based on analysis of ToxCast reported data from one set of assays, NovaScreen radioligand binding assays for human nuclear receptors [322], DOSS elicited the highest response for PPAR γ , with

some affinity for glucocorticoid receptor (GR) and progesterone receptor (PR) (Figure 2). Extremely weak or no activity was observed in these assays for androgen (AR) and estrogen receptor (ER α) as well as PPAR α (Figure 1). Together with data presented in Chapter 2, this suggests the primary mechanism of action regarding DOSS and nuclear receptors would be through the PPAR γ pathway, further demonstrated in Chapters 3. However, it should be noted that the reliability of ToxCast assays for identifying obesogens in particular may not be highly reliable. Results from similar assays do not overlap very well and such data should be interpreted with caution and careful validation is required [112]. Similarly, the presence of pan assay interference compounds (PAINS) can confound results [323]. Others have suggested DOSS may be a PAIN since it delivers several positive hits in the ToxCast dashboard [112]. However, in the assays presented here DOSS does not behave as a PAIN showing specificity for PPAR receptors (PPAR γ and PPAR β/δ ,) with no activity on RXR α , or estrogen receptors, and furthermore increases adipogenesis, indicative of PPAR γ activation.

In Chapter 3 evidence was provided in support of DOSS as a PPAR γ agonist and its ability to act as an obesogen *in vitro* primarily using adipogenic differentiation assays in three cell types. DOSS significantly increases the adipogenic differentiation of mouse 3T3L1 preadipocytes and human bone marrow derived mesenchymal stem cells and to a lesser extent mouse BM-MSCs. Importantly, this suggests that DOSS has affinity for both the mouse and human PPAR γ receptor.

While adipogenic differentiation was investigated, a process highly regulated by PPAR γ , the effects of DOSS on osteogenic or chondrogenic differentiation were not investigate beyond DXA scan measurements of bone area and density in mice. MSCs can

differentiate into multiple lineages including fat, bone, cartilage and others. Lineage commitment to either fat or bone have been shown to be a delicate, highly regulated process that can be influenced by environmental factors [211]. Furthermore, commitment to one of these lineages often occurs at the expense of the other. The obesogen and PPAR γ agonist tributyltin predisposes MSCs to an adipogenic lineage and reduces the ability of this cell type to differentiate into the bone lineage. Similarly, when MSCs are treated with the pharmaceutical PPAR γ agonist rosiglitazone, their ability for osteogenesis is reduced, while adipogenesis is greatly increased [324]. Given that DOSS activates PPAR γ and increases adipogenesis it is reasonable to propose the hypothesis that DOSS treatment in conjunction with osteogenic differentiation inducers, would similarly lead to a reduction or inhibition of osteogenic differentiation in MSCs. The Chapter 4 DXA scan results showing increased adiposity and decreased bone area provide some support for this hypothesis.

Similarly, this investigation did not test function in adipocytes that were produced by cells treated with DOSS and how this may differ from that of a rosiglitazone derived adipocyte. This is a relevant question given that pharmaceutical drug development has recently started developing selective PPAR γ modulators (SPPARgMs) [325]. These compounds are designed to activate PPAR γ but only initiate gene transcription and signaling of specific pathways. For example, a compound that activates PPAR γ eliciting insulin-sensitizing effects without the adipogenic effects (weight gain symptoms) would be more desirable than the currently available thiazolidinedione drugs, which have these and many other adverse side effects. However, it will not be a trivial task developing SPPARMs, not only with PPAR γ specificity, but also with selective transactivation

activities considering population variants in these pathways (e.g. coactivators, corepressors, etc.).

Industrial chemicals, such as the phthalate monoester, MEHP, have also been identified as adipogenic SPPARMs [86]. MEHP promotes adipogenesis but does not reach the maximum effect elicited from rosiglitazone, a result which we also observed for DOSS in our BM-MSC experiments (Chapter 3). MEHP is also involved in the recruitment of different coactivators and corepressors than rosiglitazone and, although many of the same genes are up or downregulated by MEHP and rosiglitazone, there is a unique set of genes that are regulated by each agonist as well. Unpublished work from our group studying the transcriptome of iPSCs exposed to either DOSS or rosiglitazone also identified a group of genes consistent with both exposures but also a set of genes unique to each exposure (correspondence with Demetri Spyropoulos; Theresa Cantu, PhD Thesis, MUSC 2017). TBT, another well studied environmental obesogen, may also be considered a SPPARM. It has been documented that TBT promotes a phenotypically distinct adipocyte compared to the troglitazone derived adipocyte but with equal potency (eliciting equal PPAR γ induction) [234]. TBT adipocytes secrete less adiponectin and have higher basal rates of glucose uptake but lower rates of insulin stimulated glucose uptake compared to troglitazone derived adipocytes. Evaluating the DOSS adipocyte for basal and insulin stimulated glucose uptake is a logical and important next step to further characterize DOSS as an obesogen.

DOSS, as the pharmaceutical docusate sodium, is often prescribed as a stool softener to pregnant women who suffer from pregnancy-induced constipation. Thus, pregnant women, and potentially their fetuses, are exposed to DOSS during a very

sensitive window of fetal development. In Chapter 4, multiple experiments for the phenotypic evaluation and characterization of DOSS as a metabolic disruptor were performed *in vivo* using a standard inbred mouse strain with dosing scenarios relevant to those experienced by pregnant women taking DOSS. We investigated the F1 adults for markers of obesity, diabetes and metabolic syndrome. Results indicate that DOSS promotes a phenotype indicative of metabolic syndrome in male mice, but not female mice. Most notably, male F1 adults of treated dams displayed marked glucose intolerance coupled with an increase in adiposity, a reduction in adiponectin, an increase in markers of inflammation particularly circulating levels of the proinflammatory cytokine IL-6, hypomethylation of the IL-6 promoter in IWAT and altered circulating phospholipids. Together, these data suggest that DOSS can act as an obesogen *in vitro* and *in vivo* and more research should be focused on further characterizing the metabolic disrupting effects of DOSS. In this study, C57BL/6 mice were used, a strain of mouse known to be susceptible to environmentally induced metabolic changes especially in males [326]. This is a limitation of this study, given that several strains of mice exist with the majority of metabolic disruptors research split between C57BL/6 and CD-1 strains (Table 1). Determining which strains of mice are susceptible to DOSS induced metabolic effects, and which ones are not, will provide better understanding for how these results can be translated to human exposure. This could be done using Collaborative Cross mice, which are an array of mice resulting from crosses between 8 commonly used inbred strains of mice and arguably more representative of the human population than any one inbred strain of mouse [327]. SNP analysis of each affected and unaffected mouse could yield genetic elements important in the obesity phenotypes observed with DOSS.

Additionally, in this study, two cohorts of F1 mice were used in order to increase our sample size. While control F1 mice from both groups appeared to have no significant differences for the majority of variables measured, there were differences observed between the two F1 ‘treatment’ cohorts (offspring of DOSS-treated dams). Particularly noticeable was the larger increase in adiposity observed in the second cohort of treated mice. To account for this, determined variables that were correlated with fat percentage were determined, such as circulating adiponectin levels, and normalized values based on total white adipose tissue for a given mouse. There are several factors that could influence this increased variance observed in treatment cohorts. Many features of the treated dams could contribute to this variance. For instance, in this experiment water consumption by the pregnant dams or effective concentrations of DOSS in adipose, liver and placental target tissues was not measured due to the lack of an established analytical method. It is possible that dams could drink different amounts of DOSS-containing water therefore altering the effective dose, increasing response variability in the offspring. Similarly, food consumption, lipid absorption and metabolism or energy output were not measured in the pregnant dams or offspring, all of which would have impacts on metabolic function. While littermates are genetically identical and the same mothers, natural behavioral dominance (i.e. alpha males) would contribute to altered feeding and activity levels among littermates that likely contribute to variable phenotypes. In fact, outlayers in multiple studies tend to be the same individuals. Due to experimental procedures, mice in one cohort (Cohort A) were transferred to USC Medical Center for oGTT and DXA measurements, while Cohort B was housed in MUSC CRI the entire time. It is possible that the transfer or different housing conditions could also affect these

mice physiologically. Lastly, pups from Cohort A and pups from Cohort B were born roughly six months apart and perhaps seasonal differences could have an effect on obesogen susceptibility. This would be a particularly interesting question to address.

To identify phenotypes that supersede the variability observed in the treatment cohorts, we performed multiple linear regression analysis to track individuals through multiple end point analyses. Significant correlations between adiposity and circulating adiponectin and leptin levels, but not IL-6 levels were observed. This was also observed for circulating levels of leptin and adiponectin compared with IWAT tissue gene expression, but not EWAT tissue gene expression. Additionally, a significant positive correlation between adiposity and glucose intolerance, as well as a significant negative correlation between circulating adiponectin and glucose intolerance were observed. Similarly, several phospholipid species were directly correlated with each other as well as adiposity. This is notable because some phospholipid species identified in adult F1 male offspring of DOSS-treated dams are also observed in the same strain of adult male mice after long-term high fat diet exposure [288, 303]. Correlations between gene expression and DNA methylation changes were not observed, although there was a significant inverse correlation between IL-6 gene CpG 2 methylation and circulating IL-6 levels. CpG methylation in IWAT could be acting as a proxy for overall IL-6 methylation levels. So, although we did not see correlation with expression in IWAT, expression from another tissue could be contributing to overall circulating levels that has similar methylation patterns to those observed in IWAT. Additionally, although promoter methylation is typically associated with decreased gene expression, there are other

functions for DNA methylation as well as several different CpG sites within a promoter that could be regulatory[37, 328].

In these experiments, maternal DOSS exposure was either a) acting directly on the F1 offspring via placental transfer; b) acting indirectly on the F1 offspring by eliciting one or more responses in the dams that altered fetal programming; or c) both a and b. The ability to measure DOSS in the placenta and fetus would greatly aid in assessing these possibilities, especially scenario A. DOSS is thought to be minimally absorbed when taken orally (<5%); however, Dujovne and Shoeman showed that DOSS taken orally can be measured in human bile at concentrations ranging from 40-90uM (20-40 ppm), indicative that DOSS is absorbed through the GI tract into the blood stream, followed by biliary excretion back into the GI track and enterohepatic circulation [329]. Metabolism and excretion studies in rat, rabbit and dog using radiolabeled DOSS suggest that a percentage of DOSS is metabolized to 2-ethylhexanol cleavage product within 96 hours of administration, and primarily excreted in the urine and feces; it can be detected in the blood up to 8 hours after administration with trace detection in tissues [330]. This indicates that DOSS may be able to enter the blood stream and potentially be present in cord blood. Follow-up pharmacokinetics studies should be repeated, in this case with pregnant dams, using current high resolution analytical techniques. Results of the studies presented herein also warrant studies that analyze maternal blood of pregnant women (who took DOSS containing or DOSS free laxative) and associated cord blood samples in order to help address this question.

Intriguingly, work from Sigurdsson et al. indicates that maternal bile acids can act as chemical chaperones and influence fetal hematopoietic stem cell expansion in the fetal

liver [331]. This may provide a unique mechanism of action, by which fetal DOSS exposure (via maternal bile) could influence fetal stem cell expansion and programming. To investigate this, fetal HSC number, lineage commitment and bile acid composition could be assessed in fetuses (E15.5) from pregnant dams exposed to DOSS (E10-15).

Quantitative methods for DOSS using high performance liquid chromatography and tandem mass spectrometry (HPLC-MS/MS) exist for sea water and fish tissues [162, 314, 332]. Both of these methods were developed quickly with the specific intention of quantifying contamination due to the use of Corexit 9500 in the remediation of the Deepwater Horizon oil spill in 2010. Unpublished, preliminary data from our group suggests that these methods are not suitable for biological samples given the extreme differences in matrix composition, lipid over aqueous partitioning of DOSS and the high limits of detection. Blood and breast milk are biological matrices important in understanding the body burden of DOSS, potential exposure to offspring and to test the hypotheses that a) DOSS can be detected in circulating blood and deposited to other tissues and b) Colace users have greater levels of DOSS in blood and breast milk compared to non-Colace users. Research projects to address this would likely involve optimization of efficient extraction from blood and breast milk as well as modifying current LC-MS/MS protocols to effectively quantify DOSS in these biological samples.

With regard to scenario B (above), it is certainly possible for DOSS to have indirect effects that were not measured in this study. Several EDCs can have multiple mechanisms of action which are often identified at different points in time with new mechanisms of action under investigation [257]. One such example is diethylstilbestrol (DES), a potent estrogen that also has metabolic disrupting effects that are independent of

estrogen signaling [160]. Similarly, phthalates are often classified as anti androgenic chemicals, of which there are multiple mechanisms, but can also act as metabolic disruptors. A likely mechanism whereby DOSS could indirectly effect obesity and metabolic syndrome is low grade chronic inflammation. In fact, changes to inflammatory cytokines were observed at the epigenetic, expression, and protein level, indicating the role of DOSS in mediating inflammation may be a major mechanism of action by which it can elicit metabolic disrupting effects. The non-ionic detergent 4-nonylphenol (4-NP) may be most similar to DOSS as an inflammatory inducer (COX-2 and PGE₂ production) and an obesogen [333, 334].

While data in this work indicate that DOSS is primarily acting through a PPAR γ dependent mechanism, another logical indirect effect of DOSS exposure could be through alterations to the gut microbiota. Understanding the role of the gut microbiome in relation to diabetes and obesity is an extremely exciting area of research. Studies have shown that there are significant differences in species composition and diversity between lean and obese individuals, in both rodents and humans [335]. In fact, DOSS is used in agriculture to effectively remove gut fauna from livestock, suggesting DOSS could also alter the microbiome in humans or mice [311]. Although a low sample size, ruminal dosing of cows with DOSS had altered fatty acid composition in their milk compared to cows with no DOSS induced defaunation [311]. Furthermore, when gut fauna are transferred from an obese mouse to a germ free lean mouse, the previously lean mouse gains weight despite no changes in food consumption and vice versa [336]. Transplant of human obese and lean associated gut microbiota to mice yields similar results with regard to obese and lean phenotype development [337]. Studies have also shown that the

maternal microbiome can have an impact on obesity and diabetes development in offspring particularly as it relates to maternal obesity [309].

Several emulsifiers and surfactants similar to and including DOSS are used as common food additives at up to 1% of the food content. Research has begun to assess biological effects of these emulsifiers as it relates to human health. Chassaing et al. found that mice exposed to two common food emulsifiers (Carboxymethylcellulose and Tween 80) at environmentally relevant concentrations (1% w/v or v/v) altered gut microbiota composition to that of a population that promoted inflammatory bowel disease and obesity [208]. Additionally, Lecomte et al. found that in combination with a high fat diet, different types of emulsifiers (polar lipids from milk and soybean) can exaggerate the effects of the diet through impacts on intestinal absorption further promoting metabolic syndrome [310]. In order to test the hypothesis that DOSS alters the maternal microbiome of exposed dams thereby influencing metabolic syndrome development in the pups, meta genomic sequencing of fecal samples from dams, as well as weaning pups, should be performed as part of the studies produced by this work.

The aforementioned work brings up another relevant area of research that is combinatorial exposures and multiple stressors. While several metabolic disruptors elicit their effects through treatment with the compound of interest only, researchers have begun to assess how exposure effects metabolic outcomes when combined with high fat diet, or other contributors to obesity. For instance, Wei et al. (2011) demonstrated that animals prenatally exposed to BPA developed markers of metabolic syndrome and that these results were exacerbated in conjunction with a high fat diet [338]. Interestingly, these results were only observed at a relevant low dose of BPA exposure, but not a high

dose. Investigating DOSS exposure in the context of a high fat diet or a high carb diet reflective of a typical Western diet is interesting and relevant.

In summary, the work presented in this Dissertation lead to the identification and preliminary characterization of a novel probable metabolic disruptor, DOSS, which has important implications for human health and likely will significantly impact the field. Despite the fact that this investigation initiated with oil originating from the DWH oil spill as an exposure source and held the hypothesis that PAHs in the oil would be the predominating obesogenic/EDC compounds, to the results of these studies identified the Corexit component DOSS as the primary obesogenic compound, a finding that may have far-reaching impacts on human health due to its use in a wide array of pharmaceuticals, foods, flavoring/coloring agents, as well as industrial and household cleaners. Therefore, human exposure to DOSS is likely to be widespread over the lifetime of individuals and perhaps predominantly occurs during sensitive and vulnerable times of fetal and childhood development. Although DOSS may be rapidly metabolized with minimal absorption, due to its pervasive use, DOSS may be considered a “pseudo-persistent” chemical, as is the case with phthalate esters. Further work into the pharmacokinetics of DOSS, as well as longitudinal epidemiological studies following growth and metabolic outcomes of children of mothers prescribed and taking DOSS during pregnancy and nursing, will help address these major questions associated with DOSS.

While this work generates several questions surrounding DOSS exposure, its ability to act as a metabolic disruptor, and its relevance towards human health, this work was foundational in beginning to answer those questions and shape this body of research.

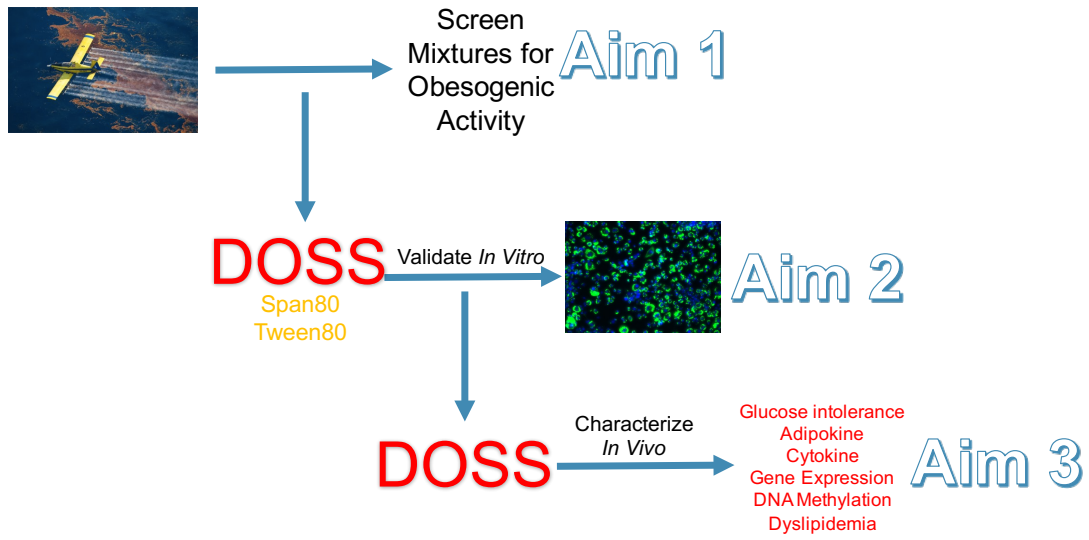


Figure 1. Summary of results presented in Chapters 2, 3 and 4.

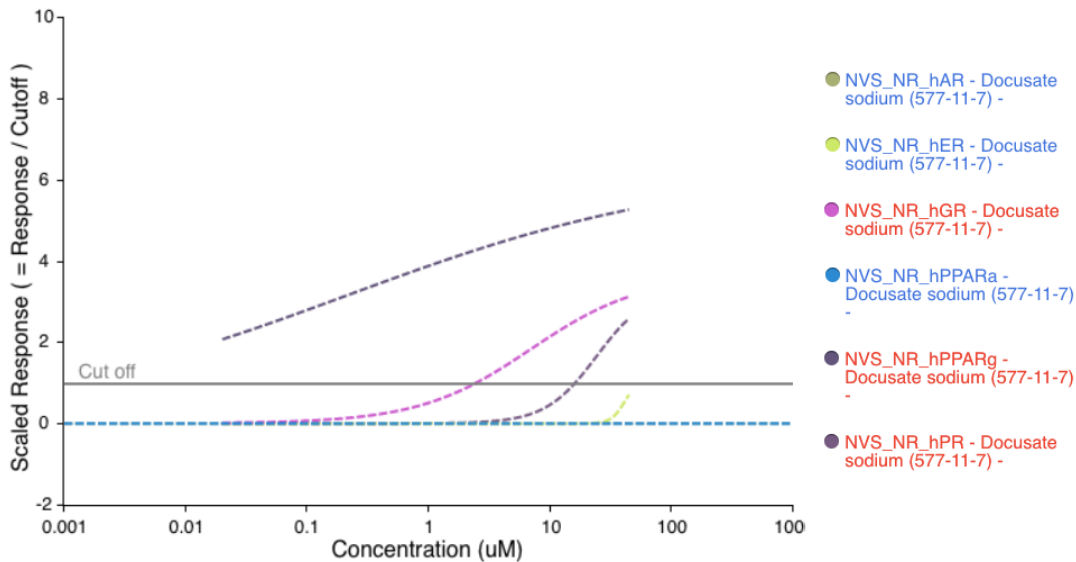


Figure 2. EPA ToxCast data for docusate sodium activation of several nuclear receptors using the NovaScreen radioligand binding assay.

The EPA iCSS ToxCast Dashboard was used to compile data available for human nuclear receptor radioligand assay binding. The action of docusate sodium on ligand binding is compared for PPAR γ , GR, PR, ER, PPAR α and AR.

REFERENCES

1. Flegal, K.M., et al., *Trends in Obesity Among Adults in the United States, 2005 to 2014*. JAMA, 2016. **315**(21): p. 2284-91.
2. Ogden, C.L., et al., *Trends in Obesity Prevalence Among Children and Adolescents in the United States, 1988-1994 Through 2013-2014*. JAMA, 2016. **315**(21): p. 2292-9.
3. Geiss, L.S., et al., *Prevalence and incidence trends for diagnosed diabetes among adults aged 20 to 79 years, United States, 1980-2012*. JAMA, 2014. **312**(12): p. 1218-26.
4. Menke, A., et al., *Prevalence of and Trends in Diabetes Among Adults in the United States, 1988-2012*. JAMA, 2015. **314**(10): p. 1021-9.
5. Smyth, S. and A. Heron, *Diabetes and obesity: the twin epidemics*. Nat Med, 2006. **12**(1): p. 75-80.
6. Kaur, J., *A comprehensive review on metabolic syndrome*. Cardiol Res Pract, 2014. **2014**: p. 943162.
7. Aguilar, M., et al., *Prevalence of the metabolic syndrome in the United States, 2003-2012*. JAMA, 2015. **313**(19): p. 1973-4.
8. Wang, Y.C., et al., *Health and economic burden of the projected obesity trends in the USA and the UK*. Lancet, 2011. **378**(9793): p. 815-25.
9. Boudreau, D.M., et al., *Health care utilization and costs by metabolic syndrome risk factors*. Metab Syndr Relat Disord, 2009. **7**(4): p. 305-14.
10. Walker, G.E., et al., *The pathophysiology of abdominal adipose tissue depots in health and disease*. Horm Mol Biol Clin Investig, 2014. **19**(1): p. 57-74.
11. Janssen, I., P.T. Katzmarzyk, and R. Ross, *Waist circumference and not body mass index explains obesity-related health risk*. Am J Clin Nutr, 2004. **79**(3): p. 379-84.
12. Friedman, J.M., *Modern science versus the stigma of obesity*. Nat Med, 2004. **10**(6): p. 563-9.
13. Carr, D. and M.A. Friedman, *Is obesity stigmatizing? Body weight, perceived discrimination, and psychological well-being in the United States*. J Health Soc Behav, 2005. **46**(3): p. 244-59.
14. Scherer, P.E., *Adipose tissue: from lipid storage compartment to endocrine organ*. Diabetes, 2006. **55**(6): p. 1537-45.
15. Ingalls, A.M., M.M. Dickie, and G.D. Snell, *Obese, a new mutation in the house mouse*. J Hered, 1950. **41**(12): p. 317-8.
16. Hummel, K.P., M.M. Dickie, and D.L. Coleman, *Diabetes, a new mutation in the mouse*. Science, 1966. **153**(3740): p. 1127-8.
17. Zhang, Y., et al., *Positional cloning of the mouse obese gene and its human homologue*. Nature, 1994. **372**(6505): p. 425-32.
18. Chen, H., et al., *Evidence that the diabetes gene encodes the leptin receptor: identification of a mutation in the leptin receptor gene in db/db mice*. Cell, 1996. **84**(3): p. 491-5.
19. Montague, C.T., et al., *Congenital leptin deficiency is associated with severe early-onset obesity in humans*. Nature, 1997. **387**(6636): p. 903-8.

20. Ghalandari, H., F. Hosseini-Esfahani, and P. Mirmiran, *The Association of Polymorphisms in Leptin/Leptin Receptor Genes and Ghrelin/Ghrelin Receptor Genes With Overweight/Obesity and the Related Metabolic Disturbances: A Review*. *Int J Endocrinol Metab*, 2015. **13**(3): p. e19073.
21. Li, M.D., *Leptin and beyond: an odyssey to the central control of body weight*. *Yale J Biol Med*, 2011. **84**(1): p. 1-7.
22. Maeda, K., et al., *cDNA cloning and expression of a novel adipose specific collagen-like factor, apM1 (AdiPose Most abundant Gene transcript 1)*. *Biochem Biophys Res Commun*, 1996. **221**(2): p. 286-9.
23. Scherer, P.E., et al., *A novel serum protein similar to C1q, produced exclusively in adipocytes*. *J Biol Chem*, 1995. **270**(45): p. 26746-9.
24. Hu, E., P. Liang, and B.M. Spiegelman, *AdipoQ is a novel adipose-specific gene dysregulated in obesity*. *J Biol Chem*, 1996. **271**(18): p. 10697-703.
25. Maeda, N., et al., *Diet-induced insulin resistance in mice lacking adiponectin/ACRP30*. *Nat Med*, 2002. **8**(7): p. 731-7.
26. Combs, T.P., et al., *A transgenic mouse with a deletion in the collagenous domain of adiponectin displays elevated circulating adiponectin and improved insulin sensitivity*. *Endocrinology*, 2004. **145**(1): p. 367-83.
27. Nakashima, Y., et al., *Involvement of low adiponectin levels in impaired glucose tolerance*. *Metabolism*, 2008. **57**(10): p. 1350-4.
28. Aleidi, S., et al., *Adiponectin serum levels correlate with insulin resistance in type 2 diabetic patients*. *Saudi Pharm J*, 2015. **23**(3): p. 250-6.
29. Hotta, K., et al., *Plasma concentrations of a novel, adipose-specific protein, adiponectin, in type 2 diabetic patients*. *Arterioscler Thromb Vasc Biol*, 2000. **20**(6): p. 1595-9.
30. Arita, Y., et al., *Paradoxical decrease of an adipose-specific protein, adiponectin, in obesity*. *Biochem Biophys Res Commun*, 1999. **257**(1): p. 79-83.
31. Haluzik, M., J. Parizkova, and M.M. Haluzik, *Adiponectin and its role in the obesity-induced insulin resistance and related complications*. *Physiol Res*, 2004. **53**(2): p. 123-9.
32. Khalil, R.B. and C. El Hachem, *Adiponectin in eating disorders*. *Eat Weight Disord*, 2014. **19**(1): p. 3-10.
33. Maeda, N., et al., *PPARgamma ligands increase expression and plasma concentrations of adiponectin, an adipose-derived protein*. *Diabetes*, 2001. **50**(9): p. 2094-9.
34. Pyrzak, B., et al., *Adiponectin as a biomarker of the metabolic syndrome in children and adolescents*. *Eur J Med Res*, 2010. **15 Suppl 2**: p. 147-51.
35. Ryo, M., et al., *Adiponectin as a biomarker of the metabolic syndrome*. *Circ J*, 2004. **68**(11): p. 975-81.
36. Tajtakova, M., et al., *Adiponectin as a biomarker of clinical manifestation of metabolic syndrome*. *Endocr Regul*, 2006. **40**(1): p. 15-9.
37. Jones, P.A., *Functions of DNA methylation: islands, start sites, gene bodies and beyond*. *Nat Rev Genet*, 2012. **13**(7): p. 484-92.
38. Yin, Y., et al., *Impact of cytosine methylation on DNA binding specificities of human transcription factors*. *Science*, 2017. **356**(6337).

39. Gonda, T.A., et al., *Folic acid increases global DNA methylation and reduces inflammation to prevent Helicobacter-associated gastric cancer in mice*. Gastroenterology, 2012. **142**(4): p. 824-833 e7.
40. Mathers, J.C., *Reversal of DNA hypomethylation by folic acid supplements: possible role in colorectal cancer prevention*. Gut, 2005. **54**(5): p. 579-81.
41. Pufulete, M., et al., *Effect of folic acid supplementation on genomic DNA methylation in patients with colorectal adenoma*. Gut, 2005. **54**(5): p. 648-53.
42. Dolinoy, D.C., D. Huang, and R.L. Jirtle, *Maternal nutrient supplementation counteracts bisphenol A-induced DNA hypomethylation in early development*. Proc Natl Acad Sci U S A, 2007. **104**(32): p. 13056-61.
43. Sala, P., et al., *Tissue-specific methylation profile in obese patients with type 2 diabetes before and after Roux-en-Y gastric bypass*. Diabetol Metab Syndr, 2017. **9**: p. 15.
44. Ronn, T., et al., *A six months exercise intervention influences the genome-wide DNA methylation pattern in human adipose tissue*. PLoS Genet, 2013. **9**(6): p. e1003572.
45. Pietilainen, K.H., et al., *DNA methylation and gene expression patterns in adipose tissue differ significantly within young adult monozygotic BMI-discordant twin pairs*. Int J Obes (Lond), 2016. **40**(4): p. 654-61.
46. Kim, A.Y., et al., *Obesity-induced DNA hypermethylation of the adiponectin gene mediates insulin resistance*. Nat Commun, 2015. **6**: p. 7585.
47. Houde, A.A., et al., *Leptin and adiponectin DNA methylation levels in adipose tissues and blood cells are associated with BMI, waist girth and LDL-cholesterol levels in severely obese men and women*. BMC Med Genet, 2015. **16**: p. 29.
48. Shen, W., et al., *Epigenetic modification of the leptin promoter in diet-induced obese mice and the effects of N-3 polyunsaturated fatty acids*. Sci Rep, 2014. **4**: p. 5282.
49. Houde, A.A., et al., *Cross-tissue comparisons of leptin and adiponectin: DNA methylation profiles*. Adipocyte, 2014. **3**(2): p. 132-40.
50. Weisberg, S.P., et al., *Obesity is associated with macrophage accumulation in adipose tissue*. J Clin Invest, 2003. **112**(12): p. 1796-808.
51. Monteiro, R. and I. Azevedo, *Chronic inflammation in obesity and the metabolic syndrome*. Mediators Inflamm, 2010. **2010**.
52. Fried, S.K., D.A. Bunkin, and A.S. Greenberg, *Omental and subcutaneous adipose tissues of obese subjects release interleukin-6: depot difference and regulation by glucocorticoid*. J Clin Endocrinol Metab, 1998. **83**(3): p. 847-50.
53. Spranger, J., et al., *Inflammatory cytokines and the risk to develop type 2 diabetes: results of the prospective population-based European Prospective Investigation into Cancer and Nutrition (EPIC)-Potsdam Study*. Diabetes, 2003. **52**(3): p. 812-7.
54. Hu, F.B., et al., *Inflammatory markers and risk of developing type 2 diabetes in women*. Diabetes, 2004. **53**(3): p. 693-700.
55. Wallenius, V., et al., *Interleukin-6-deficient mice develop mature-onset obesity*. Nat Med, 2002. **8**(1): p. 75-9.

56. Konukoglu, D., et al., *Relationship between serum concentrations of interleukin-6 and tumor necrosis factor alpha in female Turkish subjects with normal and impaired glucose tolerance*. *Horm Metab Res*, 2006. **38**(1): p. 34-7.
57. Pedersen, M., et al., *Circulating levels of TNF-alpha and IL-6-relation to truncal fat mass and muscle mass in healthy elderly individuals and in patients with type-2 diabetes*. *Mech Ageing Dev*, 2003. **124**(4): p. 495-502.
58. Ryan, A.S. and B.J. Nicklas, *Reductions in plasma cytokine levels with weight loss improve insulin sensitivity in overweight and obese postmenopausal women*. *Diabetes Care*, 2004. **27**(7): p. 1699-705.
59. Fasshauer, M., et al., *Adiponectin gene expression and secretion is inhibited by interleukin-6 in 3T3-L1 adipocytes*. *Biochem Biophys Res Commun*, 2003. **301**(4): p. 1045-50.
60. Lagathu, C., et al., *Chronic interleukin-6 (IL-6) treatment increased IL-6 secretion and induced insulin resistance in adipocyte: prevention by rosiglitazone*. *Biochem Biophys Res Commun*, 2003. **311**(2): p. 372-9.
61. Goyal, R., et al., *Evaluation of TNF-alpha and IL-6 Levels in Obese and Non-obese Diabetics: Pre- and Postinsulin Effects*. *N Am J Med Sci*, 2012. **4**(4): p. 180-4.
62. Hotamisligil, G.S., N.S. Shargill, and B.M. Spiegelman, *Adipose expression of tumor necrosis factor-alpha: direct role in obesity-linked insulin resistance*. *Science*, 1993. **259**(5091): p. 87-91.
63. Stanley, T.L., et al., *TNF-alpha antagonism with etanercept decreases glucose and increases the proportion of high molecular weight adiponectin in obese subjects with features of the metabolic syndrome*. *J Clin Endocrinol Metab*, 2011. **96**(1): p. E146-50.
64. Borges, R.L., et al., *[Impact of weight loss on adipocytokines, C-reactive protein and insulin sensitivity in hypertensive women with central obesity]*. *Arq Bras Cardiol*, 2007. **89**(6): p. 409-14.
65. Attie, A.D. and P.E. Scherer, *Adipocyte metabolism and obesity*. *J Lipid Res*, 2009. **50 Suppl**: p. S395-9.
66. Baillie-Hamilton, P.F., *Chemical toxins: a hypothesis to explain the global obesity epidemic*. *J Altern Complement Med*, 2002. **8**(2): p. 185-92.
67. Neel, B.A. and R.M. Sargis, *The paradox of progress: environmental disruption of metabolism and the diabetes epidemic*. *Diabetes*, 2011. **60**(7): p. 1838-48.
68. Sargis, R.M., *Metabolic disruption in context: Clinical avenues for synergistic perturbations in energy homeostasis by endocrine disrupting chemicals*. *Endocr Disruptors (Austin)*, 2015. **3**(1): p. e1080788.
69. Heindel, J.J., et al., *Parma consensus statement on metabolic disruptors*. *Environ Health*, 2015. **14**: p. 54.
70. Klimentidis, Y.C., et al., *Canaries in the coal mine: a cross-species analysis of the plurality of obesity epidemics*. *Proc Biol Sci*, 2011. **278**(1712): p. 1626-32.
71. Barker, D.J., *The origins of the developmental origins theory*. *J Intern Med*, 2007. **261**(5): p. 412-7.
72. Barker, D.J., et al., *Fetal nutrition and cardiovascular disease in adult life*. *Lancet*, 1993. **341**(8850): p. 938-41.

73. Roseboom, T.J., et al., *Effects of prenatal exposure to the Dutch famine on adult disease in later life: an overview*. Mol Cell Endocrinol, 2001. **185**(1-2): p. 93-8.
74. Janesick, A. and B. Blumberg, *Obesogens, stem cells and the developmental programming of obesity*. Int J Androl, 2012. **35**(3): p. 437-48.
75. Guillette, L.J., Jr., et al., *Serum concentrations of various environmental contaminants and their relationship to sex steroid concentrations and phallus size in juvenile American alligators*. Arch Environ Contam Toxicol, 1999. **36**(4): p. 447-55.
76. Crain, D.A., et al., *Alterations in steroidogenesis in alligators (Alligator mississippiensis) exposed naturally and experimentally to environmental contaminants*. Environ Health Perspect, 1997. **105**(5): p. 528-33.
77. Semenza, J.C., et al., *Reproductive toxins and alligator abnormalities at Lake Apopka, Florida*. Environ Health Perspect, 1997. **105**(10): p. 1030-2.
78. Reed, C.E. and S.E. Fenton, *Exposure to diethylstilbestrol during sensitive life stages: a legacy of heritable health effects*. Birth Defects Res C Embryo Today, 2013. **99**(2): p. 134-46.
79. Iguchi, T., et al., *Polyovular follicles in mouse ovaries exposed neonatally to diethylstilbestrol in vivo and in vitro*. Biol Reprod, 1990. **43**(3): p. 478-84.
80. Bern, H.A., et al., *Altered mammary responsiveness to estradiol and progesterone in mice exposed neonatally to diethylstilbestrol*. Cancer Lett, 1992. **63**(2): p. 117-24.
81. Iguchi, T., et al., *Vaginal abnormalities in ovariectomized BALB/cCrgl mice after neonatal exposure to different doses of diethylstilbestrol*. Cancer Lett, 1988. **43**(3): p. 207-14.
82. Aranda, A. and A. Pascual, *Nuclear hormone receptors and gene expression*. Physiol Rev, 2001. **81**(3): p. 1269-304.
83. le Maire, A., W. Bourguet, and P. Balaguer, *A structural view of nuclear hormone receptor: endocrine disruptor interactions*. Cell Mol Life Sci, 2010. **67**(8): p. 1219-37.
84. Henley, D.V. and K.S. Korach, *Endocrine-disrupting chemicals use distinct mechanisms of action to modulate endocrine system function*. Endocrinology, 2006. **147**(6 Suppl): p. S25-32.
85. Shanle, E.K. and W. Xu, *Endocrine disrupting chemicals targeting estrogen receptor signaling: identification and mechanisms of action*. Chem Res Toxicol, 2011. **24**(1): p. 6-19.
86. Feige, J.N., et al., *The endocrine disruptor monoethyl-hexyl-phthalate is a selective peroxisome proliferator-activated receptor gamma modulator that promotes adipogenesis*. J Biol Chem, 2007. **282**(26): p. 19152-66.
87. Fisher, J.S., *Are all EDC effects mediated via steroid hormone receptors?* Toxicology, 2004. **205**(1-2): p. 33-41.
88. Vaiserman, A., *Early-life Exposure to Endocrine Disrupting Chemicals and Later-life Health Outcomes: An Epigenetic Bridge?* Aging Dis, 2014. **5**(6): p. 419-29.
89. Newbold, R.R., et al., *Perinatal exposure to environmental estrogens and the development of obesity*. Mol Nutr Food Res, 2007. **51**(7): p. 912-7.

90. Newbold, R.R., E. Padilla-Banks, and W.N. Jefferson, *Environmental estrogens and obesity*. Mol Cell Endocrinol, 2009. **304**(1-2): p. 84-9.
91. Gray, S.L., et al., *Chronic exposure to PCBs (Aroclor 1254) exacerbates obesity-induced insulin resistance and hyperinsulinemia in mice*. J Toxicol Environ Health A, 2013. **76**(12): p. 701-15.
92. Grun, F. and B. Blumberg, *Environmental obesogens: organotins and endocrine disruption via nuclear receptor signaling*. Endocrinology, 2006. **147**(6 Suppl): p. S50-5.
93. Chamorro-Garcia, R., et al., *Transgenerational inheritance of increased fat depot size, stem cell reprogramming, and hepatic steatosis elicited by prenatal exposure to the obesogen tributyltin in mice*. Environ Health Perspect, 2013. **121**(3): p. 359-66.
94. Kirchner, S., et al., *Prenatal exposure to the environmental obesogen tributyltin predisposes multipotent stem cells to become adipocytes*. Mol Endocrinol, 2010. **24**(3): p. 526-39.
95. Zuo, Z., et al., *Tributyltin causes obesity and hepatic steatosis in male mice*. Environ Toxicol, 2011. **26**(1): p. 79-85.
96. Li, X., J. Ycaza, and B. Blumberg, *The environmental obesogen tributyltin chloride acts via peroxisome proliferator activated receptor gamma to induce adipogenesis in murine 3T3-L1 preadipocytes*. J Steroid Biochem Mol Biol, 2011. **127**(1-2): p. 9-15.
97. Biemann, R., et al., *Tributyltin affects adipogenic cell fate commitment in mesenchymal stem cells by a PPARgamma independent mechanism*. Chem Biol Interact, 2014. **214**: p. 1-9.
98. Chandra, V., et al., *Structure of the intact PPAR-gamma-RXR- nuclear receptor complex on DNA*. Nature, 2008. **456**(7220): p. 350-6.
99. Tugwood, J.D., et al., *The mouse peroxisome proliferator activated receptor recognizes a response element in the 5' flanking sequence of the rat acyl CoA oxidase gene*. EMBO J, 1992. **11**(2): p. 433-9.
100. Frohnert, B.I., T.Y. Hui, and D.A. Bernlohr, *Identification of a functional peroxisome proliferator-responsive element in the murine fatty acid transport protein gene*. J Biol Chem, 1999. **274**(7): p. 3970-7.
101. Nagasawa, M., et al., *Identification of a functional peroxisome proliferator-activated receptor (PPAR) response element (PPRE) in the human apolipoprotein A-IV gene*. Biochem Pharmacol, 2009. **78**(5): p. 523-30.
102. Nakachi, Y., et al., *Identification of novel PPARgamma target genes by integrated analysis of ChIP-on-chip and microarray expression data during adipocyte differentiation*. Biochem Biophys Res Commun, 2008. **372**(2): p. 362-6.
103. MacDougald, O.A. and M.D. Lane, *Transcriptional regulation of gene expression during adipocyte differentiation*. Annu Rev Biochem, 1995. **64**: p. 345-73.
104. Kliewer, S.A., et al., *Fatty acids and eicosanoids regulate gene expression through direct interactions with peroxisome proliferator-activated receptors alpha and gamma*. Proc Natl Acad Sci U S A, 1997. **94**(9): p. 4318-23.
105. Yanase, T., et al., *Differential expression of PPAR gamma1 and gamma2 isoforms in human adipose tissue*. Biochem Biophys Res Commun, 1997. **233**(2): p. 320-4.

106. Zhu, Y., et al., *Structural organization of mouse peroxisome proliferator-activated receptor gamma (mPPAR gamma) gene: alternative promoter use and different splicing yield two mPPAR gamma isoforms*. Proc Natl Acad Sci U S A, 1995. **92**(17): p. 7921-5.
107. Tontonoz, P., et al., *mPPAR gamma 2: tissue-specific regulator of an adipocyte enhancer*. Genes Dev, 1994. **8**(10): p. 1224-34.
108. Ahmadian, M., et al., *PPARgamma signaling and metabolism: the good, the bad and the future*. Nat Med, 2013. **19**(5): p. 557-66.
109. Staels, B. and J.C. Fruchart, *Therapeutic roles of peroxisome proliferator-activated receptor agonists*. Diabetes, 2005. **54**(8): p. 2460-70.
110. Casals-Casas, C., J.N. Feige, and B. Desvergne, *Interference of pollutants with PPARs: endocrine disruption meets metabolism*. Int J Obes (Lond), 2008. **32 Suppl 6**: p. S53-61.
111. Janesick, A. and B. Blumberg, *Minireview: PPARgamma as the target of obesogens*. J Steroid Biochem Mol Biol, 2011. **127**(1-2): p. 4-8.
112. Janesick, A.S., et al., *On the Utility of ToxCast and ToxPi as Methods for Identifying New Obesogens*. Environ Health Perspect, 2016. **124**(8): p. 1214-26.
113. Sargis, R.M., et al., *Environmental endocrine disruptors promote adipogenesis in the 3T3-L1 cell line through glucocorticoid receptor activation*. Obesity (Silver Spring), 2010. **18**(7): p. 1283-8.
114. Pettersson, U.S., et al., *Female mice are protected against high-fat diet induced metabolic syndrome and increase the regulatory T cell population in adipose tissue*. PLoS One, 2012. **7**(9): p. e46057.
115. Regnier, S.M., et al., *Dietary exposure to the endocrine disruptor tolylfluanid promotes global metabolic dysfunction in male mice*. Endocrinology, 2015. **156**(3): p. 896-910.
116. Mauvais-Jarvis, F., A.P. Arnold, and K. Reue, *A Guide for the Design of Pre-clinical Studies on Sex Differences in Metabolism*. Cell Metab, 2017. **25**(6): p. 1216-1230.
117. Yaghjian, L., et al., *Associations of urinary phthalates with body mass index, waist circumference and serum lipids among females: National Health and Nutrition Examination Survey 1999-2004*. Int J Obes (Lond), 2015. **39**(6): p. 994-1000.
118. Stahlhut, R.W., et al., *Concentrations of urinary phthalate metabolites are associated with increased waist circumference and insulin resistance in adult U.S. males*. Environ Health Perspect, 2007. **115**(6): p. 876-82.
119. Braun, J.M., et al., *Prenatal perfluoroalkyl substance exposure and child adiposity at 8 years of age: The HOME study*. Obesity (Silver Spring), 2016. **24**(1): p. 231-7.
120. Buyun Liu, H.-J.L., Yangbo Sun, Guifeng Xu, Yuewei Liu, Geng Zong, Qi Sun, Frank B Hu, Robert B Wallace, Wei Bao, *Bisphenol A substitutes and obesity in US adults: analysis of a population-based, cross-sectional study*. The Lancet Planetary Health, 2017. **1**(3).
121. Harley, K.G., et al., *Prenatal and postnatal bisphenol A exposure and body mass index in childhood in the CHAMACOS cohort*. Environ Health Perspect, 2013. **121**(4): p. 514-20.

122. Braun, J.M., et al., *Early-life bisphenol a exposure and child body mass index: a prospective cohort study*. Environ Health Perspect, 2014. **122**(11): p. 1239-45.
123. Legler, J., et al., *The OBELIX project: early life exposure to endocrine disruptors and obesity*. Am J Clin Nutr, 2011. **94**(6 Suppl): p. 1933S-1938S.
124. Iszatt, N., et al., *Prenatal and Postnatal Exposure to Persistent Organic Pollutants and Infant Growth: A Pooled Analysis of Seven European Birth Cohorts*. Environ Health Perspect, 2015. **123**(7): p. 730-6.
125. Crone, T.J. and M. Tolstoy, *Magnitude of the 2010 Gulf of Mexico oil leak*. Science, 2010. **330**(6004): p. 634.
126. Rico-Martinez, R., T.W. Snell, and T.L. Shearer, *Synergistic toxicity of Macondo crude oil and dispersant Corexit 9500A((R)) to the Brachionus plicatilis species complex (Rotifera)*. Environ Pollut, 2013. **173**: p. 5-10.
127. Ramachandran, S.D., et al., *Oil dispersant increases PAH uptake by fish exposed to crude oil*. Ecotoxicol Environ Saf, 2004. **59**(3): p. 300-8.
128. de Soysa, T.Y., et al., *Macondo crude oil from the Deepwater Horizon oil spill disrupts specific developmental processes during zebrafish embryogenesis*. BMC Biol, 2012. **10**: p. 40.
129. Incardona, J.P., et al., *Deepwater Horizon crude oil impacts the developing hearts of large predatory pelagic fish*. Proc Natl Acad Sci U S A, 2014. **111**(15): p. E1510-8.
130. Schwacke, L.H., et al., *Health of common bottlenose dolphins (Tursiops truncatus) in Barataria Bay, Louisiana, following the deepwater horizon oil spill*. Environ Sci Technol, 2014. **48**(1): p. 93-103.
131. D'Andrea, M.A. and G.K. Reddy, *Health risks associated with crude oil spill exposure*. Am J Med, 2014. **127**(9): p. 886 e9 -13.
132. D'Andrea, M.A. and G.K. Reddy, *Health consequences among subjects involved in Gulf oil spill clean-up activities*. Am J Med, 2013. **126**(11): p. 966-74.
133. Shi, Y., A.M. Roy-Engel, and H. Wang, *Effects of COREXIT dispersants on cytotoxicity parameters in a cultured human bronchial airway cells, BEAS-2B*. J Toxicol Environ Health A, 2013. **76**(13): p. 827-35.
134. Adedara, I.A., et al., *Nigerian bonny light crude oil induces endocrine disruption in male rats*. Drug Chem Toxicol, 2014. **37**(2): p. 198-203.
135. Tracey, R., et al., *Hydrocarbons (jet fuel JP-8) induce epigenetic transgenerational inheritance of obesity, reproductive disease and sperm epimutations*. Reprod Toxicol, 2013. **36**: p. 104-16.
136. Yan, Z., et al., *Prenatal polycyclic aromatic hydrocarbon, adiposity, peroxisome proliferator-activated receptor (PPAR) gamma methylation in offspring, grand-offspring mice*. PLoS One, 2014. **9**(10): p. e110706.
137. Kim, J.H., et al., *Evaluation of polycyclic aromatic hydrocarbons in the activation of early growth response-1 and peroxisome proliferator activated receptors*. Toxicol Sci, 2005. **85**(1): p. 585-93.
138. Truter, J.C., et al., *An evaluation of the endocrine disruptive potential of crude oil water accommodated fractions and crude oil contaminated surface water to freshwater organisms using in vitro and in vivo approaches*. Environ Toxicol Chem, 2017. **36**(5): p. 1330-1342.

139. Vrabie, C.M., et al., *Specific in vitro toxicity of crude and refined petroleum products: 3. Estrogenic responses in mammalian assays*. Environ Toxicol Chem, 2011. **30**(4): p. 973-80.
140. Judson, R.S., et al., *Analysis of eight oil spill dispersants using rapid, in vitro tests for endocrine and other biological activity*. Environ Sci Technol, 2010. **44**(15): p. 5979-85.
141. Petrovic, M. and D. Barcelo, *Determination of anionic and nonionic surfactants, their degradation products, and endocrine-disrupting compounds in sewage sludge by liquid chromatography/mass spectrometry*. Anal Chem, 2000. **72**(19): p. 4560-7.
142. Schlenk, D., et al., *Reconstitution studies of pesticides and surfactants exploring the cause of estrogenic activity observed in surface waters of the San Francisco Bay Delta*. Environ Sci Technol, 2012. **46**(16): p. 9106-11.
143. Routledge EJ, S.J., *Estrogenic activity of surfactants and some of their degradation products assessed using a recombinant yeast screen*. Environmental Toxicology and Chemistry, 1996. **15**(3): p. 241-248.
144. White, R., et al., *Environmentally persistent alkylphenolic compounds are estrogenic*. Endocrinology, 1994. **135**(1): p. 175-82.
145. Xie, L., et al., *Evaluation of estrogenic activities of aquatic herbicides and surfactants using an rainbow trout vitellogenin assay*. Toxicol Sci, 2005. **87**(2): p. 391-8.
146. Miles-Richardson, S.R., et al., *Effects of waterborne exposure to 4-nonylphenol and nonylphenol ethoxylate on secondary sex characteristics and gonads of fathead minnows (*Pimephales promelas*)*. Environ Res, 1999. **80**(2 Pt 2): p. S122-S137.
147. Guenther, K., et al., *Endocrine disrupting nonylphenols are ubiquitous in food*. Environ Sci Technol, 2002. **36**(8): p. 1676-80.
148. FDA, *Code of Federal Regulations Title 21. Secondary Direct Food Additives Permitted in Food for Human Consumption*. Food and Drug Administration. 2015.
149. Karlin, D.A., R.T. O'Donnell, and W.E. Jensen, *Effect of dioctyl sodium sulfosuccinate feeding on rat colorectal 1,2-dimethylhydrazine carcinogenesis*. J Natl Cancer Inst, 1980. **64**(4): p. 791-3.
150. MacKenzie, K., et al., *Three-generation reproduction study with dioctyl sodium sulfosuccinate in rats*. Fundam Appl Toxicol, 1990. **15**(1): p. 53-62.
151. Jick, H., et al., *First-trimester drug use and congenital disorders*. JAMA, 1981. **246**(4): p. 343-6.
152. Aselton, P., et al., *First-trimester drug use and congenital disorders*. Obstet Gynecol, 1985. **65**(4): p. 451-5.
153. Trottier, M., A. Erebara, and P. Bozzo, *Treating constipation during pregnancy*. Can Fam Physician, 2012. **58**(8): p. 836-8.
154. Greenhalf, J.O. and H.S. Leonard, *Laxatives in the treatment of constipation in pregnant and breast-feeding mothers*. Practitioner, 1973. **210**(256): p. 259-63.
155. Godfrey, H., *Dangers of dioctyl sodium sulfosuccinate in mixtures*. JAMA, 1971. **215**(4): p. 643.

156. Hines, E.P., et al., *Phenotypic dichotomy following developmental exposure to perfluorooctanoic acid (PFOA) in female CD-1 mice: Low doses induce elevated serum leptin and insulin, and overweight in mid-life*. Mol Cell Endocrinol, 2009. **304**(1-2): p. 97-105.
157. Kloting, N., et al., *Di-(2-Ethylhexyl)-Phthalate (DEHP) Causes Impaired Adipocyte Function and Alters Serum Metabolites*. PLoS One, 2015. **10**(12): p. e0143190.
158. Hao, C., et al., *The endocrine disruptor mono-(2-ethylhexyl) phthalate promotes adipocyte differentiation and induces obesity in mice*. Biosci Rep, 2012. **32**(6): p. 619-29.
159. Li, X., et al., *Triflumizole is an obesogen in mice that acts through peroxisome proliferator activated receptor gamma (PPARgamma)*. Environ Health Perspect, 2012. **120**(12): p. 1720-6.
160. Newbold, R.R., et al., *Developmental exposure to estrogenic compounds and obesity*. Birth Defects Res A Clin Mol Teratol, 2005. **73**(7): p. 478-80.
161. Angle, B.M., et al., *Metabolic disruption in male mice due to fetal exposure to low but not high doses of bisphenol A (BPA): evidence for effects on body weight, food intake, adipocytes, leptin, adiponectin, insulin and glucose regulation*. Reprod Toxicol, 2013. **42**: p. 256-68.
162. Kujawinski, E.B., et al., *Fate of dispersants associated with the deepwater horizon oil spill*. Environ Sci Technol, 2011. **45**(4): p. 1298-306.
163. Almeda, R., et al., *Interactions between zooplankton and crude oil: toxic effects and bioaccumulation of polycyclic aromatic hydrocarbons*. PLoS One, 2013. **8**(6): p. e67212.
164. Hemmer, M.J., M.G. Barron, and R.M. Greene, *Comparative toxicity of eight oil dispersants, Louisiana sweet crude oil (LSC), and chemically dispersed LSC to two aquatic test species*. Environ Toxicol Chem, 2011. **30**(10): p. 2244-52.
165. Vrabie, C.M., et al., *Specific in vitro toxicity of crude and refined petroleum products: II. Estrogen (alpha and beta) and androgen receptor-mediated responses in yeast assays*. Environ Toxicol Chem, 2010. **29**(7): p. 1529-36.
166. Swedenborg, E., et al., *Endocrine disruptive chemicals: mechanisms of action and involvement in metabolic disorders*. J Mol Endocrinol, 2009. **43**(1): p. 1-10.
167. Lee, H.R., et al., *Molecular mechanism(s) of endocrine-disrupting chemicals and their potent oestrogenicity in diverse cells and tissues that express oestrogen receptors*. J Cell Mol Med, 2013. **17**(1): p. 1-11.
168. Molehin, D., M. Dekker Nitert, and K. Richard, *Prenatal Exposures to Multiple Thyroid Hormone Disruptors: Effects on Glucose and Lipid Metabolism*. J Thyroid Res, 2016. **2016**: p. 8765049.
169. De Coster, S. and N. van Larebeke, *Endocrine-disrupting chemicals: associated disorders and mechanisms of action*. J Environ Public Health, 2012. **2012**: p. 713696.
170. Gronemeyer, H., J.A. Gustafsson, and V. Laudet, *Principles for modulation of the nuclear receptor superfamily*. Nat Rev Drug Discov, 2004. **3**(11): p. 950-64.
171. Delfosse, V., et al., *A structural perspective on nuclear receptors as targets of environmental compounds*. Acta Pharmacol Sin, 2014.

172. Couse, J.F., et al., *Estrogen receptor-alpha knockout mice exhibit resistance to the developmental effects of neonatal diethylstilbestrol exposure on the female reproductive tract*. Dev Biol, 2001. **238**(2): p. 224-38.
173. Ma, R. and D.A. Sassoon, *PCBs exert an estrogenic effect through repression of the Wnt7a signaling pathway in the female reproductive tract*. Environ Health Perspect, 2006. **114**(6): p. 898-904.
174. Bitman, J. and H.C. Cecil, *Estrogenic activity of DDT analogs and polychlorinated biphenyls*. J Agric Food Chem, 1970. **18**(6): p. 1108-12.
175. Welshons, W.V., S.C. Nagel, and F.S. vom Saal, *Large effects from small exposures. III. Endocrine mechanisms mediating effects of bisphenol A at levels of human exposure*. Endocrinology, 2006. **147**(6 Suppl): p. S56-69.
176. Vandenberg, L.N., et al., *Hormones and endocrine-disrupting chemicals: low-dose effects and nonmonotonic dose responses*. Endocr Rev, 2012. **33**(3): p. 378-455.
177. Clemons, J.H., et al., *Evidence of Estrogen- and TCDD-Like Activities in Crude and Fractionated Extracts of PM10 Air Particulate Material Using in Vitro Gene Expression Assays*. Environmental Science and Technology, 1998. **32**(12): p. 1853-1860.
178. Rundle, A., et al., *Association of childhood obesity with maternal exposure to ambient air polycyclic aromatic hydrocarbons during pregnancy*. Am J Epidemiol, 2012. **175**(11): p. 1163-72.
179. Athas, J.C., et al., *An effective dispersant for oil spills based on food-grade amphiphiles*. Langmuir, 2014. **30**(31): p. 9285-94.
180. Forman, B.M., et al., *15-Deoxy-delta 12, 14-prostaglandin J2 is a ligand for the adipocyte determination factor PPAR gamma*. Cell, 1995. **83**(5): p. 803-12.
181. Katsu, Y., et al., *Molecular cloning, characterization, and chromosome mapping of reptilian estrogen receptors*. Endocrinology, 2010. **151**(12): p. 5710-20.
182. Lieberman, B.A., et al., *The constitution of a progesterone response element*. Mol Endocrinol, 1993. **7**(4): p. 515-27.
183. Hvattum, E., et al., *Characterization of polysorbate 80 with liquid chromatography mass spectrometry and nuclear magnetic resonance spectroscopy: specific determination of oxidation products of thermally oxidized polysorbate 80*. J Pharm Biomed Anal, 2012. **62**: p. 7-16.
184. Chen, R., X. Yu, and L. Li, *Characterization of poly(ethylene glycol) esters using low energy collision-induced dissociation in electrospray ionization mass spectrometry*. J Am Soc Mass Spectrom, 2002. **13**(7): p. 888-97.
185. Mathew, J., et al., *Dioctyl sulfosuccinate analysis in near-shore Gulf of Mexico water by direct-injection liquid chromatography-tandem mass spectrometry*. J Chromatogr A, 2012. **1231**: p. 46-51.
186. Ramirez, C.E., S.R. Batchu, and P.R. Gardinali, *High sensitivity liquid chromatography tandem mass spectrometric methods for the analysis of dioctyl sulfosuccinate in different stages of an oil spill response monitoring effort*. Anal Bioanal Chem, 2013. **405**(12): p. 4167-75.
187. Zhang, R., et al., *Analysis of polysorbate 80 and its related compounds by RP-HPLC with ELSD and MS detection*. J Chromatogr Sci, 2012. **50**(7): p. 598-607.

188. Berman, H.M., et al., *The Protein Data Bank*. Nucleic Acids Res, 2000. **28**(1): p. 235-42.
189. Liberato, M.V., et al., *Medium chain fatty acids are selective peroxisome proliferator activated receptor (PPAR) gamma activators and pan-PPAR partial agonists*. PLoS One, 2012. **7**(5): p. e36297.
190. Hopkins, C.R., et al., *Design and synthesis of novel N-sulfonyl-2-indole carboxamides as potent PPAR-gamma binding agents with potential application to the treatment of osteoporosis*. Bioorg Med Chem Lett, 2006. **16**(21): p. 5659-63.
191. Williams, C.M., *Effects of Exposure to 17 β -Estradiol (E2) and Corexit-Enhanced Water Accommodated Fraction of Crude Oil (CWAFF) In Vitro on Sex Determination in the American Alligator, Alligator mississippiensis*, in *Marine Biology*. 2016, College of Charleston: ProQuest.
192. McNabb, N., *Investigating Estrogenic Activity of the Dispersant Corexit 9500 in the American Alligator and Diamondback Terrapin*, in *Marine Biology*. 2016, College of Charleston: ProQuest.
193. Behr, M., J. Oehlmann, and M. Wagner, *Estrogens in the daily diet: in vitro analysis indicates that estrogenic activity is omnipresent in foodstuff and infant formula*. Food Chem Toxicol, 2011. **49**(10): p. 2681-8.
194. Spitz, I.M., H.B. Croxatto, and A. Robbins, *Antiprogestins: mechanism of action and contraceptive potential*. Annu Rev Pharmacol Toxicol, 1996. **36**: p. 47-81.
195. Mangelsdorf, D.J. and R.M. Evans, *The RXR heterodimers and orphan receptors*. Cell, 1995. **83**(6): p. 841-50.
196. Keller, H., et al., *Fatty acids and retinoids control lipid metabolism through activation of peroxisome proliferator-activated receptor-retinoid X receptor heterodimers*. Proc Natl Acad Sci U S A, 1993. **90**(6): p. 2160-4.
197. Grun, F., et al., *Endocrine-disrupting organotin compounds are potent inducers of adipogenesis in vertebrates*. Mol Endocrinol, 2006. **20**(9): p. 2141-55.
198. Jones, B.L., et al., *Conservation of estrogen receptor function in invertebrate reproduction*. BMC Evol Biol, 2017. **17**(1): p. 65.
199. Escriva, H., S. Bertrand, and V. Laudet, *The evolution of the nuclear receptor superfamily*. Essays Biochem, 2004. **40**: p. 11-26.
200. Konkel, L., *A Closer Look at Obesogens: Lipid Homeostasis Disruption in Daphnia*. Environ Health Perspect, 2015. **123**(8): p. A219.
201. Cocci, P., et al., *Effects of Diisodecyl Phthalate on PPAR:RXR-Dependent Gene Expression Pathways in Sea Bream Hepatocytes*. Chem Res Toxicol, 2015. **28**(5): p. 935-47.
202. Bility, M.T., et al., *Activation of mouse and human peroxisome proliferator-activated receptors (PPARs) by phthalate monoesters*. Toxicol Sci, 2004. **82**(1): p. 170-82.
203. Ogden, C.L., et al., *Prevalence of childhood and adult obesity in the United States, 2011-2012*. JAMA, 2014. **311**(8): p. 806-14.
204. Kelly, T., et al., *Global burden of obesity in 2005 and projections to 2030*. Int J Obes (Lond), 2008. **32**(9): p. 1431-7.

205. Villareal, D.T., et al., *Obesity in older adults: technical review and position statement of the American Society for Nutrition and NAASO, The Obesity Society*. *Obes Res*, 2005. **13**(11): p. 1849-63.
206. Grun, F. and B. Blumberg, *Endocrine disruptors as obesogens*. *Mol Cell Endocrinol*, 2009. **304**(1-2): p. 19-29.
207. Bray, G.A., S.J. Nielsen, and B.M. Popkin, *Consumption of high-fructose corn syrup in beverages may play a role in the epidemic of obesity*. *Am J Clin Nutr*, 2004. **79**(4): p. 537-43.
208. Chassaing, B., et al., *Dietary emulsifiers impact the mouse gut microbiota promoting colitis and metabolic syndrome*. *Nature*, 2015. **519**(7541): p. 92-6.
209. Heindel, J.J., *Endocrine disruptors and the obesity epidemic*. *Toxicol Sci*, 2003. **76**(2): p. 247-9.
210. Nielsen, R., et al., *Genome-wide profiling of PPARgamma:RXR and RNA polymerase II occupancy reveals temporal activation of distinct metabolic pathways and changes in RXR dimer composition during adipogenesis*. *Genes Dev*, 2008. **22**(21): p. 2953-67.
211. Chen, Q., et al., *Fate decision of mesenchymal stem cells: adipocytes or osteoblasts? Cell Death Differ*, 2016. **23**(7): p. 1128-39.
212. Rodeheffer, M.S., K. Birsoy, and J.M. Friedman, *Identification of white adipocyte progenitor cells in vivo*. *Cell*, 2008. **135**(2): p. 240-9.
213. Gavin, K.M., et al., *De novo generation of adipocytes from circulating progenitor cells in mouse and human adipose tissue*. *FASEB J*, 2016. **30**(3): p. 1096-108.
214. Lengqvist, J., et al., *Polyunsaturated fatty acids including docosahexaenoic and arachidonic acid bind to the retinoid X receptor alpha ligand-binding domain*. *Mol Cell Proteomics*, 2004. **3**(7): p. 692-703.
215. Yanik, S.C., et al., *Organotins are potent activators of PPARgamma and adipocyte differentiation in bone marrow multipotent mesenchymal stromal cells*. *Toxicol Sci*, 2011. **122**(2): p. 476-88.
216. Hurst, C.H. and D.J. Waxman, *Activation of PPARalpha and PPARgamma by environmental phthalate monoesters*. *Toxicol Sci*, 2003. **74**(2): p. 297-308.
217. Takacs, M.L. and B.D. Abbott, *Activation of mouse and human peroxisome proliferator-activated receptors (alpha, beta/delta, gamma) by perfluorooctanoic acid and perfluorooctane sulfonate*. *Toxicol Sci*, 2007. **95**(1): p. 108-17.
218. Riu, A., et al., *Peroxisome proliferator-activated receptor gamma is a target for halogenated analogs of bisphenol A*. *Environ Health Perspect*, 2011. **119**(9): p. 1227-32.
219. Iida, K., et al., *Sodium dodecyl sulfate and sodium dodecyl benzenesulfonate are ligands for peroxisome proliferator-activated receptor gamma*. *J Toxicol Sci*, 2013. **38**(5): p. 697-702.
220. Wang, D., et al., *Peroxisome proliferator-activated receptor delta promotes colonic inflammation and tumor growth*. *Proc Natl Acad Sci U S A*, 2014. **111**(19): p. 7084-9.
221. Hudak, C.S. and H.S. Sul, *Pref-1, a gatekeeper of adipogenesis*. *Front Endocrinol (Lausanne)*, 2013. **4**: p. 79.
222. Hemming, S., et al., *EZH2 and KDM6A act as an epigenetic switch to regulate mesenchymal stem cell lineage specification*. *Stem Cells*, 2014. **32**(3): p. 802-15.

223. Shimizu, H., et al., *Troglitazone reduces plasma leptin concentration but increases hunger in NIDDM patients*. Diabetes Care, 1998. **21**(9): p. 1470-4.
224. Schwartz, A.V., *TZDs and Bone: A Review of the Recent Clinical Evidence*. PPAR Res, 2008. **2008**: p. 297893.
225. Hanhoff, T., et al., *Branched-chain fatty acids as activators of peroxisome proliferator-activated receptors*. Eur J Lipid Sci Technol, 2005. **107**: p. 716-729.
226. Fan, Y.Y., et al., *Chemopreventive n-3 fatty acids activate RXRalpha in colonocytes*. Carcinogenesis, 2003. **24**(9): p. 1541-8.
227. Gosselin, R.E. and M.N. Gleason, *Clinical toxicology of commercial products : acute poisoning*. 4th ed. 1976, Baltimore: Williams & Wilkins. 1794 p. in various pagings.
228. Ingram, A.J., et al., *Short-term toxicity study of sorbitan mono-oleate (Span 80) in rats*. Food Cosmet Toxicol, 1978. **16**(6): p. 535-42.
229. Staff, P.O., *Correction: Comprehensive profiling of plasma fatty acid concentrations in young healthy Canadian adults*. PLoS One, 2015. **10**(5): p. e0128167.
230. Song He, W., T.Y. Nara, and M.T. Nakamura, *Delayed induction of delta-6 and delta-5 desaturases by a peroxisome proliferator*. Biochem Biophys Res Commun, 2002. **299**(5): p. 832-8.
231. Li, Y., T.Y. Nara, and M.T. Nakamura, *Peroxisome proliferator-activated receptor alpha is required for feedback regulation of highly unsaturated fatty acid synthesis*. J Lipid Res, 2005. **46**(11): p. 2432-40.
232. Kampf, J.P. and A.M. Kleinfeld, *Fatty acid transport in adipocytes monitored by imaging intracellular free fatty acid levels*. J Biol Chem, 2004. **279**(34): p. 35775-80.
233. Wang, Q., et al., *Expression of PPAR, RXR isoforms and fatty acid transporting proteins in the rat and human gastrointestinal tracts*. J Pharm Sci, 2005. **94**(2): p. 363-72.
234. Regnier, S.M., et al., *Tributyltin differentially promotes development of a phenotypically distinct adipocyte*. Obesity (Silver Spring), 2015. **23**(9): p. 1864-71.
235. Hughes, T.S., et al., *An alternate binding site for PPARgamma ligands*. Nat Commun, 2014. **5**: p. 3571.
236. EWG. *Environmental Working Group: Skin deep cosmetics databse*. 2015 [cited 2015 May 20]; Available from: http://www.ewg.org/skindeep/ingredient/702082/DIOCTYL_SODIUM_SULFOSUCCINATE/
237. Taratino, L., *Cytec Industries, Inc. - GRAS Notification for Dioctyl Sodium Sulfosuccinate*, in CY04825/05, F.D.o.H.a.H. Services, Editor. July 20 1998.
238. Jewell, D.J. and G. Young, *Interventions for treating constipation in pregnancy*. Cochrane Database Syst Rev, 2001(2): p. CD001142.
239. Ellett, R.P., Jr., *Dioctyl sodium sulfosuccinate in constipation of pregnancy*. Obstet Gynecol, 1957. **10**(3): p. 322-5.
240. Beltran-Sanchez, H., et al., *Prevalence and trends of metabolic syndrome in the adult U.S. population, 1999-2010*. J Am Coll Cardiol, 2013. **62**(8): p. 697-703.

241. Finkelstein, E.A., et al., *Obesity and severe obesity forecasts through 2030*. Am J Prev Med, 2012. **42**(6): p. 563-70.
242. Maes, H.H., M.C. Neale, and L.J. Eaves, *Genetic and environmental factors in relative body weight and human adiposity*. Behav Genet, 1997. **27**(4): p. 325-51.
243. Waalen, J., *The genetics of human obesity*. Transl Res, 2014. **164**(4): p. 293-301.
244. Speliotes, E.K., et al., *Association analyses of 249,796 individuals reveal 18 new loci associated with body mass index*. Nat Genet, 2010. **42**(11): p. 937-48.
245. Llewellyn, C.H., et al., *Finding the missing heritability in pediatric obesity: the contribution of genome-wide complex trait analysis*. Int J Obes (Lond), 2013. **37**(11): p. 1506-9.
246. Trerotola, M., et al., *Epigenetic inheritance and the missing heritability*. Hum Genomics, 2015. **9**: p. 17.
247. Heindel, J.J., et al., *Metabolism disrupting chemicals and metabolic disorders*. Reprod Toxicol, 2017. **68**: p. 3-33.
248. Brantley, P.J., V.H. Myers, and H.J. Roy, *Environmental and lifestyle influences on obesity*. J La State Med Soc, 2005. **157 Spec No 1**: p. S19-27.
249. Wild, C.P., *The exposome: from concept to utility*. Int J Epidemiol, 2012. **41**(1): p. 24-32.
250. Gluckman, P.D. and M.A. Hanson, *Living with the past: evolution, development, and patterns of disease*. Science, 2004. **305**(5691): p. 1733-6.
251. Calkins, K. and S.U. Devaskar, *Fetal origins of adult disease*. Curr Probl Pediatr Adolesc Health Care, 2011. **41**(6): p. 158-76.
252. Rappaport, S.M. and M.T. Smith, *Epidemiology. Environment and disease risks*. Science, 2010. **330**(6003): p. 460-1.
253. Kim, S.H. and M.J. Park, *Phthalate exposure and childhood obesity*. Ann Pediatr Endocrinol Metab, 2014. **19**(2): p. 69-75.
254. Vafeiadi, M., et al., *Association of Prenatal Exposure to Persistent Organic Pollutants with Obesity and Cardiometabolic Traits in Early Childhood: The Rhea Mother-Child Cohort (Crete, Greece)*. Environ Health Perspect, 2015. **123**(10): p. 1015-21.
255. Mendez, M.A., et al., *Prenatal organochlorine compound exposure, rapid weight gain, and overweight in infancy*. Environ Health Perspect, 2011. **119**(2): p. 272-8.
256. Grun, F. and B. Blumberg, *Minireview: the case for obesogens*. Mol Endocrinol, 2009. **23**(8): p. 1127-34.
257. Tabb, M.M. and B. Blumberg, *New modes of action for endocrine-disrupting chemicals*. Mol Endocrinol, 2006. **20**(3): p. 475-82.
258. Temkin, A.M., et al., *Effects of Crude Oil/Dispersant Mixture and Dispersant Components on PPARgamma Activity in Vitro and in Vivo: Identification of Dioctyl Sodium Sulfosuccinate (DOSS; CAS #577-11-7) as a Probable Obesogen*. Environ Health Perspect, 2016. **124**(1): p. 112-9.
259. Fraulob, J.C., et al., *A Mouse Model of Metabolic Syndrome: Insulin Resistance, Fatty Liver and Non-Alcoholic Fatty Pancreas Disease (NAFPD) in C57BL/6 Mice Fed a High Fat Diet*. J Clin Biochem Nutr, 2010. **46**(3): p. 212-23.
260. Collins, S., et al., *Genetic vulnerability to diet-induced obesity in the C57BL/6J mouse: physiological and molecular characteristics*. Physiol Behav, 2004. **81**(2): p. 243-8.

261. Wang, C.Y. and J.K. Liao, *A mouse model of diet-induced obesity and insulin resistance*. *Methods Mol Biol*, 2012. **821**: p. 421-33.
262. Johnson, P., K. Mount, and S. Graziano, *Functional bowel disorders in pregnancy: effect on quality of life, evaluation and management*. *Acta Obstet Gynecol Scand*, 2014. **93**(9): p. 874-9.
263. Berger, A., *Bone mineral density scans*. *BMJ*, 2002. **325**(7362): p. 484.
264. Deng, H.W., et al., *Differences in bone mineral density, bone mineral content, and bone areal size in fracturing and non-fracturing women, and their interrelationships at the spine and hip*. *J Bone Miner Metab*, 2002. **20**(6): p. 358-66.
265. Cordey, J., et al., *Effect of bone size, not density, on the stiffness of the proximal part of normal and osteoporotic human femora*. *J Bone Miner Res*, 1992. **7 Suppl 2**: p. S437-44.
266. Bolger, A.M., M. Lohse, and B. Usadel, *Trimmomatic: a flexible trimmer for Illumina sequence data*. *Bioinformatics*, 2014. **30**(15): p. 2114-20.
267. Langmead, B. and S.L. Salzberg, *Fast gapped-read alignment with Bowtie 2*. *Nat Methods*, 2012. **9**(4): p. 357-9.
268. Krueger, F. and S.R. Andrews, *Bismark: a flexible aligner and methylation caller for Bisulfite-Seq applications*. *Bioinformatics*, 2011. **27**(11): p. 1571-2.
269. Bligh, E.G. and W.J. Dyer, *A rapid method of total lipid extraction and purification*. *Can J Biochem Physiol*, 1959. **37**(8): p. 911-7.
270. Koelmel, J.P., et al., *Expanding Lipidome Coverage Using LC-MS/MS Data-Dependent Acquisition with Automated Exclusion List Generation*. *J Am Soc Mass Spectrom*, 2017. **28**(5): p. 908-917.
271. Al-Hamodi, Z., et al., *Association of adipokines, leptin/adiponectin ratio and C-reactive protein with obesity and type 2 diabetes mellitus*. *Diabetol Metab Syndr*, 2014. **6**(1): p. 99.
272. Guo, J., et al., *Persistent diet-induced obesity in male C57BL/6 mice resulting from temporary obesigenic diets*. *PLoS One*, 2009. **4**(4): p. e5370.
273. Fan, Y., et al., *Diet-induced obesity in male C57BL/6 mice decreases fertility as a consequence of disrupted blood-testis barrier*. *PLoS One*, 2015. **10**(4): p. e0120775.
274. Lihn, A.S., S.B. Pedersen, and B. Richelsen, *Adiponectin: action, regulation and association to insulin sensitivity*. *Obes Rev*, 2005. **6**(1): p. 13-21.
275. Wolfson, N., et al., *Relation of adiponectin to glucose tolerance status, adiposity, and cardiovascular risk factor load*. *Exp Diabetes Res*, 2012. **2012**: p. 250621.
276. Aguirre, L., et al., *Increasing adiposity is associated with higher adipokine levels and lower bone mineral density in obese older adults*. *J Clin Endocrinol Metab*, 2014. **99**(9): p. 3290-7.
277. Gollisch, K.S., et al., *Effects of exercise training on subcutaneous and visceral adipose tissue in normal- and high-fat diet-fed rats*. *Am J Physiol Endocrinol Metab*, 2009. **297**(2): p. E495-504.
278. Friedman, J.M. and J.L. Halaas, *Leptin and the regulation of body weight in mammals*. *Nature*, 1998. **395**(6704): p. 763-70.

279. Maffei, M., et al., *Leptin levels in human and rodent: measurement of plasma leptin and ob RNA in obese and weight-reduced subjects*. Nat Med, 1995. **1**(11): p. 1155-61.
280. Al Maskari, M.Y. and A.A. Alnaqdy, *Correlation between Serum Leptin Levels, Body Mass Index and Obesity in Omanis*. Sultan Qaboos Univ Med J, 2006. **6**(2): p. 27-31.
281. Surmi, B.K. and A.H. Hasty, *Macrophage infiltration into adipose tissue: initiation, propagation and remodeling*. Future Lipidol, 2008. **3**(5): p. 545-556.
282. Den Hartigh, L.J., et al., *Adipocyte-Specific Deficiency of NADPH Oxidase 4 Delays the Onset of Insulin Resistance and Attenuates Adipose Tissue Inflammation in Obesity*. Arterioscler Thromb Vasc Biol, 2017. **37**(3): p. 466-475.
283. Hsieh, P.S., et al., *COX-2-mediated inflammation in fat is crucial for obesity-linked insulin resistance and fatty liver*. Obesity (Silver Spring), 2009. **17**(6): p. 1150-7.
284. Wong, C.P., N.A. Rinaldi, and E. Ho, *Zinc deficiency enhanced inflammatory response by increasing immune cell activation and inducing IL6 promoter demethylation*. Mol Nutr Food Res, 2015. **59**(5): p. 991-9.
285. Hur, K., et al., *Aberrant methylation of the specific CpG island portion regulates cyclooxygenase-2 gene expression in human gastric carcinomas*. Biochem Biophys Res Commun, 2003. **310**(3): p. 844-51.
286. Markgraf, D.F., H. Al-Hasani, and S. Lehr, *Lipidomics-Reshaping the Analysis and Perception of Type 2 Diabetes*. Int J Mol Sci, 2016. **17**(11).
287. Meikle, P.J. and M.J. Christopher, *Lipidomics is providing new insight into the metabolic syndrome and its sequelae*. Curr Opin Lipidol, 2011. **22**(3): p. 210-5.
288. Eisinger, K., et al., *Lipidomic analysis of serum from high fat diet induced obese mice*. Int J Mol Sci, 2014. **15**(2): p. 2991-3002.
289. Barber, M.N., et al., *Plasma lysophosphatidylcholine levels are reduced in obesity and type 2 diabetes*. PLoS One, 2012. **7**(7): p. e41456.
290. Hwang, L.L., et al., *Sex differences in high-fat diet-induced obesity, metabolic alterations and learning, and synaptic plasticity deficits in mice*. Obesity (Silver Spring), 2010. **18**(3): p. 463-9.
291. Rabe, K., et al., *Adipokines and insulin resistance*. Mol Med, 2008. **14**(11-12): p. 741-51.
292. Guo, R., et al., *Adiponectin knockout accentuates high fat diet-induced obesity and cardiac dysfunction: role of autophagy*. Biochim Biophys Acta, 2013. **1832**(8): p. 1136-48.
293. Chand, L.a.S., S, *Serum adiponectin level in obese and non obese type 2 diabetes mellitus*. International Journal of Clinical and Biomedical Research, 2016. **2**(3): p. 8-12.
294. Mohammadzadeh, G. and N. Zarghami, *Serum leptin level is reduced in non-obese subjects with type 2 diabetes*. Int J Endocrinol Metab, 2013. **11**(1): p. 3-10.
295. Hagman, J., A. Travis, and R. Grosschedl, *A novel lineage-specific nuclear factor regulates mb-1 gene transcription at the early stages of B cell differentiation*. EMBO J, 1991. **10**(11): p. 3409-17.

296. Modan, M., et al., *Hyperinsulinemia. A link between hypertension obesity and glucose intolerance.* J Clin Invest, 1985. **75**(3): p. 809-17.
297. Zisman, A., et al., *Targeted disruption of the glucose transporter 4 selectively in muscle causes insulin resistance and glucose intolerance.* Nat Med, 2000. **6**(8): p. 924-8.
298. Garvey, W.T., et al., *Evidence for defects in the trafficking and translocation of GLUT4 glucose transporters in skeletal muscle as a cause of human insulin resistance.* J Clin Invest, 1998. **101**(11): p. 2377-86.
299. Kirchner, H., et al., *Altered promoter methylation of PDK4, IL1 B, IL6, and TNF after Roux-en Y gastric bypass.* Surg Obes Relat Dis, 2014. **10**(4): p. 671-8.
300. Na, Y.K., et al., *Increased methylation of interleukin 6 gene is associated with obesity in Korean women.* Mol Cells, 2015. **38**(5): p. 452-6.
301. Chan, P.C., et al., *Importance of adipocyte cyclooxygenase-2 and prostaglandin E2-prostaglandin E receptor 3 signaling in the development of obesity-induced adipose tissue inflammation and insulin resistance.* FASEB J, 2016. **30**(6): p. 2282-97.
302. Rai, S. and S. Bhatnagar, *Novel Lipidomic Biomarkers in Hyperlipidemia and Cardiovascular Diseases: An Integrative Biology Analysis.* OMICS, 2017. **21**(3): p. 132-142.
303. van Ginneken, V., Verheij, E., de Vries, E., van der Greef, J., *The Discovery of Two Novel Biomarkers in a High-Fat Diet C56bl6 Obese Mouse Model for Non-Adipose Tissue: A Comprehensive LCMS Study at Hind Limb, Heart, Carcass Muscle, Liver, Brain, Blood Plasma and Food Composition Following a Lipidomics LCMS-Based Approach.* Cellular and Molecular Medicine: Open access, 2016. **2**(3).
304. Floegel, A., et al., *Identification of serum metabolites associated with risk of type 2 diabetes using a targeted metabolomic approach.* Diabetes, 2013. **62**(2): p. 639-48.
305. Kim, H.J., et al., *Metabolomic analysis of livers and serum from high-fat diet induced obese mice.* J Proteome Res, 2011. **10**(2): p. 722-31.
306. Delahunty, K.M., et al., *Gender- and compartment-specific bone loss in C57BL/6J mice: correlation to season?* J Clin Densitom, 2009. **12**(1): p. 89-94.
307. Bartness, T.J. and G.N. Wade, *Photoperiodic control of seasonal body weight cycles in hamsters.* Neurosci Biobehav Rev, 1985. **9**(4): p. 599-612.
308. Nazari, M., M. Kurdi, and H. Heerklotz, *Classifying surfactants with respect to their effect on lipid membrane order.* Biophys J, 2012. **102**(3): p. 498-506.
309. Paul, H.A., et al., *Diet-induced changes in maternal gut microbiota and metabolomic profiles influence programming of offspring obesity risk in rats.* Sci Rep, 2016. **6**: p. 20683.
310. Lecomte, M., et al., *Dietary emulsifiers from milk and soybean differently impact adiposity and inflammation in association with modulation of colonic goblet cells in high-fat fed mice.* Mol Nutr Food Res, 2016. **60**(3): p. 609-20.
311. Yang, C.M. and G.A. Varga, *The effects of continuous ruminal dosing with dioctyl sodium sulphosuccinate on ruminal and metabolic characteristics of lactating Holstein cows.* Br J Nutr, 1993. **69**(2): p. 397-408.

312. Goodman, J., J. Pang, and A.N. Bessman, *Dioctyl sodium sulfosuccinate- an ineffective prophylactic laxative*. J Chronic Dis, 1976. **29**(1): p. 59-63.
313. MacMillan, T.E., R. Kamali, and R.B. Cavalcanti, *Missed Opportunity to Deprescribe: Docusate for Constipation in Medical Inpatients*. Am J Med, 2016. **129**(9): p. 1001 e1-7.
314. Flurer RA, B.B., Gamble B, Gratz S, Muligan KJ, Benner Jr RA, El Said KR, Jester E, Burrows DG, da Silva D, Krahn M, Reichert W, Ylitalo G, *DETERMINATION OF DIOCTYLSULFOSUCCINATE IN SELECT SEAFOODS USING A QuEChERS EXTRACTION WITH LIQUID CHROMATOGRAPHY-TRIPLE QUADRUPOLE MASS SPECTROMETRY*, in *Laboratory Information Bulletin*. 2010, FDA/ORR/DFS.
315. Domingo-Gonzalez, R., et al., *COX-2 expression is upregulated by DNA hypomethylation after hematopoietic stem cell transplantation*. J Immunol, 2012. **189**(9): p. 4528-36.
316. Giacchetti, G., et al., *Decreased expression of insulin-sensitive glucose transporter mRNA (GLUT-4) in adipose tissue of non-insulin-dependent diabetic and obese patients: evaluation by a simplified quantitative PCR assay*. J Endocrinol Invest, 1994. **17**(9): p. 709-15.
317. Gracia, A., et al., *Fatty acid synthase methylation levels in adipose tissue: effects of an obesogenic diet and phenol compounds*. Genes Nutr, 2014. **9**(4): p. 411.
318. Cortese, R., et al., *Epigenomic profiling in visceral white adipose tissue of offspring of mice exposed to late gestational sleep fragmentation*. Int J Obes (Lond), 2015. **39**(7): p. 1135-42.
319. Jais, A., et al., *Heme oxygenase-1 drives metaflammation and insulin resistance in mouse and man*. Cell, 2014. **158**(1): p. 25-40.
320. Fujiki, K., et al., *Expression of the peroxisome proliferator activated receptor gamma gene is repressed by DNA methylation in visceral adipose tissue of mouse models of diabetes*. BMC Biol, 2009. **7**: p. 38.
321. Filer, D., et al., *Test driving ToxCast: endocrine profiling for 1858 chemicals included in phase II*. Curr Opin Pharmacol, 2014. **19**: p. 145-52.
322. Sipes, N.S., et al., *Profiling 976 ToxCast chemicals across 331 enzymatic and receptor signaling assays*. Chem Res Toxicol, 2013. **26**(6): p. 878-95.
323. Baell, J.B. and G.A. Holloway, *New substructure filters for removal of pan assay interference compounds (PAINS) from screening libraries and for their exclusion in bioassays*. J Med Chem, 2010. **53**(7): p. 2719-40.
324. Cho, E.S., et al., *The effects of rosiglitazone on osteoblastic differentiation, osteoclast formation and bone resorption*. Mol Cells, 2012. **33**(2): p. 173-81.
325. Doshi, L.S., et al., *Discovery and development of selective PPAR gamma modulators as safe and effective antidiabetic agents*. Expert Opin Investig Drugs, 2010. **19**(4): p. 489-512.
326. Ingvorsen, C., N.A. Karp, and C.J. Lelliott, *The role of sex and body weight on the metabolic effects of high-fat diet in C57BL/6N mice*. Nutr Diabetes, 2017. **7**(4): p. e261.
327. Threadgill, D.W., et al., *The collaborative cross: a recombinant inbred mouse population for the systems genetic era*. ILAR J, 2011. **52**(1): p. 24-31.

328. Spruijt, C.G. and M. Vermeulen, *DNA methylation: old dog, new tricks?* Nat Struct Mol Biol, 2014. **21**(11): p. 949-54.
329. Dujovne, C.A. and D.W. Shoeman, *Toxicity of a hepatotoxic laxative preparation in tissue culture and excretion in bile in man.* Clin Pharmacol Ther, 1972. **13**(4): p. 602-8.
330. Fiume, M.M., et al., *Safety Assessment of Dialkyl Sulfosuccinate Salts as Used in Cosmetics.* Int J Toxicol, 2016. **35**(3 suppl): p. 34S-46S.
331. Sigurdsson, V., et al., *Bile Acids Protect Expanding Hematopoietic Stem Cells from Unfolded Protein Stress in Fetal Liver.* Cell Stem Cell, 2016. **18**(4): p. 522-32.
332. Gray, J.L., et al., *Presence of the Corexit component dioctyl sodium sulfosuccinate in Gulf of Mexico waters after the 2010 Deepwater Horizon oil spill.* Chemosphere, 2014. **95**: p. 124-30.
333. Zhang, H.Y., et al., *Perinatal exposure to 4-nonylphenol affects adipogenesis in first and second generation rats offspring.* Toxicol Lett, 2014. **225**(2): p. 325-32.
334. Han, E.H., et al., *Upregulation of cyclooxygenase-2 by 4-nonylphenol is mediated through the cyclic amp response element activation pathway.* J Toxicol Environ Health A, 2010. **73**(21-22): p. 1451-64.
335. John, G.K. and G.E. Mullin, *The Gut Microbiome and Obesity.* Curr Oncol Rep, 2016. **18**(7): p. 45.
336. Turnbaugh, P.J., et al., *An obesity-associated gut microbiome with increased capacity for energy harvest.* Nature, 2006. **444**(7122): p. 1027-31.
337. Ridaura, V.K., et al., *Gut microbiota from twins discordant for obesity modulate metabolism in mice.* Science, 2013. **341**(6150): p. 1241214.
338. Wei, J., et al., *Perinatal exposure to bisphenol A exacerbates nonalcoholic steatohepatitis-like phenotype in male rat offspring fed on a high-fat diet.* J Endocrinol, 2014. **222**(3): p. 313-25.